

University of Montana

ScholarWorks at University of Montana

Graduate Student Theses, Dissertations, &
Professional Papers

Graduate School

2005

Gallium and arsenic/selenium recoveries from aqueous systems using silica based chelating composites

Paul J. Miranda

The University of Montana

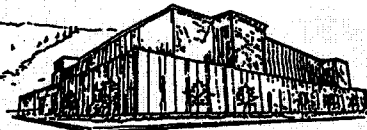
Follow this and additional works at: <https://scholarworks.umt.edu/etd>

Let us know how access to this document benefits you.

Recommended Citation

Miranda, Paul J., "Gallium and arsenic/selenium recoveries from aqueous systems using silica based chelating composites" (2005). *Graduate Student Theses, Dissertations, & Professional Papers*. 9569.
<https://scholarworks.umt.edu/etd/9569>

This Dissertation is brought to you for free and open access by the Graduate School at ScholarWorks at University of Montana. It has been accepted for inclusion in Graduate Student Theses, Dissertations, & Professional Papers by an authorized administrator of ScholarWorks at University of Montana. For more information, please contact scholarworks@mso.umt.edu.



**Maureen and Mike
MANSFIELD LIBRARY**

The University of
Montana

Permission is granted by the author to reproduce this material in its entirety, provided that this material is used for scholarly purposes and is properly cited in published works and reports.

****Please check "Yes" or "No" and provide signature****

Yes, I grant permission

X

No, I do not grant permission

Author's Signature:

[Handwritten Signature]

Date:

8-31-05

Any copying for commercial purposes or financial gain may be undertaken only with the author's explicit consent.

Gallium and Arsenic/Selenium
Recoveries from Aqueous Systems
Using Silica Based Chelating
Composites

By

Paul J. Miranda

B Sc. Montana Tech

M. Sc. Montana Tech of the University of Montana Tech

presented in partial fulfillment of the requirements

for the degree of

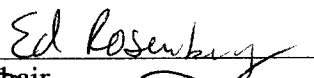
Doctor of Philosophy


Department of Chemistry

The University of Montana

July 2005

Approved by


Chair


Dean, Graduate School

8-31-05
Date

UMI Number: 3184233

Copyright 2005 by
Miranda, Paul J.

All rights reserved.

INFORMATION TO USERS

The quality of this reproduction is dependent upon the quality of the copy submitted. Broken or indistinct print, colored or poor quality illustrations and photographs, print bleed-through, substandard margins, and improper alignment can adversely affect reproduction.

In the unlikely event that the author did not send a complete manuscript and there are missing pages, these will be noted. Also, if unauthorized copyright material had to be removed, a note will indicate the deletion.

UMI[®]

UMI Microform 3184233

Copyright 2005 by ProQuest Information and Learning Company.

All rights reserved. This microform edition is protected against unauthorized copying under Title 17, United States Code.

ProQuest Information and Learning Company
300 North Zeeb Road
P.O. Box 1346
Ann Arbor, MI 48106-1346

Gallium and Arsenic/Selenium Recoveries from Aqueous Systems Using Silica Based Chelating Composites

Chair: Edward Rosenberg

EK

Abstract

During the last decade, silica based ion exchange resins have been developed and have the ability to successfully remove both cations and anions from aqueous systems. The synthesized materials are chemically strong enough to withstand both temperature and pH extremes in aqueous environments. Modifications of silica based ion exchange resins can be done with straightforward chemistry using a variety of chemical reactions.

The focus of the work presented is two-fold. Initially, a new silica based ion exchange resin was chemically developed with a functional group of 8-hydroxyquinoline or oxine. The oxine group was placed onto both polyallyl amine and polyetheneimine silica based ion exchange resin using the Mannich reaction. After successful grafting of the oxine group to the experimental composite, experimental work revealed that the new resin was able to successfully separate gallium from other metals such as ferrous iron, aluminum, and zinc, in acidic conditions. Further experimental work revealed the oxine based silica gel had a very high affinity for removal of ferric iron from nickel in acidic environments.

Secondly, a highly charged metal, zirconium, was successfully immobilized onto a silica based ion change resin with a functional group of aminoacetic acid. After loading the resin with the metal, experimental results have shown the resin has a very high affinity to successfully remove both selenium and arsenic from solution with little loss of the metal on the silica gel during stripping and regeneration.

Acknowledgements

I would initially like to thank my advisor, Dr. Edward Rosenberg, for providing me support academically, financially, and spiritually. During my time at the University of Montana, Dr. Rosenberg was more than a mentor to me. Besides being my advisor, Dr. Rosenberg was a true friend in many ways including becoming a father figure to me. His generosity and his commitment to me and other students are incredible. I have the utmost respect for Dr. Rosenberg as a researcher as well as a person. His scientific background and knowledge on many subjects amazed me on a daily basis. Personally, these years at the University of Montana have been exceptional because of my advisor, Dr. Edward Rosenberg.

A special thanks to Dr. Heiko Langer for allowing me to use the Inductively Coupled Plasma Spectrometer whenever possible for sample analysis. I am also thankful for the entire Rosenberg group and the University of Montana Department of Chemistry for friendships acquired during my time obtaining my doctorate degree.

Finally, I want to express my gratitude for the love of my life, Jennifer Marie Miranda, for her encouragement and patience during my coursework and final preparation of my dissertation. I also want to express my deepest love to my children, Conner Christopher and Lauren Ashleigh, for their inspiration to me of all that is good throughout the world.

To my children,
Conner and Lauren
may this dissertation make
their lives easier in the future.

Table of Contents

Authorization to Submit Dissertation.....	i
Abstract.....	ii
Acknowledgements.....	iii
Dedication.....	iv
Table of Contents.....	v
List of Figures.....	x
List of Tables.....	xiii
Chapter 1. Recovery of Metal Ions from Aqueous Systems	1
1.1 Purity Systems Introduction and Background	1
1.2 Proposed Research	5
Chapter 2. Experimental Methods	8
2.1 General Need Section	8
2.2 Infrared Spectra Experimental Procedure	8
2.3 Syntheses of the Polyamine Composites	8
2.4 Acid Washing of Silica Gel	9
2.5 Humidification of Silica Gel	9
2.6 Silinization of Silica Gel	10
2.7 Polyethylene Imine Gel (PEI)	11
2.8 Polyallyl Amine Gel (PAA)	12
2.9 Chromium Simulated Solution Experimental Work	14
2.10 Chromium Electroplating Solution on WP-1	15

2.11 Copper Removal with Cu-WRAM after pH adjustment	15
2.12 Testing of Cu-WRAM with pH Adjustment Using Sodium Hydroxide	15
2.13 Pre-Filtered Testing Solution	16
2.14 Formation of Sodium 8-Hydroxyquinoline Salt	16
2.15 Fries Rearrangement	16
2.16 Thomas Fries Rearrangement Experimental Procedure	17
2.17 Thomas Product Silica Gel Synthesis Procedure	18
2.18 Mannich Reaction Procedure (BPOX and WPOX)	18
2.19 Tethered Experimental Procedure	20
2.20 Tethered BPOX Procedure	21
2.21 Experimental Testing of WPOX and BPOX for Gallium Recoveries	21
2.22 Zirconium(IV) Loading Procedure on WP-2	22
2.23 WPAN Flow Testing Procedures	22
2.24 WPAN Batch Testing Procedures	23
2.25 Experimental Error Determination.....	23
Chapter 3. Chromium Recovery Using PSI Technology	24
3.1 Preliminary Work of Chromium Recovery and Removal of Plating Solutions.....	24
3.2 Chromium Simulated Solution Experimental Work	24
3.3 Chromium Remediation on U.S. Filter Solutions	25
3.4 Chromium Electroplating Solution on WP-1	25
3.5 Testing of Chromium Rinse Solution on WP-1	30
3.6 Conclusions	32
Chapter 4. Separation of Cobalt from Copper and Arsenic from a Cobalite Ore Leach	34

4.1 Introduction	34
4.2 NSC Pressure Leaching Fundamentals	34
4.3 Partial Nitrogen Species Catalyzed Pressure Oxidation of a Cobaltite Chalcopyrite Concentrate	36
4.4 Copper Removal with Cu-WRAM after pH adjustment	37
4.5 Testing of Cu-WRAM with pH Adjustment using Sodium Hydroxide.....	38
4.6 Testing of Cu-WRAM at pH=1.0	39
4.7 Pre-Filtered Testing Solution	41
4.8 CuWRAM Testing Results at pH 4.0	41
4.9 WP-1 Testing Results	42
4.10 WP-2 Testing Results	44
4.11 Conclusions	45
Chapter 5. Recovery of Gallium from Aqueous Systems	46
5.1 8-hydroxyquinoline Background Chemistry and Research Goals	46
5.2 Fries Rearrangement Experimental Procedure.....	49
5.3 Thomas Fries Rearrangement Results	50
5.4 Bonding of 8-Hydroxyquinoline to BP-1 and WP-1 Using the Mannich Reaction	51
5.5 Mannich Reaction Results	53
5.6 Infrared Spectra Analysis of Mannich Reaction Products	55
5.7 Elemental Analysis and Results	59
5.8 Results	62
Chapter 6. Experimental Testing of WPOX and BPOX for Gallium Recoveries	65

6.1 Background and Introduction.....	65
6.2 Gallium Recovery with WPOX	67
6.3 Gallium recovery with BPOX	68
6.4 Gallium Recovery from Alkaline Bayer Solutions	70
6.5 BPOX/WPOX Experimental Testing Results	74
6.6 Two Step Separation of Germanium and Gallium	75
6.7 Two Step Separation Conclusions	79
Chapter 7. Tethered BPOX	81
7.1 Mounting the 8-Hydroxy Quinoline Ligand via a Tether and its Impact on Kinetics	81
7.2 Tethering Conclusions	83
Chapter 8 Nickel-Ferric Separations using BPOX	84
8.1 Experimental Testing of BPOX for Nickel-Ferric	84
8.2 BPOX pH testing	87
8.3 Nickel-Ferric Conclusions	91
Chapter 9. Arsenic and Selenium Removal Using Zirconium(IV) Loaded Silica Polyamine Composites	93
9.1 Introduction	93
9.2 Zirconium Background	94
9.3 WPAN Experimental Strip Study	96
9.4 Selenate Flow Through Experimental Testing	99
9.5 Batch Testing for Selenate	100
9.6 Flow Testing for Selenate Species	100
9.7 Flow Testing for Selenite Species	103

9.8 Selenium Process Test Solution Experimental Work	105
9.9 Batch Testing for Arsenite and Arsenate Species	108
9.10 Flow Testing for Arsenite and Arsenate Species	110
9.11 Arsenic Mining Process Solution Flow Through Testing	116
9.12 East Helena Solution Second Experimental Research	119
9.13 WPAN Testing on Arsenic and Sulfate Solution	120
9.14 WPAN Results on Arsenic and Sulfate Solution	120
9.15 Montana Tech Design Team Solution	121
9.16 Zirconium Loaded Silica Conclusions	123
References.....	126

List of Figures

Figure 1.1 Synthetic Scheme for Making Silica Polyamine Composites.....	3
Figure 1.2. The Polyamines Used to Synthesize the Silica-Polyamine Composites.....	4
Figure 2.1 Infrared Spectra of Polyethylene Imine(PEI) Gel.....	12
Figure 2.2 Infrared Spectra of Polyallyl Amine(PAA) Gel.....	14
Figure 2.3. Infrared Spectra of WPOX Silica Gel.....	20
Figure 2.4. Infrared Spectra of BPOX Silica Gel.....	20
Figure 3.1 Chromium (III) Electroplating Breakthrough Curve.....	26
Figure 3.2 Chromium (III) Electroplating Breakthrough Curve (Slower Flow Rate).....	27
Figure 3.3 Electroplating Breakthrough after Carbon Pretreatment.....	29
Figure 3.4 Electroplating Breakthrough with U.S. Filter Carbon Pretreatment.....	30
Figure 3.5 Chromium Rinse Breakthrough on WP-1.....	31
Figure 4.1. Structure of Cu-WRAM Silica Gel.....	37
Figure 5.1. Structure of WP-1.....	47
Figure 5.2. Structure of BP-1.....	48
Figure 5.3. Schiff Base Formation and Reaction.....	48
Figure 5.4. Formation of Ester.....	49
Figure 5.5. Fries Rearrangement Mechanism.....	50
Figure 5.6. Infrared Spectra of Thomas Fries Rearrangement Product of 5-Acetyl-8-hydroxyquinoline.....	51
Figure 5.7. Mannich Reaction Example.....	52
Figure 5.8. Mannich Reaction Mechanism.....	53
Figure 5.9. BPOX Structure.....	54

Figure 5.10. WPOX Structure.....	55
Figure 5.11. Infrared Spectrum of BP-1.....	56
Figure 5.12 Infrared Spectrometer of BPOX.....	57
Figure 5.13. Infrared Spectrometer of WP-1.....	58
Figure 5.14 Infrared Spectrometer of WPOX.....	59
Figure 5.15. BPOX Structure Determination after Elemental Analysis.....	62
Figure 6.1 pH Profile for Gallium Recovery Using WPOX	66
Figure 6.2 Gallium Breakthrough Curve for WPOX with the Acidic Ore Leach Solution.....	67
Figure 6.3 Comparison of Feed and Flow Through Concentrations for Acidic Ore Leach Containing Gallium.....	68
Figure 6.4 Gallium Break Through Curve for BPOX with Acidic Leach Solution...	69
Figure 6.5 Comparison of Feed and Flow Through Concentrations Containing Gallium.....	70
Figure 6.6. Breakthrough Curves for the Acidic Ore Leach after Adjustment to pH = 2.1 and Passing Through the WP-2 Column.....	78
Figure 6.7. Break Through Curve for Acidic Ore Leach after Readjusting pH to 2.1 on BPOX.....	79
Figure 7.1. Tethered BPOX Structure.....	82
Figure 7.2. Kinetics Test of BPOX vs. Tethered BPOX.....	82
Figure 8.1 Nickel-Iron Flow Through Results.....	85
Figure 8.2 Nickel-Iron Flow Through and Strip Results.....	86
Figure 8.3. Ferric Flow Through Testing on WPOX.....	89
Figure 8.4. Nickel Flow Through Testing on BPOX.....	90
Figure 9.1 Schematic Representation of the Immobilization of Zirconium on WP-2.....	95

Figure 9.2. Selenate Break Through Curve.....	101
Figure 9.3. Sulfate Break Through Curve with Selenate.....	101
Figure 9.4. Selenite Break Through Curve.....	104
Figure 9.5. Sulfate Break Through Curve with Selenite.....	105
Figure 9.6. Kennecott Flow Through Curve.....	106
Figure 9.7. Kennecott Stripping Curve.....	107
Figure 9.8. Arsenate Species in Aqueous Systems.....	109
Figure 9.9. Arsenite Species in Aqueous Systems.....	110
Figure 9.10. Arsenate Flow Through Results.....	113
Figure 9.11. Sulfate Flow Through Results in Arsenate Solution.....	113
Figure 9.12. Sulfate Flow Through Results in Arsenite Solution.....	115
Figure 9.13. Sulfate Flowthrough Results in Presence of Arsenite.....	115
Figure 9.14. Flowthrough Results of East Helena Solution.....	117
Figure 9.15. Strip Results of East Helena Solution.....	117
Figure 9.16. East Helena Experimental Work.....	119
Figure 9.17. WPAN Results on Arsenic and Sulfate Solution.....	121
Figure 9.18. Experimental Results of Arsenic Solution from Design Team.....	122

Tables List

Table 1.1 Advantages of PSI Composite Resins Over Polystyrene Resins	5
Table 2.1. Elemental Analysis of Silanized Silica Gel	11
Table 2.2 Elemental Analysis of Polyethylene Imine(PEI) gel	12
Table 2.3 Elemental Analysis of Polyallyl Amine(PAA) gel	13
Table 2.4 Elemental Analysis of BPOX and WPOX	19
Table 2.5 Elemental Analysis of BPOX and Tethered BPOX	21
Table 3.1 Synthetic Solution Results	25
Table 4.1. NSC Leach Results	36
Table 4.2. Initial ICP Results with Cu-WRAM	38
Table 4.3. Strip Results with Cu-WRAM	38
Table 4.4. Flowthrough Solutions with Liquid Sodium Hydroxide	39
Table 4.5. Strip Solutions with Liquid Sodium Hydroxide	39
Table 4.6. Flow Through Solutions with Cu-WRAM at pH=1.0	40
Table 4.7. Strip Solutions with Cu-WRAM at pH=1.0	40
Table 4.8. Strip Solution Results after Prefiltering	41
Table 4.9. Flow Through Solutions after Cu-WRAM	42
Table 4.10. Strips Solutions from Cu-WRAM	42
Table 4.11. Strip Solution Weight Ratios Using Cu-WRAM	42

Table 4.12. Flow Through Solutions Using Cu-WRAM and WP-1	43
Table 4.13. Strip Solutions Using Cu-WRAM and WP-1	43
Table 4.14. Cobalt to Arsenic Weight Ratios Using WP-1	43
Table 4.15. Flow Through Solutions Using Cu-WRAM and WP-2	44
Table 4.16. Strip Solutions with Cu-WRAM and WP-2	44
Table 4.17. Mole Ratios using Cu-WRAM and WP-2	44
Table 5.1. Elemental Analysis of BP-1 and WP-1	60
Table 5.2. Molar Elemental Analysis of BP-1 and WP-1.....	60
Table 5.3. Elemental Analysis of BPOX and WPOX.....	60
Table 5.4. Molar Elemental Analysis of BPOX and WPOX.....	60
Table 5.5. Oxine Loading Calculation.....	61
Table 5.6. Oxine Loading Molar Calculation.....	61
Table 5.7. Nitrogen-Oxine Ratio.....	61
Table 6.1 Metal Profile of Pasminco Challenge Solution.....	66
Table 6.2 WPOX Metal Strip Ratio.....	68
Table 6.3 WPOX Metal Strip Ratio.....	69
Table 6.4 Initial Bayer Challenge Solution.....	71
Table 6.5 BPOX Flow Through Data for Bayer Solutions.....	71
Table 6.6 WPOX Flow Through Data for Bayer Solutions.....	71
Table 6.7 Tethered BPOX Flow Through Data for Bayer Solutions.....	71
Table 6.8 BPOX Strip Data for Bayer Solutions.....	72

Table 6.9 WPOX Strip Data for Bayer Solutions.....	72
Table 6.10 Tethered BPOX Strip Data for Bayer Solutions.....	72
Table 6.11 Tethered BPOX Strip Data for Bayer Solutions.....	74
Table 6.12. Flow Through Results for the WP-2-BPOX Two Column System.....	76
Table 6.13. Strip Results for the WP-2-BPOX Two Column System.....	76
Table 6.14. ICP Data for Pasminco Flow Through Using BPOX.....	77
Table 6.15. ICP Data for Pasminco Flow Through Using WP-2.....	79
Table 7.1. Elemental Results of Tethered Product, BPOX and WPOX.....	81
Table 8.1 Nickel-Iron Separation Results.....	85
Table 8.2. Ferric Capacity Calculations.....	86
Table 8.3 Nickel Iron Strip Results.....	87
Table 8.4. Nickel-Iron Flow Through at pH 1.0.....	87
Table 8.5 Nickel-Ferric Loading Calculations at pH 1.0.....	88
Table 8.6 Nickel-Iron Flow Through at pH 2.0.....	88
Table 8.7 Nickel-Ferric Loading Calculations at pH 2.0.....	89
Table 8.8. Nickel-Ferric Loading Calculations.....	90
Table 9.1 Zirconium Capacity Loading onto WP-2 Silica Gel.....	95
Table 9.2. Hydrochloric Acid Stripping Results.....	97
Table 9.3. Sulfuric Acid Stripping Results.....	97
Table 9.4. Sodium Phosphate Strip.....	98
Table 9.5. Sulfuric Acid Strip.....	98
Table 9.6. Duplicate Experimental Work for Selenate Strip Data.....	99
Table 9.7. Selenate Flow Through Data.....	99

Table 9.8. Selenate Capacity Calculations.....	100
Table 9.9. WPAN Loading Calculations of Selenate.....	102
Table 9.10. WPAN Loading Calculations of Sulfate in Presence of Selenate.....	102
Table 9.11. WPAN Loading Calculations of Selenite.....	103
Table 9.12. WPAN Loading Calculations of Sulfate in Presence of Selenite.....	104
Table 9.13. Kennecott Flow Through Data.....	107
Table 9.14. Kennecott Stripping Data.....	107
Table 9.15. Selenium Mass Balance.....	108
Table 9.16. Arsenate Batch Capacity.....	108
Table 9.17. Arsenite Batch Capacity.....	108
Table 9.18. Arsenite Flow Through Results.....	111
Table 9.19. Arsenate Flow Through Results.....	111
Table 9.20. Phosphate Strip Results.....	111
Table 9.21. Sulfate Strip Results.....	112
Table 9.22. Arsenate Capacity Calculations.....	114
Table 9.23. WPAN Loading Calculations of Sulfate in Presence of Arsenate.....	114
Table 9.24. Arsenite Capacity Calculations.....	116
Table 9.25. WPAN Loading Calculations of Sulfate in Presence of Arsenite.....	116
Table 9.26. Flow Through Results of East Helena Solution.....	118
Table 9.27. Strip Results of East Helena Solution.....	118
Table 9.28. Experimental Results of Second East Helena Testing Solution.....	119
Table 9.29. Arsenic Results from Montana Tech Design Team.....	122

Chapter 1. Recovery of Metal Ions from Aqueous Systems

1.1 Purity Systems Introduction and Background

Environmental contamination due to wastewater discharges containing high concentrations of toxic ions is ubiquitous. Sources include metal plating, pickling, pigments industries, tanneries, municipal landfills and wastewater treatment facilities, nuclear weapons production facilities and nuclear power generators, as well as mining waste. Increasing regulation on natural resource extraction and industrial wastewater discharge has caused an increased interest in removal and recovery of these ions from waste streams as well as the remediation of contaminated sites.¹ The growing scarcity of high grade mineral ores and the environmental problems associated with pyrometallurgy has lead to a steady increase in the use of hydrometallurgical techniques.² By far, the most popular solution mining technique is solvent extraction.³ However, this technique also suffers from some environmental drawbacks including the use of flammable and toxic organic solvents, the build up of “crud” at the aqueous-organic interface and an inability to extract the desired metal to very low levels. Recently, there has been increased interest in the use of solid phase adsorbents for mining and metal ion remediation applications.

The materials needed to effectively and economically treat these wastewaters will ideally have the following properties: 1) the ability to reduce heavy metal ion concentrations to below allowable discharge limits; 2) high adsorption capacities for the target metal ions, even in solutions containing high levels of alkali and alkaline earth metal ions; 3) the capability of processing wastewater or ore leaches at high throughput rates.¹⁻⁴ Many materials are currently being developed for these purposes but few can be

said to have all of these features. Simple methods involve the use of agricultural waste materials and other biomass.^{5,6} More sophisticated methods involve the ultrafiltration of soluble metal binding polymers and resins containing intricately designed ligands.^{3,7-10} The more advanced materials incorporate ligands designed to bind only one specific metal ion or a group of similar metal ions. This is accomplished in a number of ways; in some cases molecular species or elements are used in the ligand that demonstrate a preference for binding to the metal of interest and/or the atoms in the ligand molecule are “preformed” to match the size and coordination geometry of the metal ion.⁸⁻¹⁰ With these considerations in mind materials can be synthesized that are very effective at removing the target ions, but the synthesis of these materials is often complicated and costly and the resulting material chemically delicate. An alternative to this method of rendering separations is to create a material composed of a single binding element in high density that is conformationally mobile. This type of material is not intrinsically selective for a specific metal ion, but based on the stability constant of the metal-ligand complex formed, the material selectively extracts metal ions in a series retaining those ions with high stability constants more than those with low stability constants.

Recently, patented polyamine-silica composite materials designed to remove transition metal ions from aqueous solutions have been developed at The University of Montana in collaboration with Purity Systems Inc.^{11, 12} The materials consisted of linear or branched water soluble chelating polyamines covalently bound to a silica gel support.

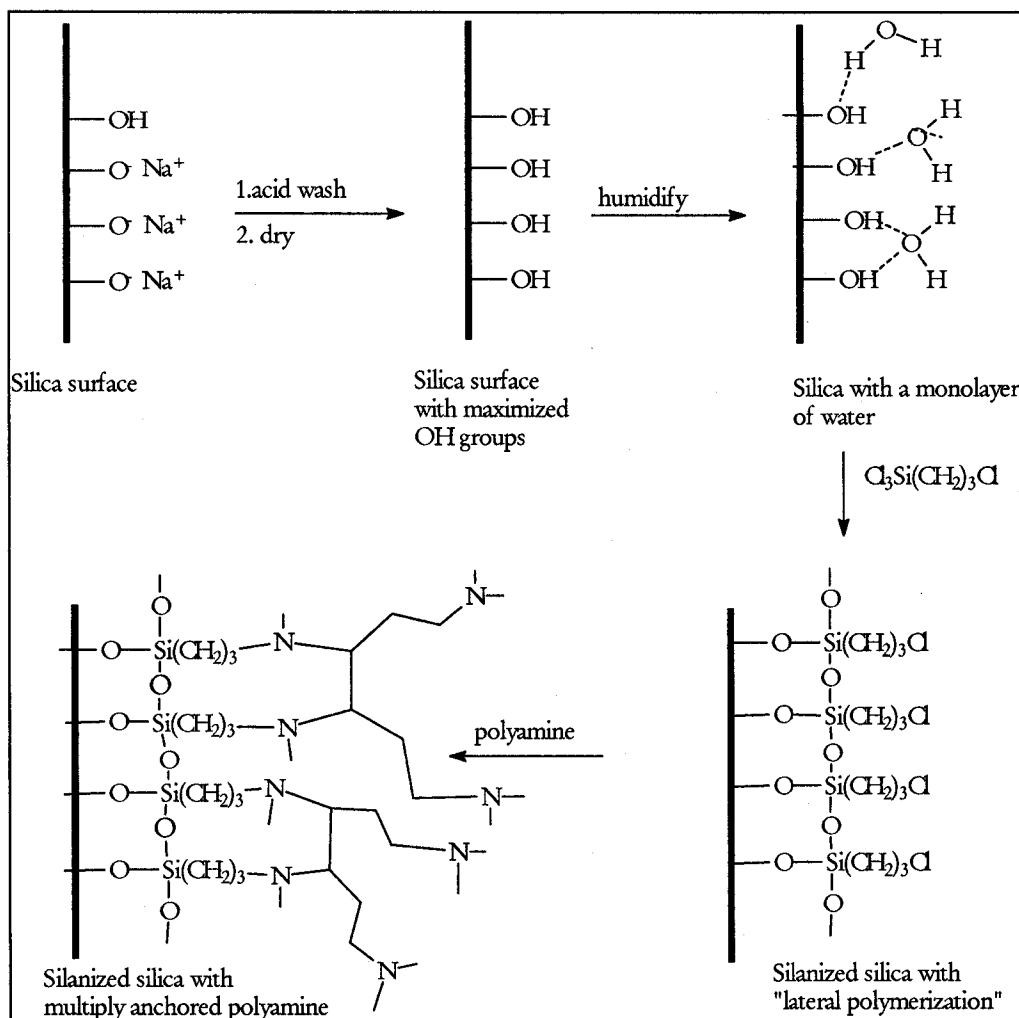


Figure 1.1 Synthetic scheme for making silica polyamine composites, illustrating the key features of humidification to promote “lateral polymerization,” for maximization of surface coverage.

For example, the material designated as WP-1 consists of poly(ethylene imine), M.W. 1,200 covalently bound to porous silica gel. Poly(ethylene imine) is a highly branched, water soluble amine polymer containing 1°, 2°, and 3° amino groups in a ratio of 0.35:0.35:0.30, respectively. The synthetic route (Figure 1.1), which yielded almost complete coverage of the silica gel with an organic coating, used a polymer where the chelating agent and was an integral part of the matrix coating. These are key factors in creating a material that has remarkable durability.

These resins have been tested through 3000 cycles with no visible loss of physical stability and less than 10% loss in capacity.^{12c} The copper capacity of the basic polyamine composites is in the range of 0.7-1.1 mmol/g, and depends on the polymer being used. To date we have tried three polyamines, poly(ethylene imine) (PEI), poly(vinyl amine) (PVA) and poly(allyl amine) (PAA) (Figure 1.2).

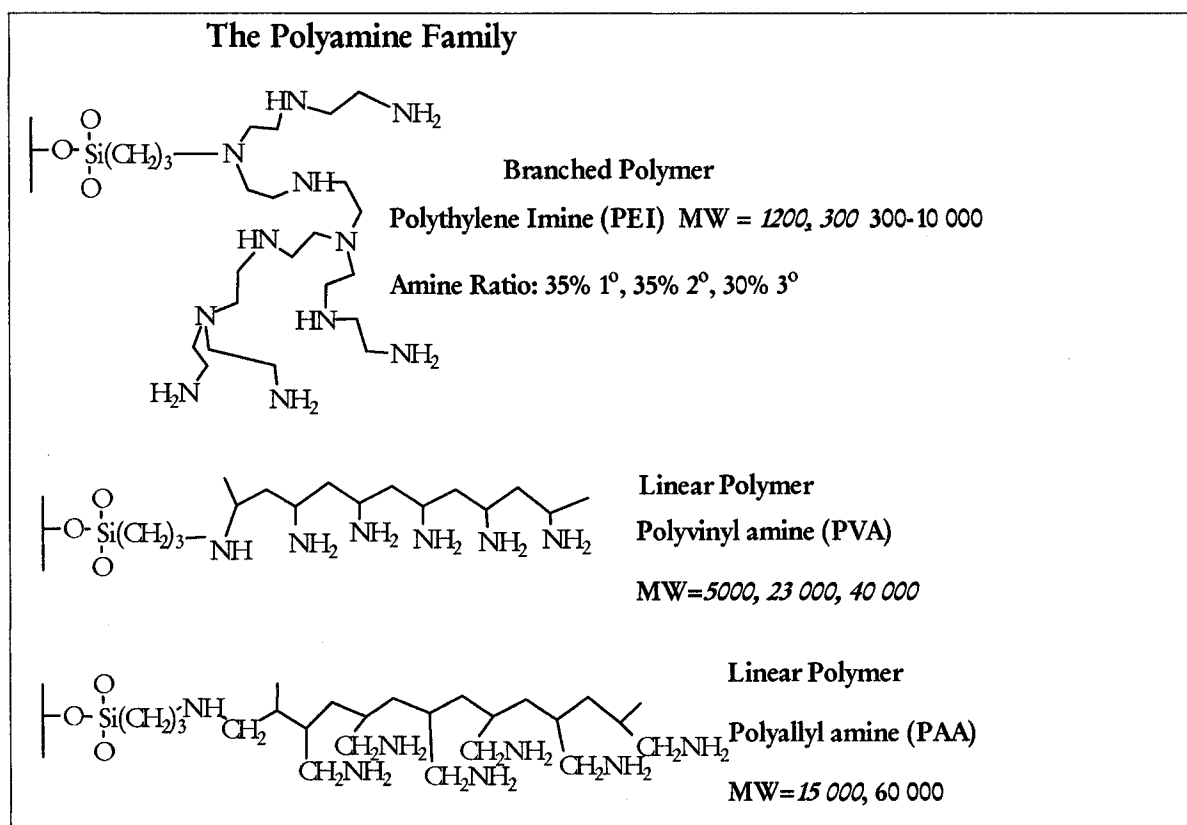


Figure 1.2. The polyamines used to synthesize the silica-polyamine composites, showing the schematic structure and the available molecular weights (only MW values in *italics* were used).

These polyamine composites can be readily modified to make them selective for a given metal or group of metals over a particular pH range, in similar ways to those used for polystyrene resins.^{12, 13} These materials offer distinct advantages over polystyrene resins (Table 1.1). These advantages have been demonstrated through studies that directly

compare the properties of the polyamine composites with commercially available polystyrene resins.^{12c, 13}

Table 1.1 Advantages of Purity Systems Inc Composite Resins Over Polystyrene Resins.

1. No shrink-swell in load-strip-regenerate cycles.
2. Faster capture kinetics allows use of shallower beds.
3. Available in four particle sizes: 200-165, 94-74, 74-38, and 38-22 mesh
4. Faster operational flow rates at higher capacities than conventional resins.
5. More porous structure gives lower pressure drops at comparable particle sizes.
6. Much longer usable lifetimes due to more rigid structure.
7. Shipped dry (<10% water) compared with 45-50% water for polystyrene
8. Higher maximum operating temperature (110 °C) compared with 70 °C for polystyrene
9. More stable to radiolytic decomposition.
10. Stable over a wide range of alkalinities and acidities.

1.2 Proposed Research

The primary goals of this thesis were to expand the base of application of the silica polyamine resin technology to the solution of environmental and industrial problems involving the removal and recovery of valuable and toxic metals from real industrial wastewater and mining solutions.

The particular projects that were addressed were the result of the contacts made with industry by the members of my committee, Dr. Corby Anderson and Professor Edward Rosenberg and by agents of the company that is the sole practitioner of the technology, Purity Systems Inc. (www.puritysystemsinc.com). The projects were very diverse and allowed me to develop skills in analytical chemistry, materials synthesis and analysis and metal removal process development. Below are the accounts of how these projects were brought to my attention and what the initial goals of each project were:

For chromium recovery work, U.S. Filter, a company specializing in water and

wastewater treatment, contacted Purity Systems Inc. through an east coast agent named Tony Metzner. The company was looking for methods to remove and recover chromium from electroplating and rinse solutions. Previous attempted technologies of styrene based ion exchange resins for removal of chromium to the required discharge level was never achieved. The project goal for removal and recovery of chromium from solution was to lower chromium concentrations to the required discharge level of 3 mg/L in both electroplating and rinse solutions using Purity Systems Inc. technology.

For cobalt recovery work, The Formation Capital Corporation Idaho Cobalt Project (www.formcap.com) currently hosts a potential 3 million ton cobalt-copper-gold ore body located in the central portion of eastern Idaho. The company was looking for potential technologies needed to successfully separate copper and cobalt from arsenic and iron using hydrometallurgical and other processes. This project was initiated by a committee member, Dr. Corby Anderson, Director for the Center for Advanced Mineral and Metallurgical Processes. The project goal was to use silica based technology to develop methods which could successfully remove, recover, and concentrate copper and cobalt from arsenic in leach solutions.

For gallium recovery work, Pasminco Inc. was looking for a technology to recover gallium and germanium from a solid waste product at a zinc electroplating refinery located in Clarksville, Tennessee. The company was looking for a technology that could recover and concentrate gallium and germanium from the leached solid waste product. An individual name Todd Fayram, Chief Mill Supervisor at the Gordonsville, Tennessee, contacted Dr. Corby Anderson looking for new innovative technologies which could be used for recovery of valuable metals. The project goal was to find a PSI technology

that could successfully and economically remove, recover, and concentrate gallium and germanium from the leached solid waste product. Secondly, a college design team from Montana Tech of the University of Montana was interested in developing a technology which could remove gallium and arsenic from a synthetic solution. The overall goal for the design team was to remove and recover the valuable gallium and to successfully lower arsenic concentrations to below required discharge levels of 10 ug/L.

For the selenium recovery work, Kennecott Mining, located in Magna, Utah, was interested in a technology that could successfully remove selenium from mine waste solutions. Jennifer Saran, a fellow Montana Tech graduate, contacted PSI for information on possible technologies for selenium removal. The overall goal was to find a technology that could successfully lower selenium in the presence of sulfate solutions to less than the required discharge levels of 50 ug/L.

For arsenic recovery work, MSE Technology Applications, located in Butte, Montana, was interested in finding new technologies capable of removing arsenic from a smelter process solution. Mr. Jay McCloskey, senior process engineer, contacted PSI for a possible technology to remove and recover arsenic from solution. The overall goal was to take a process solution and reduce arsenic levels to the required amount of 10 ug/L using PSI technology. Secondly, the Montana Tech of the University of Montana environmental design team was interested in developing a technology that could remove arsenic from a synthetic solution. The overall goal for the design team was to lower arsenic concentrations to below a required discharge level of 10 ug/L.

Chapter 2. Experimental Methods

2.1 General Need Section

For experimental work, all chemicals were purchased from Aldrich Chemical Company. Chemicals were 99% pure, unless otherwise stated, from manufacturer data sheets. For all infrared spectra produced, a Nicolet Nexus 870 Fourier Transform Infrared Spectrometer (FTIR) with Omnic E.S.P. software located in the Chemistry Department of the University of Montana was used for determination of organic materials and silica based products. For determination of metals and non metals from solution, a Thermo Electron Model IRIS Inductively Coupled Plasma (ICP) Spectrometer located in the Geology Department of the University of Montana was used. Standard deviation on the ICP using known standards is 10%. All samples were diluted to less than 100 mg/L using a 5% nitric acid solution. Elemental analysis was performed by the Schwarzkopf Microanalytical Laboratory Inc. located in Woodside, New York.

2.2 Infrared Spectra Experimental Procedure

Initially, materials were placed into a 100°C oven for 24 hours to remove any residual water in pores of the silica gel from the rinsing steps of the experimental procedure. Next, the gel surface area was increased by grinding with a ceramic mortar and pestle. Then, infrared samples were made using a 10:1 ratio of anhydrous potassium bromide to analyte and pressed into a thin pellet for analysis. A one minute scan on a Nicolet Nexus determined organic groups in silica products.

2.3 Syntheses of the Polyamine Composites

From Figure 1.1 in the introduction section, several experimental steps are required for making the silica based ion exchange resins into the final product for

industrial usage. These steps include acid washing, humidifying, silanization, and polymerization of the silica gel.

2.4 Acid Washing of Silica Gel

For formation of the silica based ion exchange resins, Crossfield or Hai Yong silica gel was used for the initial acid washing procedure. In a 3-neck 5-liter flask, 500 grams of Crossfield Huy Young silica gel were placed into the flask. Next, two liters of 1 molar nitric acid was placed into the flask. The slurry was mixed using a paddle stirrer and heated for six hours under reflux temperature of 95°C. The paddle mixer and heater were turned off and the solution was allowed to cool to room temperature. The mixture was placed into a Buchner funnel and the acid solution was then filtered off. To the wet silica gel, distilled water was placed over the gel and continuously added and vacuum suctioned until a neutral pH of the effluent solution was achieved. The gel was then air dried for 16 hours. Finally, the gel was placed into an oven at a temperature of 100°C and, the sample was weighed every hour until no gel weight loss occurred.

2.5 Humidification of Silica Gel

For the humidification process, 500 grams acid washed Crossfield Huy Young silica gel were placed into a sealed humidification apparatus, a 4-inch diameter, 24-inch length polyvinyl chloride (PVC) pipe sealed at both ends by a frit material and PVC end caps fittings, and barbed fittings for air passage. For this procedure, a compressed air hose was attached to hollowed glass tubing placed into a stopper of a 500-mL side arm flask filled with 400 mLs of distilled water. By allowing the air to flow over the top of

the distilled water, humidified air was created for the system. To the side arm flask, another compressed air hose was attached and then attached to the humidification apparatus. The humidified air was then allowed to bubble up through the dried silica gel. The entire apparatus is weighed at 6-hour intervals until a constant weight was measured. The apparatus was then weighed hourly to maintain the consistent weight. For the humidification procedure, the approximate weight gain for the silica gel was 10%.

2.6 Silinization of Silica Gel

For the silanization of Crossfield or HaiYong silica gel, 50 grams of humidified silica gel was placed into a 3-neck 500-milliter flask. To the flask, 100 milliliters of heptane were added to form a slurried solution. The slurry was mixed using a paddle stirrer. In a 200 mL flask, 100 mL of heptane was placed into solution. Next 26.8 mLs of chloropropyl trichloro silane (CPTCS) were placed into the 2-liter flask. The heptane-CPTCS mixture was slowly titrated, over a 30 minute time span, into the 3-neck 100-mL flask. After the titration was completed, the slurried solution was then vacuumed degassed for 30 minutes. The slurry was then allowed to mix for 24 hours.

After the reaction was completed, a series of rinses was performed on the silinized product. Initially, the heptane-CPTCS silica mixture was decanted to remove the unreacted CPCTS. Next, the wet silica gel was placed into a rotovap apparatus under vacuum pressure and heated to remove all the heptane and unreacted CPTCS until the silica gel was dry. Next, three 200 mLs of methanol was placed into a 3-neck 500-mL flask and the dry silica gel was added. The slurry was mixed for 30 minutes and then suction filtered using a Buchner funnel to remove all the ethanol. Two methanol rinses of 200 mL were added on top of the silica gel in the Buchner filter and suction filtered.

Next, three 200 mL volumes of distilled water was placed onto the funneled gel and allowed to suction dry. Next, three additional amounts of 200 mLs of methanol were placed through the suction filter and allowed to suction dry. The gel was then air dried for 48 hours. Finally, the gel was placed into a 100° C oven until a consistent weight was measured. The final weight after silanization step was 57.5 grams and the percent weight gain in 15%. Elemental analysis of silanized silica gel are shown in Table 2.1.

Table 2.1. Elemental Analysis of Silanized Silica Gel.

	% Carbon	% Hydrogen	% Chlorine
Silanized Gel	6.07	1.35	6.05

2.7 Polyethylene Imine Gel (PEI)

For formation of polyethylene imine(PEI) gel, 15 mLs of Nippon Shukubai polyethylene imine polymer (MW=1200), 15 mLs of distilled water, 10 mLs of methanol gel, and 10 grams of silanized gel were placed into a 3-neck 100-mL flask and mixed using a paddle stirrer. The solution mixture was then degassed using a vacuum line for 10 minutes. Next, the mixture was placed into an oil bath with a temperature of 70°C for 48 hours. The mixture was then allowed to come to room temperature for final rinsing.

For the final rinsing procedure, the remaining polymer was decanted from the silica gel. The wet gel was then vacuum filtered to remove any residual polymer in a small Buchner funnel. Next, three sets of 40 mLs of distilled water were placed onto the top of the gel and allowed to suction dry. After the water was suctioned through, 40 mLs of 1 molar sulfuric acid was suctioned through the gel followed by an additional three sets of 40 mLs of distilled water. Then, 40 mLs of 1 molar ammonium hydroxide were suctioned through the gel followed by an additional three sets of 40 mLs of distilled

water. Finally, 40 mLs of methanol were suctioned through the gel. The PEI gel was then allowed to air dry. Overall weight gain for this procedure was 20%. Elemental analysis and the infrared spectrum of PEI are shown in Table 2.2 and Figure 2.1.

Table 2.2 Elemental Analysis of Polyethylene Imine(PEI) gel.

	% Carbon	% Hydrogen	% Nitrogen
PEI Gel	11.22	2.26	4.77

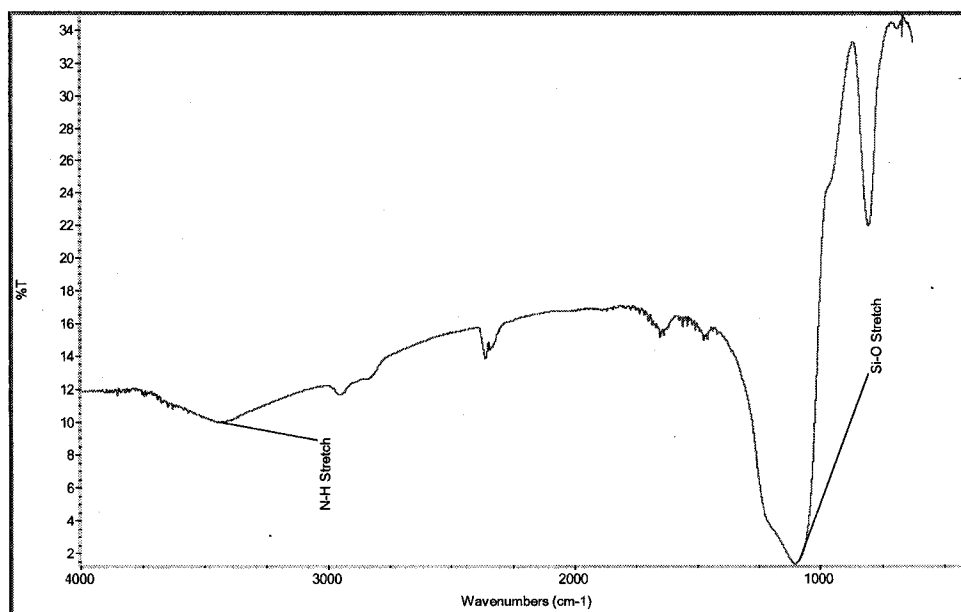


Figure 2.1 Infrared Spectrum of Polyethylene Imine (PEI) Gel.

2.8 Polyallyl Amine Gel (PAA)

For formation of polyallyl amine gel (PAA), 15 mLs of a 15% solution of Nitobo Chemical Tokyo polyallyl amine polymer (MW=15000), 15 mLs of distilled water, 10 mLs of methanol gel, and 10 grams of silanized gel were placed into a 3-neck 100-mL flask and mixed using a paddle stirrer. The solution mixture was then degassed using a vacuum line for 10 minutes. Next, the mixture was placed into an oil bath with a temperature of 70°C for 48 hours. The mixture was then allowed to come to room temperature for final rinsing.

For the final rinsing procedure, the remaining polymer was decanted from the silica gel. The wet gel was then vacuumed filtered in a small Buchner funnel to remove any residual polymer. Next, three sets of 40 mLs of distilled water were placed onto the top of the gel and allowed to suction through. After the water was suctioned through, 40 mLs of 1 molar sulfuric acid were suctioned through the gel followed by an additional three sets of 40 mLs of distilled water. Then, 40 mLs of 1 molar ammonium hydroxide were suctioned through the gel followed by an additional three sets of 40 mLs of distilled water. Finally, 40 mLs of methanol were suctioned through the gel. The PAA gel was then allowed to air dry. Overall weight gain for this procedure was 20%. Elemental analysis and the infrared spectrum of PAA are shown in Table 2.3 and Figure 2.2.

Table 2.3 Elemental Analysis of Polyallyl Amine(PAA) gel.

	% Carbon	% Hydrogen	% Nitrogen
PAA Gel	13.61	2.90	2.69

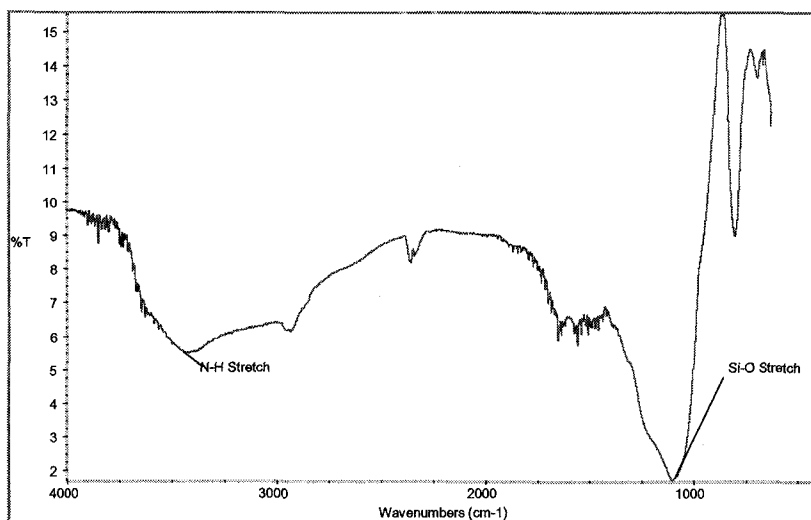


Figure 2.2 Infrared Spectra of Polyallyl Amine (PAA) Gel.

2.9 Chromium Simulated Solution Experimental Work

During initial experimental testing, 18 grams of WP-1 silica gel was placed into a 30-mL syringe column. The column was then initially rinsed with distilled water followed by 2 molar sulfuric acid rinse to clean any residual metals from the gel. Next, the column was regenerated by addition of 4 molar ammonium hydroxide through the column. The column was finally rinsed with ten bed volumes of distilled water. The flow rate for the system was kept constant for the initial testing procedures at two bed volumes per minute. The pH of the feed solution was adjusted to mimic both the rinse and electroplating solutions of incoming samples. For electroplating, the solution pH was adjusted to 3.5, while the pH of the rinse solution was adjusted to 5.5 for testing.

Each test procedure consisted of pumping 100 mL of 50 mM chromium(III) solution through the syringe column. Flow through was collected during each test. The columns were then stripped with sulfuric acid and solution was captured for analysis. Both flow

through and strips were then analyzed using the Ultraviolet-Visible (UV-VIS) spectrometer.

2.10 Chromium Electroplating Solution on WP-1

The initial testing of the electroplating was performed in a 5 mL syringe column with a testing volume of 100 mLs being used. Flow rate for the tests was 10 mLs/min or 2 bed volumes per minute. A breakthrough curve was performed by taking samples at 1, 2, 5, 10, 15, and 20 bed volumes.

2.11 Copper Removal with Cu-WRAM after pH adjustment

The pH of the test solution was increased to 1.8 by addition of granular sodium carbonate. The solution was pushed through a 5 mL column containing 3.83 grams of silica gel called Cu-WRAM (Figure 4.1). Testing flow rate for the system was 0.5 bed volumes per minute. The pressure leach solution was pumped through the column and collected for reloading the column. The column was then stripped using concentrated sulfuric acid followed by addition of distilled water.

2.12 Testing of Cu-WRAM with pH Adjustment using Sodium Hydroxide.

For the experimental work, a 5 mL column filled with 3.83 grams of Cu-WRAM silica gel was used for testing. Initially, 25 mLs of distilled water was passed through the column at a flow rate of 1 mL per minute. Next, 50 mLs of test solution was pushed through the column and flow through was captured. Rinsing of the column consisted of running an additional 25 mLs of distilled water through the column. The loaded Cu-WRAM column was then stripped and captured using a 5 mL solution of 2 molar sulfuric acid followed by 5 mL of distilled water. After stripping the column, an additional 25

mLs of distilled water was pushed through the column for the next flow through test. The loading and stripping process were completed four times for the experimental testing.

2.13 Pre-Filtered Testing Solution

The experimental procedure used two columns, one containing Cu-WRAM and the other containing either WP-1 or WP-2. Flow through, bottom to top, from the first column was directly fed into the column. During the stripping, the columns were selectively separated and stripped after loading by additions of the sulfuric acid. Column sizes for testing procedures were increased from 5 to 30 mLs containing 18 grams of Cu-WRAM, WP-1, and WP-2 in each separate column. Testing flow rate was decreased from 0.5 to 0.33 bed volumes per minute. The volume of solution used for each test was 0.2 liters.

2.14 Formation of Sodium 8-Hydroxyquinoline Salt

In a 100 mL flask, 43.55 grams (0.3 moles) of 8-hydroxyquinoline were placed into 200 mLs of methanol. To the solution, 0.3 moles of sodium hydroxide (in 30 mLs of distilled water) were added to the solution. The yellow precipitate was then filtered and separated from solution using a Buchner funnel. The filter cake was also rinsed with 100 mLs of methanol. After complete drying, the filter cake weighed 45.09 grams. Percent yield was calculated at 90%.

2.15 Fries Rearrangement

In a 500-mL round bottom 3-neck flask, 100 mLs of carbon disulfide were placed. 13.2 grams of anhydrous aluminum chloride were then placed into the solvent along with 16.7 grams of the sodium 8-hydroxyquinoline acetyl ester. The mixture vessel was then purged with nitrogen and sealed from the atmosphere. The reaction vessel was placed

into an oil bath and mixed for 24 hours at 85°C. After heating, the mixture was allowed to cool to room for sixty minutes. Next, 200 mLs of 6 molar hydrochloric acid were added to the vessel. An addition 200 mLs of distilled water were also added to dissolve the product salt. The solution mixture was placed into a separatory funnel overnight. Next, the aqueous phase was separated from the organic phase using the separatory funnel. To the aqueous phase, 50 mLs of a saturated solution of sodium by carbonate were added. Next 100 mLs of methylene chloride was placed into the solution. The methylene chloride layer was isolated using a separatory funnel and distilled off to yield the final product. Total recovered weight of the solid was 0.924 grams which represented a 7% recovery of the final product.

2.16 Thomas Fries Rearrangement Experimental Procedure

In a 500-mL round bottom 3-neck flask, 16.7 grams (0.1 moles) of 8-hydroxyquinoline were placed into 200 mLs of 1,2-dichloroethane. The vessel mixture was placed into a separate large container containing methanol and dry ice. A thermometer was placed into the solvent mixture and temperatures recorded. When the solvent temperature lowered to -35°C, 10 mLs of acetyl chloride and 13.2 grams of anhydrous aluminum chloride were placed into the flask. The solvent temperature was recorded before the system temperature was allowed to drop back to -35°C for sixty minutes. Next, the solution mixture was removed from the dry ice bath and allowed to come to room temperature for six hours. The solution mixture was then refluxed for 18 hours at 65°C. After refluxing, the solution was allowed to come to room temperature for sixty minutes. 100 mLs of 1 molar sodium hydroxide solution were placed into the mixing vessel and stirred for 30 minutes. The solution was placed into a separatory

funnel and the aqueous phase was separated and captured from the organic phase. To the aqueous phase, glacial acetic acid was added until a neutral pH of 7 was achieved. During this step, a solid yellow slurry formed. The slurry was then filtered using a Buchner filter funnel for 60 minutes. The filter cake was then rinse with 200 mLs of distilled water. The filter cake was then dried in an oven at 100°C for 16 hours. After the filter cake was completely dried, the sample was weighed for calculation of percent yield. The product yielded 12.5 grams and which represented a 73% recovery of the final product. Samples of the ester and final product were next analyzed by Infrared Spectrometry.

2.17 Thomas Product Silica Gel Synthesis Procedure

The anchoring procedure consisted of placing 10 grams of the 5-acetyl 8-hydroxyquinoline ligand into a 100-mL reaction vessel. Next, 50 mLs of dry methanol were added and the solution was stirred for 30 minutes to allow the ligand to dissolve. The silica gel was then placed into the vessel, heated, and refluxed in an oil bath at 80°C for 48 hours. After refluxing, the silica composite was then rinsed with 60 mLs of methanol followed by 20 mLs of 1 molar sulfuric acid, then 100 mLs of water, then 60 mLs of acetone. The sample was then dried overnight in an oven at 100°C.

2.18 Mannich Reaction Procedure (BPOX and WPOX)

The procedure to place 8-hydroxy quinoline onto the silica matrix was relatively simple. Initially, a solution of 250 mLs of formaldehyde and 25 mLs acetic acid were placed into a 3 liter vessel and mixed. Next, the silica gel matrix, 250 grams of BP-1 or WP-1, was placed into the mixing chamber and allowed to react for 4 hours. The gel was

then thoroughly rinsed with methanol. Suction filtration was done on the gel using a Buchner funnel to remove the excess methanol. It should be noted the color of the gel changed from white to a light yellow color indicating a chemical reaction occurred. Next, 1000 mLs of methanol were added to the solution along with the 250 grams of 8-hydroxy quinoline. The pH of the solution was adjusted to pH 9 with base with either 4 molar ammonium hydroxide or concentrated tetramethyl ammonium hydroxide. The mixture was stirred and allowed to reflux for 16 hours. The mixture was thoroughly rinsed with 1000 mLs methanol, 1000 mLs of 1 molar ammonium hydroxide, 3000 mLs of distilled water, 1000 mLs of 1 molar acetic acid, 3000 mLs of distilled water, and 250 mLs of acetone. Finally, the gel was dried overnight for 16 hours. Elemental analysis and the infrared spectra of BPOX and WPOX are shown in Table 2.4 and Figures 2.3 and 2.4.

Table 2.4 Elemental Analysis of BPOX and WPOX.

	% Carbon	% Hydrogen	% Chlorine
BPOX	18.73	4.13	3.42
WPOX	25.95	3.23	4.02

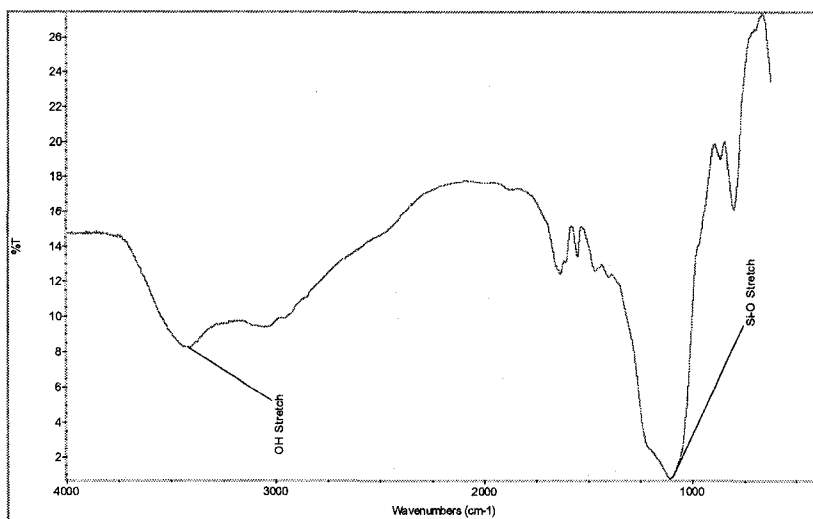


Figure 2.3. Infrared Spectrum of WPOX Silica Gel.

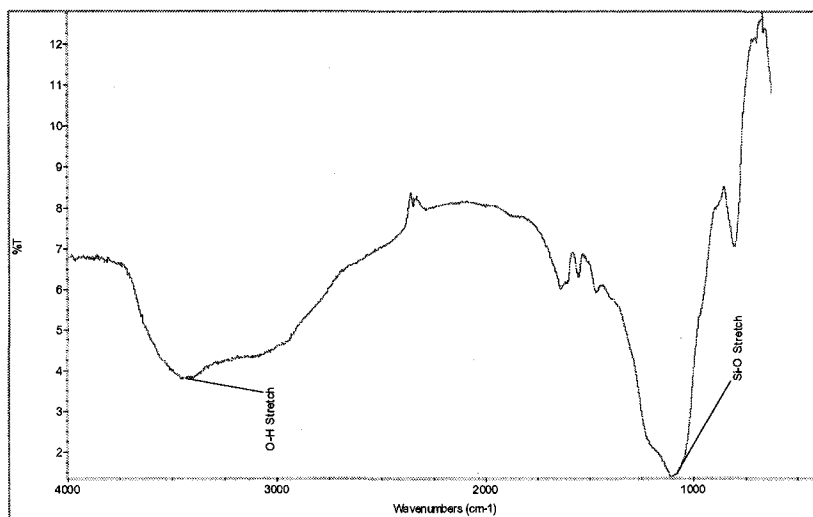


Figure 2.4. Infrared Spectrum of BPOX Silica Gel.

2.19 Tethered Experimental Procedure

Initially, 10 grams of BP-1, 15 grams of bromoethylamine, and 100 mLs of methanol were placed into a 500-mL round bottom vessel. The mixture was placed into an oil bath, heated, and refluxed for 24 hours at 65°C. The mixture was then allowed to

cool down for 60 minutes and rinsed using a Buchner funnel with 100 mLs of methanol, 300 mLs of distilled water, 100 mLs of 1 molar sulfuric acid, 300 mLs of distilled water, 100 mLs of 1 molar ammonium hydroxide, 300 mLs of distilled water, and 100 mLs of methanol. The gel was then dried overnight.

2.20 Tethered BPOX Procedure

Initially, a solution of 50 mL of formaldehyde and 5 mLs acetic acid was placed into a 250-mL vessel and mixed. Next 10 grams of modified BP-1 was placed into the mixing chamber and allowed to react for 4 hours. The gel was then thoroughly rinsed with methanol. Suction filtration was done on the gel using a Buchner funnel to remove the excess methanol. It should be noted the color of the gel changed from white to a light yellow color indicating a chemical reaction. Next, 100 mLs of methanol was added to the solution along with the 10 grams of 8-hydroxyquinoline. The pH of the solution was then adjusted to pH 9 with base with either 4 molar ammonium hydroxide or concentrated tetramethyl ammonium hydroxide. The mixture is stirred and allowed to reflux for 16 hours. The mixture was then thoroughly rinsed with 100 mLs methanol, 100 mLs of 1 molar ammonium hydroxide, 300 mLs of distilled water, 100 mLs of 1 molar acetic acid, 300 mLs of distilled water, and 25 mLs of acetone. Finally, the gel was dried overnight for 16 hours. Elemental analysis of tethered BPOX, with comparison to BPOX, are shown in Table 2.5.

Table 2.5 Elemental Analysis of BPOX and Tethered BPOX.

	% Carbon	% Hydrogen	% Chlorine
BPOX	18.73	4.13	3.42
Tethered BPOX	25.28	3.77	4.22

2.21 Experimental Testing of WPOX and BPOX for Gallium Recoveries

During the experimental testing, 18.6 grams of the resin was placed into the columns and recorded for capacity calculation of each tested resin. The flow rate used for all tests was 0.2 bed volumes per minutes. Samples were taken every bed volume and analyzed using ICP. After loading the columns, two bed volumes of water were passed through the column to remove any residual test solution. Finally, the columns were stripped and collected using 25 mLs of 4 molar sulfuric acid.

2.22 Zirconium(IV) Loading Procedure on WP-2.

Initially, 25 grams of WP-2 were added to 500-mL round bottom flask. Next, 125 mLs of 2 molar hydrochloric acid (HCl) were added to the reaction vessel. Finally, 25 grams of zirconium oxychloride ($ZrOCl_2$) were added and the mixture was stirred for 16 hours. The final mixture solution was then vacuum filtered using a Buchner filter while 300 mLs of distilled water were placed into the funnel for final rinsing. When the pH of the rinsing solution effluent reached 4, an additional 100 mLs of distilled water was filtered through the silica resin for final rinsing. The gel was then placed into an oven at 40°C for 24 hours and allowed to dry.

2.23 WPAN Flow Testing Procedures

For loading the column with either arsenic or selenium, all experimental procedures were performed with 18 grams of WPAN placed into a 30-mL syringe column. Initially, 100 mLs of distilled water were pumped through the column at a flow rate of 5 mLs per minute. Next, the arsenic or selenium solution was adjusted to pH 4 with 1 molar sulfuric acid. The adjusted solution was then pump through the syringe column at 5 mLs per minute and 20 mLs flow through samples were taken. After the solution was pumped through the column, an additional 100 mLs of distilled water were

pumped through the column to remove any residual testing solution from the column.

The stripping procedure consisted of using pH 4 adjusted 100 grams per liter phosphate solution. During stripping, 30 mLs of phosphate solution were pumped through the column followed by 200 mLs of distilled water. Samples of 20 mLs were collected. Next, 30 mLs of 4 molar sulfuric acid were placed into the column followed by 200 mLs of distilled water. Additional distilled water was passed through the column until pH 4 was achieved for regeneration of the column. All collected samples were measured by ICP.

2.24 WPAN Batch Testing Procedures

For batch testing, 0.3 grams of WPAN were placed into a 25-mLs sample vial. Next, 20 mLs of either arsenic or selenium pH 4 solution was placed into the vial. Each batch testing sample set was done in triplicate. The samples were then placed onto a shaker table for 24 hours. Next, the samples were allowed to settle for an hour after removal from the shaker table. The samples were then filtered using 0.2-micron syringe filter and analyzed on ICP for metals of interest.

2.25 Experimental Error Determination

For determination of experimental error, standard deviations were used in cases where duplicate experimental tests were conducted. For both duplicate and triplicate testing, the average of the standard deviations was used for error bars within the graphs. For tests where no duplicate tests were conducted, standard deviation was not used.

Chapter 3. Chromium Recovery Using PSI Technology

3.1 Preliminary Work of Chromium Recovery and Removal from Plating Solutions.

U.S. Filter, a company with several divisions located throughout the United States and specializing in water and wastewater treatment systems for industrial and municipal communities, contacted Purity Systems Inc. through an east coast agent named Tony Metzner located in New York. They were interested in methods for removing chromium contaminants from their customer's electroplating waste solutions. Chromium is now placed into solution using a new process which uses the less toxic form of chromium. Currently, U.S. Filter uses ion exchange resins for remediation and recovery of free chromium within the solutions, however, using this technology, the required chromium discharge level of less than 3 mg/L is never achieved. Due to this, U.S. Filter sent test solutions to evaluate PSI silica technology for chromium remediation and removal.

3.2 Chromium Simulated Solution Experimental Work

Initial testing of PSI technology consisted of using the polyethylene imine (PEI) silica gel called WP-1 which successfully captures the metals in solution (Figure 1.2) Testing of WP-1 consisted of using 50 millimolar(mM) synthetic chromium solutions made from reagent grade chromium(III) chloride hexahydrate($\text{CrCl}_3 \cdot 6\text{H}_2\text{O}$). The initial testing of plating solutions was conducted in the Chemistry Department at The University of Montana. Results from synthetic solutions testing are shown in Table 3.1.

Table 3.1 Synthetic Solution Results.

Silica Gel Composite	Synthetic Test Solution	Flow Through Capacity (mM/g)	Capacity g/l Cr⁺³ Density=0.6g/L
WP-1	Electroplating pH=3.5	0.41	13.8
WP-1	Rinse pH = 5.5	0.43	14.5

The results from Table 3.1 indicate WP-1 silica gel has the same capacity, approximately 0.41 mM/g for both electroplating and rinse solutions.

3.3 Chromium Remediation on U.S. Filter Solutions

Electroplating and rinse wastewater solutions were received from U.S. Filter. The overall goal was to successfully remove chromium in the waste streams to a discharge level less than 3 mg/L. Initial pH values and chromium concentrations of the solutions were measured using a pH meter and an inductively coupled plasma (ICP) spectrometer. The rinse solution contained 19.56 mg/L total chromium at pH of 6.0 while the electroplating solution contained 162.4 mg/L total chromium at pH of 4.0.

3.4 Chromium Electroplating Solution on WP-1

Large sized (500-1000 micron) WP-1 silica gel particles were used for chromium testing removal because this particle size was requested by U.S. Filter.

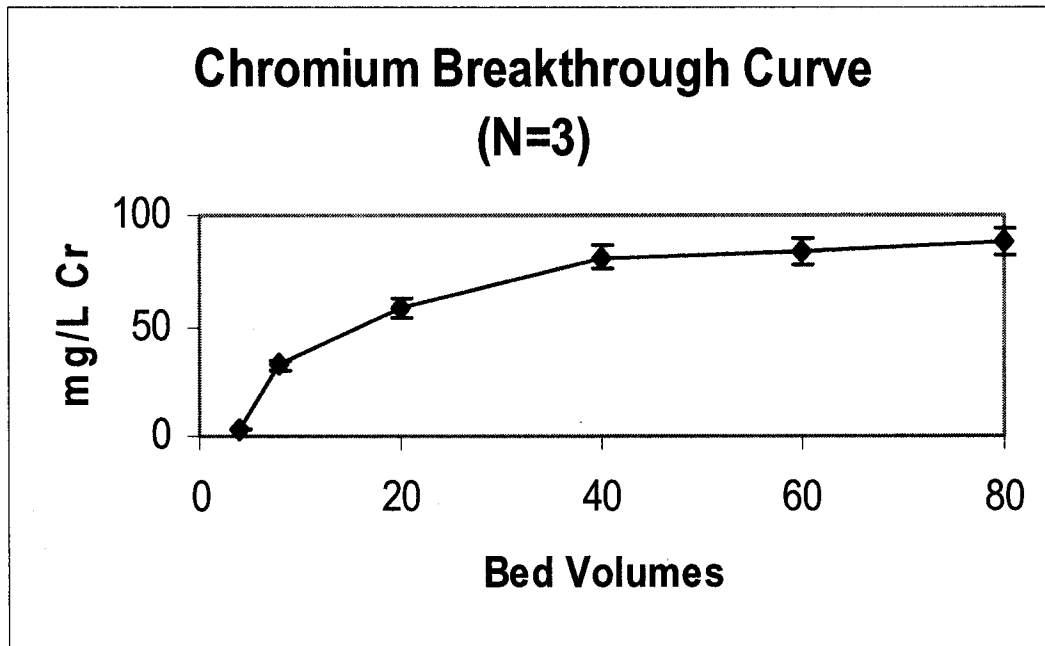


Figure 3.1 Chromium (III) Electroplating Breakthrough Curve.

Figure 3.1 indicates immediate breakthrough of chromium using WP-1 gel for electroplating solution. After the initial bed volume, chromium concentration was measured at 3.15 mg/L. As further measurements were taken, discharge levels increase dramatically.

The poor results could be kinetic rather than a chemical problem. Previous silica gel studies indicate slower flow rates produce better results. The next step was to slow down the flow rate from 2.0 to 0.5 bed volumes per minute. At a lower flow rate, samples were taken every bed volume up to 11 then at 15 and 20. A breakthrough curve is shown in Figure 3.2.

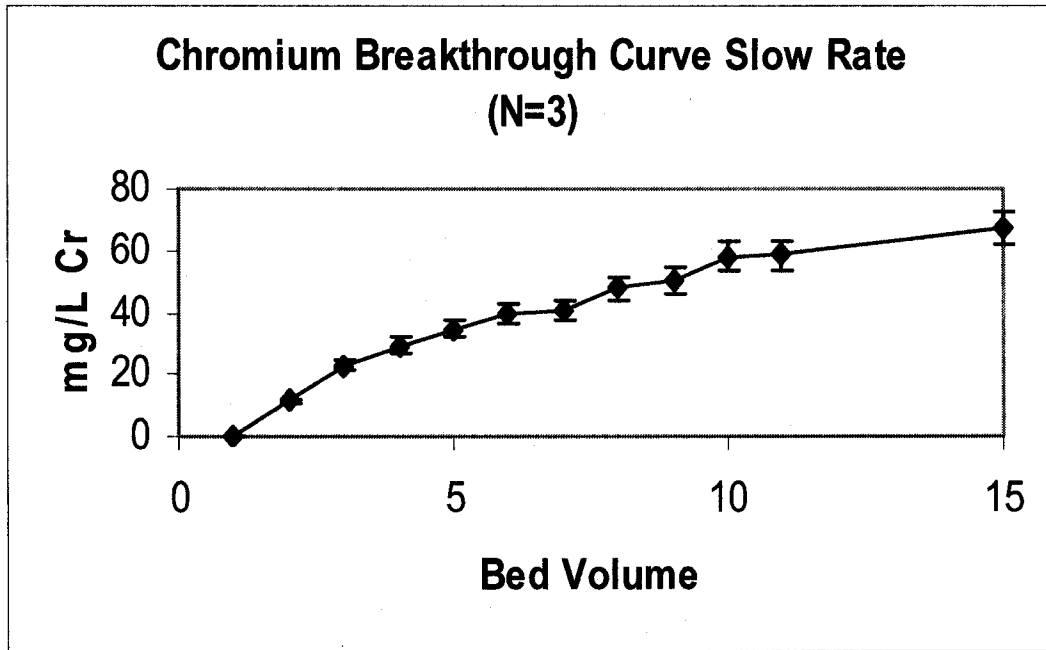
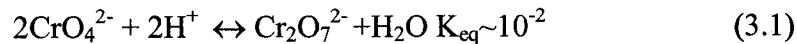


Figure 3.2 Chromium (III) Electroplating Breakthrough Curve (Slower Flow Rate).

Figure 3.2 shows better results using a slower flow rate, however, discharge chromium levels were above the requested level of 3 mg/L after 2 bed volumes. According to the data, WP-1 was somewhat effective for removal of chromium in the system, however, requested discharge levels were never achieved. There are two possible explanations for this event. First, the system may contain two valences of chromium. Some of the chromium in the system may have oxidized from chromium(III) to chromium(VI). WP-1 would not be selective for hexavalent chromium because it exists as the anions, CrO_4^{2-} or $\text{Cr}_2\text{O}_7^{2-}$ (depending on pH) from the following equation and WP-1 captures only cations.



Secondly, the chromium plating industry used organic acids as plating modifiers along with chromium(III) salts. These chemicals are required for complexation of

chromium(III) in solutions in order to control the rate of the electroplating process. The complexing agents may be competing with WP-1. Because of the possibility of complexing agents, the next step was to pretreat the solution using activated carbon which would remove the complexing agents and also any hexavalent chromium anions¹⁵.

Further laboratory studies were performed on a larger scale 220-mL column. Approximately 8 liters of electroplating solution was initially pretreated by passing the solution through a column of activated carbon and rinsed with distilled water. The solution was then collected in a clean container. The flow rate of the system was kept constant at 0.33 bed-volumes per minute. A chromium composite sample was taken before and after the pretreatment step and analyzed on the ICP. Initial measured chromium concentration was 162.4 mg/L before pretreatment and 73.02 mg/L after passing through the carbon column indicating that the carbon removed significant amount of chromium.

The solution was then passed through a large column of 500 to 1000-micron sized WP-1 silica gel. Samples were taken every bed volume and analyzed on the ICP for chromium. The results are shown in Figure 3.3.

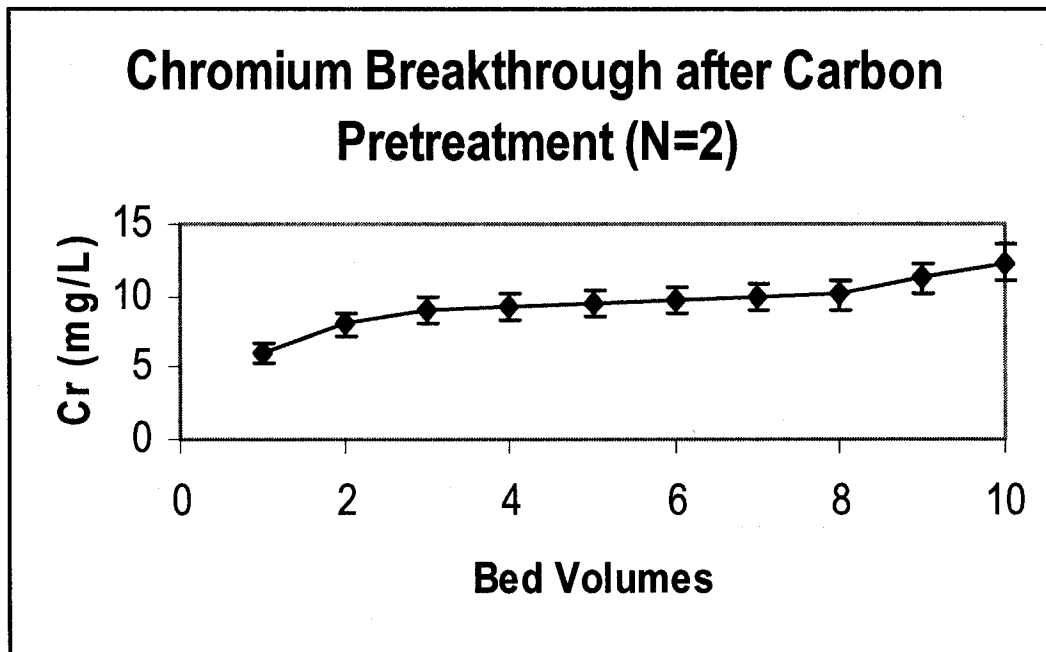


Figure 3.3 Electroplating Breakthrough after Carbon Pretreatment.

Figure 3.3 results show better removal of chromium from the wastewater after pretreatment with activated carbon, however, required discharge levels were never achieved. U.S. Filter then recommended using an activated carbon specifically designed for organic acid removal.

The new activated carbon was received and a second pre-treating column was made using the U.S Filter carbon. Electroplating stock solution was passed through the new carbon column, collected, and analyzed for chromium. Results from carbon pretreatment indicate a decrease from 162.40 to 11.56 mg/L chromium. WP-1 silica gel was used again for secondary treatment of the electroplating solution. Samples were collected and analyzed at 1, 2, 3, 4, 5, 10, 15, 20, and 25 bed volumes. Results can be seen in Figure 3.4.

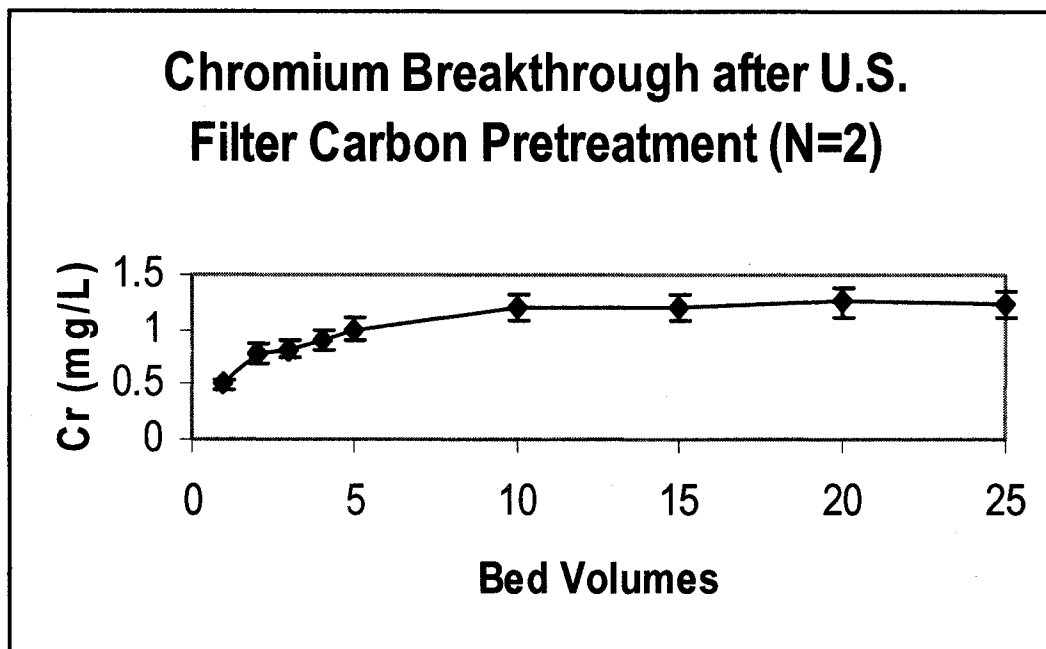


Figure 3.4 Electroplating Breakthrough with U.S. Filter Carbon Pretreatment.

Figure 3.4 results show excellent removal of chromium from electroplating solutions. Even after 25 bed-volumes, the required discharge level of 3 mg/L was achieved. Using a combination of activated carbon and WP-1 is an excellent way to remediate this system.

Chromium(III) was stripped from the WP-1 silica gel with one bed volume of 15% hydrochloric acid (HCl) at 70 °C. The strip concentration was measure at 221 ± 0.22 mg/L representing a concentration factor of 19 from the feed solution. The factor would be much higher if larger amounts of solution were added until breakthrough occurred.

3.5 Testing of Chromium Rinse Solution on WP-1

WP-1 was also tested for chromium removal in the rinse solution. Tests were performed in the larger 220 mL column. Other parameters, such as flow rate, gel size,

and gel volume, were kept the same as in previous studies. Prior to testing the rinse water, an initial chromium concentration was measured on the ICP at 19.56 mg/L. However, while testing the electroplating solution, some of the chromium precipitated and the dissolved concentration of chromium dropped to 12.18 mg/L. Ten liters of chromium rinse solution was run through the WP-1 column. Samples were taken and measured at 1, 2, 3, 4, 5, 6, 20, 35, and 50 bed volumes. Results can be seen in Figure 3.5.

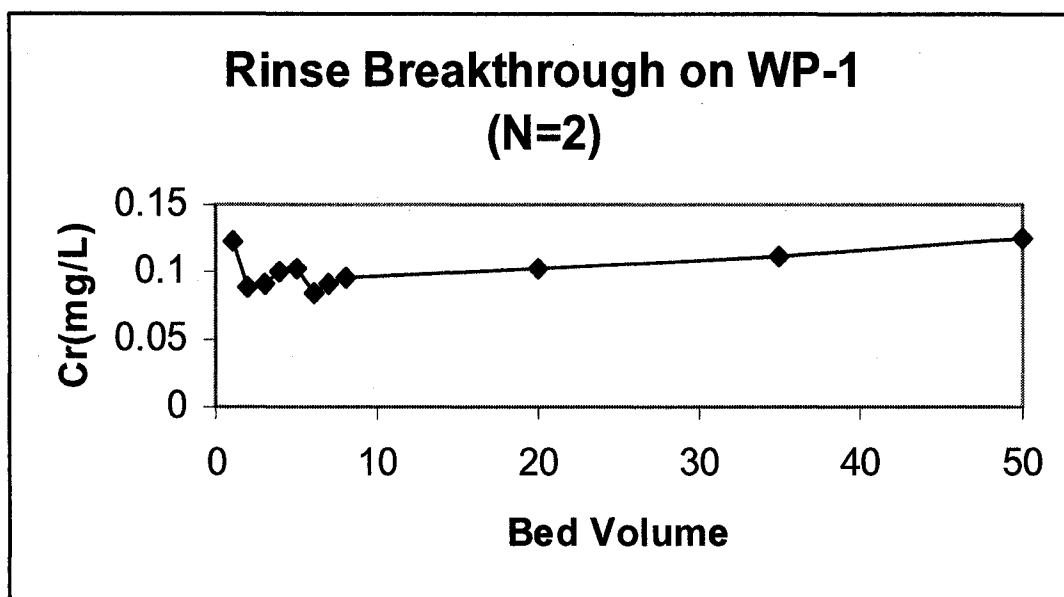


Figure 3.5 Chromium Rinse Breakthrough on WP-1.

Figure 3.5 indicates excellent results for removal of chromium from the rinse solution using WP-1. Compared to the electroplating solution, pretreatment with activated carbon was not required to remove organic acid modifiers, hexavalent chromium and some Cr(III) from solution using WP-1. After 50 bed-volumes, the treated rinse solution was well below required discharge levels of 3 mg/L.

The silica gel was then stripped with 15% HCl at 70 °C. The chromium

concentration in the strip was 576 mg/L yielding a concentration factor of 45 with respect to feed. As before, this factor would be much higher if the column was loaded to breakthrough. Mass balance analyses show a 99.1% recovery of chromium from the system.

3.6 Conclusions

Several conclusions can be drawn from the studies on chromium removal done for the electroplating solution and rinse solutions. WP-1 resin was unable to remove chromium to required discharge levels without pre-treating the solution with activated carbon. After pretreatment, the PSI technology was able to successfully remove chromium below discharge levels in 25 bed-volumes of solution. For the chromium rinse solution, the carbon pretreatment for chromium removal was not required to successfully remove the contaminant from solution. Two possible explanations could have accounted for the poor performance of the non carbon treated electroplating solution. Higher concentrations along with the presence of organic acids which compete for complexation of chromium and hexavalent chromium anions which are not captured by WP-1 accounts for the elevated required discharge levels observed in the initial tests with WP-1. Addition of a carbon pre-treatment step greatly enhanced the performance of WP-1 resin and brought the chromium discharge levels to below the required 3 mg/L by absorbing the chromium (VI) anions and the organic acids. The rinse solution did not contain these other species, therefore, the pretreatment was not needed and WP-1 performed quite well at the higher pH of this solution and lower chromium(III) levels. Finally, during stripping of the silica resin, using warm acid to strip the chromium from the resin greatly enhances the chromium concentration of the stripped solution so that the resulting strip was

sufficiently concentrated for recycling the chromium. However, the use of warm 15% HCl is not an ideal stripping method since this requires special steel for plant construction and the presence of chloride is undesirable in most electroplating systems. An alternative would be to precipitate the recovered chromium as Cr_2O_3 for reuse.

Chapter 4. Separation of Cobalt from Copper and Arsenic from a Cobalite Ore Leach

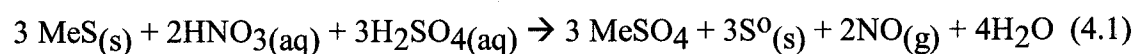
4.1 Introduction

Hydrometallurgical treatment of concentrates, ores and materials is a growing global technology. Habashi¹⁵ reports that nitric acid has been used for over 50 years in the uranium industry and in phosphate fertilizer manufacture. Its application in the treatment of sulfide concentrates is relatively recent.

The use of nitric acid in sulfide oxidation is not new, however, only the nitrogen species catalyzed (i.e., NSC) sulfuric acid oxidative pressure leach has ever been built and operated successfully on a long term industrial scale¹⁶. Moreover, it has been thoroughly studied and it has found successful application in oxidation of other feedstocks as well¹⁷. It offers several definitive advantages. First of all, it is the only proven industrial process over the long term for pressure leaching of copper sulfides and direct recovery of precious metals without the use of cyanide. Second, the rate of reaction is much faster and subsequent required reactor volume is thus smaller. Third, the process does not require excessively high temperatures or pressures.

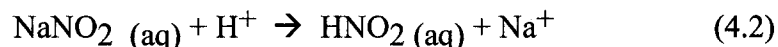
4.2 NSC Pressure Leaching Fundamentals

The commonly reported leach reaction of a sulfide mineral with nitric acid in conjunction with sulfuric acid is shown below.



However, it is postulated that the actual reaction species¹⁸ is NO^+ and not NO_3^- . The addition of or presence of NO_2^- instead of NO_3^- accelerates the formation of

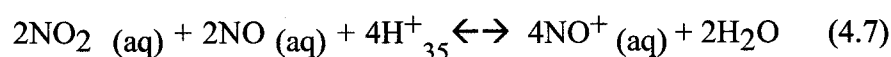
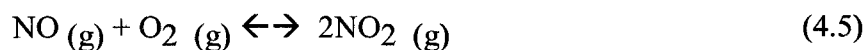
NO⁺. As shown in Table 4.1, the NO⁺/NO couple is capable of an extremely high redox potential¹⁹. So, NO⁺ is readily formed from nitrous rather than nitric acid. For example, a convenient source of nitrous acid can be sodium nitrite²⁰. When it is added to an acidic solution, nitrous acid is readily formed.



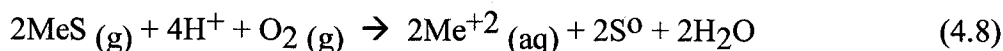
Nitrous acid further reacts to form NO⁺.

E_h^0 Oxidant	Redox Equation	(pH = 0, H ₂ ref.)
Fe ⁺³	Fe ⁺³ + e ⁻ → Fe ⁺²	0.770 V
HNO ₃	NO ₃ ⁻ + 4H ⁺ + 3e ⁻ → NO + 2H ₂ O	0.957 V
HNO ₂	NO ₂ ⁻ + 2H ⁺ + e ⁻ → NO + H ₂ O	1.202 V
O ₂ (g)	O ₂ + 4H ⁺ + 4e ⁻ → 2H ₂ O	1.230 V
Cl ₂ (g)	Cl ₂ (g) + 2e ⁻ → 2 Cl ⁻	1.358 V
NO ⁺	NO ⁺ + e ⁻ → NO	1.450 V

As are shown, nitric oxide gas, NO, was produced from the oxidation of sulfides. Since this gas had a limited solubility in aqueous phases, it tends to transfer out of solution. In the pressure leach system, a closed vessel with an oxygen overpressure was used. The nitric oxide gas emanating from the leach slurry accumulates in the headspace of the reactor where it reacted with the supplied oxygen to form nitrogen dioxide gas. The NO was then regenerated to NO⁺. Overall this can be viewed as:



Since the nitrogen species was continuously regenerated, its role in the overall reaction as the actual oxidizer was not obvious. The net overall reaction has the sulfide mineral reacting with the acid solution and oxygen to solubilize the metal value into the sulfate solution and form some elemental sulfur. Of course, at higher temperatures and/or nitrous acid concentrations, the sulfide would be fully oxidized to sulfate.



Overall, the nitrogen intermediates served as an expedient means to transport oxygen to the surface of the solid particle and allow the resulting reaction to take place at a heightened redox potential. This inherent asset of the unique system precludes the use of high temperatures and high pressures, which lead to higher costs in other pressure leach processes.

4.3 Partial Nitrogen Species Catalyzed Pressure Oxidation of a Cobaltite Chalcopyrite Concentrate.

The NSC pressure leach technology was used to treat a gold-bearing chalcopyrite and cobaltite concentrate. NSC concentrate leach testing was conducted at Montana Tech, in Butte, Montana, by Corby Anderson for a proposed mine in Idaho. The results were as follows.

Table 4.1. NSC Leach Results

Cobalt (mg/L)	Copper (mg/L)	Iron (mg/L)	Arsenic (mg/L)
12,430	5,223	18,940	3,150

As shown in Table 4.1, the solution contained significant amounts of cobalt, copper, iron, and arsenic. Attempts to separate the components of the solution were conducted at The University of Montana Chemistry Department. The overall goal for this

application of PSI technology was twofold. Our first goal was to separate and concentrate copper from the leach solution at low pH ranges (0 to 2.5). The second goal was to selectively remove cobalt from arsenic in the leach solution using PSI technologies.

4.4 Copper Removal with Cu-WRAM after pH adjustment

After receiving the pressure leach solution, pH was determined to be 0.02.

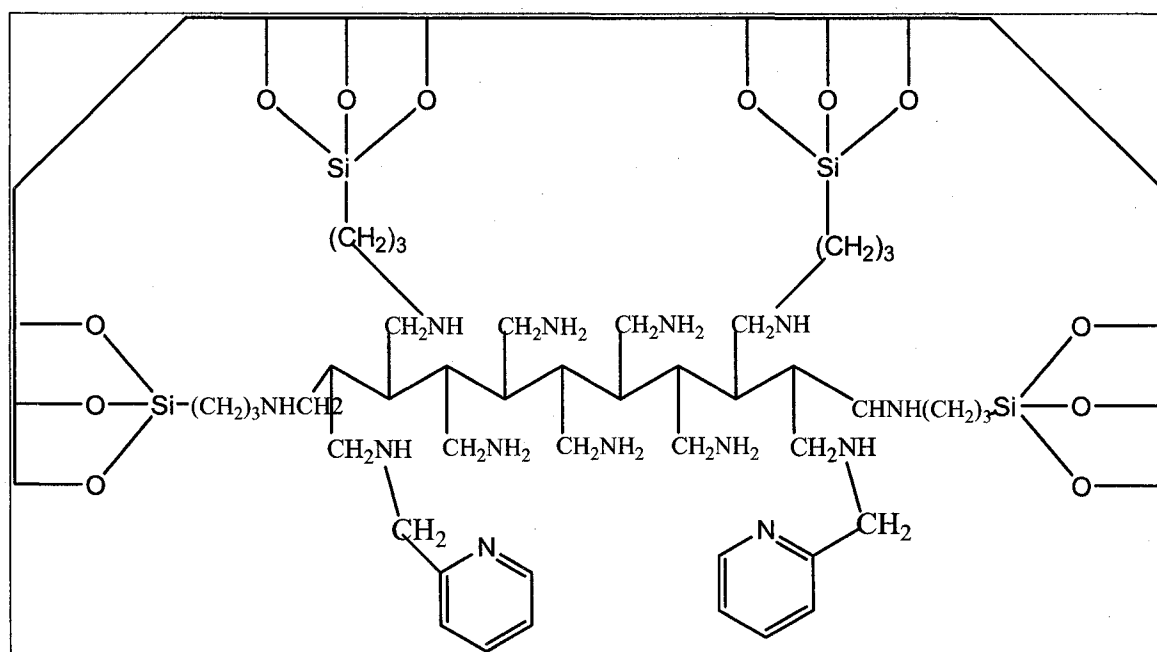


Figure 4.1. Structure of Cu-WRAM Silica Gel

Cu-WRAM gel²¹ (Figure 4.1) was used because it had a high affinity for copper as well as a high rejection rate for ferric ions in acidic conditions. Both flow through and strip samples were collected for metal concentrations on the ICP. After column stripping, it was regeneration with distilled water. This process was repeated several times. Initial test and flow through results can be observed in Table 4.2.

Table 4.2. Initial ICP Results with Cu-WRAM.

	Cobalt (mg/L)	Copper (mg/L)	Iron (mg/L)	Arsenic (mg/L)
Head	12,430	5,223	18,940	3,150
Flow Through	Cobalt (mg/L)	Copper (mg/L)	Iron (mg/L)	Arsenic (mg/L)
1	10,540	3,050	14,840	2,712
2	8,805	784	13,310	2,299
3	7,452	1.92	7,363	2,040
4	6,737	0.00	5,481	1,820
5	4,987	0.00	2,703	1,483

Table 4.2 results show excellent loading of copper onto the silica resin, however, some metals, especially iron and arsenic were also bound on the resin. Cobalt had little affinity to Cu-WRAM at this pH range. Strip results are shown in Table 4.3.

Table 4.3. Strip Results with Cu-WRAM.

Strip	Cobalt (mg/L)	Copper (mg/L)	Iron (mg/L)	Arsenic (mg/L)
1	144.2	2,496	2,601	298.1
2	179.1	2,238	2,365	302.2
3	1,627	958.7	3,185	617.7
4	1,165	65.31	2,008	518.4
5	963	9.27	1,225	484.6

The results in Table 4.3 indicate poor separation of copper from iron in the test solutions. Previous studies show Cu-WRAM to be excellent in removing copper from iron in solutions. The next testing step was to use a liquid solution of sodium hydroxide instead of granular sodium carbonate for pH control of the system.

4.5 Testing of Cu-WRAM with pH Adjustment using Sodium Hydroxide.

After previous poor results, the next idea was to raise the pH of the solution with eight molar sodium hydroxide solution instead of granular sodium carbonate. By switching pH reagents, we hope to effect the precipitation of ferric hydroxide with adsorption of arsenic from the solution and reduce the amount of precipitated particles in

the solution. Both flow through and strip samples were run for cobalt, copper, iron, and arsenic on the ICP instrument. Results are shown in Tables 4.4 and 4.5.

Table 4.4. Flowthrough Solutions with Liquid Sodium Hydroxide.

	Cobalt (mg/L)	Copper (mg/L)	Iron (mg/L)	Arsenic (mg/L)
Head	10,090	4,537	15,900	13,630
Flow Through	Cobalt (mg/L)	Copper (mg/L)	Iron (mg/L)	Arsenic (mg/L)
1	6,992	1,651	9,451	8,061
2	5,475	119.2	6,772	5,377
3	4,352	0.07	4,517	3,626
4	1,748	0.00	1,052	728

Table 4.5. Strip Solutions with Liquid Sodium Hydroxide.

Strip	Cobalt (mg/L)	Copper (mg/L)	Iron (mg/L)	Arsenic (mg/L)
1	22.96	1,435	1,801	1,927
2	12.32	1,071	472.3	496
3	10.55	235.5	848.8	927.8
4	369.2	0.085	573.6	453

Tables 4.4 and 4.5 show the same results as the previous experimental study. Cu-WRAM was able to successfully remove copper from solution, however, large amounts of both iron and arsenic were present in the strips despite earlier studies showing high selectivity of copper using Cu-WRAM. Using either granular sodium carbonate or liquid sodium hydroxide solution had little effect on copper iron separation.

4.6 Testing of Cu-WRAM at pH=1.0

The next testing step involved adjusting the pH of the solution to 1.0 instead of 1.8 with sodium hydroxide. By testing at a lower pH, we hoped precipitation of ferric hydroxide would not occur and a pure copper strip could be obtained at this pH range. Conditions remained the same as previous tests. Results are shown in Tables 4.6 and 4.7.

Table 4.6. Flow Through Solutions with Cu-WRAM at pH=1.0.

	Cobalt (mg/L)	Copper (mg/L)	Iron (mg/L)	Arsenic (mg/L)
Head	13,930	6,953	21,98	20,070
Flow Through	Cobalt (mg/L)	Copper (mg/L)	Iron (mg/L)	Arsenic (mg/L)
1	11,690	4,506	17,460	15,500
2	9,592	2,325	13,340	12,900
3	7,709	726.2	9,607	8,191
4	6,168	25.89	7,169	5,339
5	4,788	12.04	4,888	3,482

Table 4.7. Strip Solutions with Cu-WRAM at pH=1.0.

Strip	Cobalt (mg/L)	Copper (mg/L)	Iron (mg/L)	Arsenic (mg/L)
1	22.23	2,731	849	934
2	24.56	2,465	406.7	426
3	16.63	2,258	265.2	259.7
4	26.68	1,130	146.3	364.8
5	13.71	72.9	71.13	538

Even at this low pH range, it was theorized small particles of precipitated ferric hydroxide could be the cause of the poor results. With ferric hydroxide precipitates present, arsenic was able absorb onto the surface. Thus account for the high concentration of arsenic in the solution. The next proposed idea was to pre-filter the solution after initial pH adjustment. The pre-filter was done with a 0.45 micron syringe filter. The filtered solution was then passed through the Cu-WRAM column with previous parameters. Results of the strip solution are shown in Table 4.8.

Table 4.8. Strip Solution Results after Pre-filtering.

Strip	Cobalt (mg/L)	Copper(mg/L)	Iron(mg/L)	Arsenic(mg/L)
1	68.68	1,431	174.6	137.5
2	20.04	1,336	65.83	46.72
3	24.18	941.1	100.7	8.86
4	20.41	702.7	77.36	55.18

Table 4.8 showed better results for copper separation from iron at low pH ranges using the pre-filtration step. The data definitely showed that small amounts of ferric hydroxide precipitates occur in the solution even at a pH level of 1.0. The copper to iron weight ratio was approximately 9 to 1 for the strips. The overall results using the pre-filtration step were good but the strip ratios were not as high as expected at this pH range.

4.7 Pre-Filtered Testing Solution

After the low pH testing results, our collaborator, Dr. Corby Anderson, suggested it was economically feasible to raise the pH of the solution and precipitate out most of the iron as ferric hydroxide along with a large amount of adsorbed arsenic. The final pH of the new testing solution was 4.0 and metal concentrations are shown in Table 4.9. The overall goal of this strategy was to separate and concentrate cobalt and copper from arsenic in the solution. For this purpose, three separate silica gels, Cu-WRAM, WP-1, and WP-2, were employed using columns.

4.8 Cu-WRAM Testing Results at pH 4.0

Solution was pumped through the 30 mL Cu-WRAM column and flowthrough was collected. After each loading, the pH was adjusted to 4.0 with dilute sodium hydroxide. After loading, the columns were stripped with concentrated acid. Both strip and head were collected and analyzed (Tables 4.9 and 4.10).

Table 4.9. Flow through Solutions after Cu-WRAM.

	Cobalt (mg/L)	Copper (mg/L)	Arsenic (mg/L)	Iron (mg/L)
Head	8,286	2,728	160.6	0.231
Flow Through	Cobalt (mg/L)	Copper (mg/L)	Arsenic (mg/L)	Iron (mg/L)
1	6,811	0.00	126.3	0.198
2	2,084	0.00	49.45	0.236
3	1,375	0.00	41.84	0.222

Table 4.10. Strips Solutions from Cu-WRAM.

Strip	Cobalt (mg/L)	Copper (mg/L)	Arsenic (mg/L)	Iron (mg/L)
1	248.7	17,700	21.97	0.00
2	184.8	329.1	45.23	0.00
3	7,042	174.2	69.09	0.00
4	3,272	167.1	35.81	0.00
5	2,625	34.96	8.22	0.00

Table 4.9 showed excellent results for removal of copper from initial test solutions. The strip contained almost 18 grams per liter while having only a small amount of amount of cobalt. After copper loading, cobalt was the next metal to be taken from solution, however, some of the arsenic was also removed from solution. Strip ratios are shown in Table 4.11.

Table 4.11. Strip Solution Weight Ratios using Cu-WRAM.

Strip	Copper/Cobalt	Cobalt/Arsenic
1	71.17	11.31
2	1.78	41.06
3	0.024	101.11
4	0.051	91.37
5	0.013	319.34

4.9 WP-1 Testing Results

Cu-WRAM was used to remove copper from the feed solution. WP-1 was then used for removal of cobalt from arsenic in the solution. The same experimental

parameters that were used for copper removal with Cu-WRAM testing were used for this stage. After copper removal, pH of the test solution was adjusted with dilute sodium hydroxide to a pH of 4.0 and columns were stripped with concentrated sulfuric acid and analyzed (Tables 4.12 and 4.13).

Table 4.12. Flowthrough Solutions using Cu-WRAM and WP-1.

Head	Cobalt (mg/L)	Copper (mg/L)	Arsenic (mg/L)
1 (Cu-WRAM)	8,535	2,800	172.1
2 (WP-1)	7,442	47.67	138.3
3 (WP-1)	2,001	32.29	18.32
4 (WP-1)	147.6	6.62	0.00

Table 4.13. Strip Solutions using Cu-WRAM and WP-1.

Strip	Cobalt (mg/L)	Copper (mg/L)	Arsenic (mg/L)
1 (Cu-WRAM)	598.8	37,370	81.43
2 (WP-1)	11,380	128.1	234.8
3 (WP-1)	5,732	58.18	253.6

Tables 4.12 and 4.13 showed good results for removal of cobalt from arsenic in the system. By initially using Cu-WRAM, we preferentially separated copper from solution. Using WP-1, cobalt was separated from solution, however, some contamination of arsenic occurred in the system. Table 4.14 shows the cobalt to arsenic mole ratio.

Table 4.14. Cobalt to Arsenic Weight Ratios Using WP-1.

Strip	Cobalt/Arsenic
WP-1 (initial experimental run)	48.66
WP-1 (secondary experimental run)	22.6

While Table 4.14 shows good results, some contamination occurs with arsenic. Since WP-1, uses a neutral ligand for cobalt removal, arsenic may be taken out as the counter ion in the system. This could be a direct result of arsenic contamination in the strip

solutions.

4.10 WP-2 Testing Results.

As done in previous testing of cobalt solutions, Cu-WRAM was used to remove copper from the system. All other previous parameters, flowrate, etc., remained the same. Flowthrough and strip results are shown in Tables 4.15 and 4.16.

Table 4.15. Flowthrough Solutions using Cu-WRAM and WP-2.

Head	Cobalt (mg/L)	Copper (mg/L)	Arsenic (mg/L)
1 (Cu-WRAM)	7,774	2,565	150.2
2 (WP-2)	6,729	36.86	121.6
3 (WP-2)	2,387	5.16	127.4
4(WP-3)	77.64	5.95	96.82

Table 4.16. Strip Solutions with Cu-WRAM and WP-2.

Strips	Cobalt (mg/L)	Copper (mg/L)	Arsenic (mg/L)
1 (Cu-WRAM)	232.6	20,410	36.54
2 (WP-2)	13,290	76.98	16.72
3 (WP-2)	9,168	62.76	7.12

Table 4.15 shows excellent removal of cobalt using WP-2. Cu-WRAM reproduced the previous results as in other tests. Secondly, WP-2 was able to separate cobalt from arsenic in the testing solution. Since WP2 uses a carboxylic acid as the binding group, cobalt is exchanged with protons in the system. In having cation exchange instead of a neutral ligand binding the metal, arsenic is not removed as the counter ion in the system. WP-2 shows great potential for purifying cobalt from arsenic contaminated solutions. Cobalt to arsenic mole ratios can be observed in Table 4.17.

Table 4.17. Mole Ratios using Cu-WRAM and WP-2.

Strip	Cobalt/Arsenic Ratio
WP-2 (initial experimental run)	794.8
WP-2 (secondary experimental run)	1,287.6

4.11 Conclusions

Using two PSI resins, Cu-WRAM and WP-2, we successfully removed, separated, and concentrated both copper and cobalt from arsenic in an acid pressure leach solution. Cu-WRAM at pH 4, following iron precipitation, proved the best strategy for removal of copper and cobalt in a mixed element solution. After one pass of the solution through the column, all of the copper was removed from solution while passing the other remaining metals. Copper strips were concentrated to 17.7 g/l with very little contamination of other metals.

For separation of cobalt from arsenic, resin WP-1 was able to successfully remove cobalt from solution, however, the solution was contaminated with arsenic. The cobalt to arsenic weight ratio was 48.66. Using WP-2, cobalt was also taken from solution, with very little arsenic present in the stripped solutions. Using this resin, the cobalt to arsenic weight ratio of the stripped solution was 794.8 in the initial strip and increased to 1,287.6 after the second pass through the column. Because WP-2 uses a proton exchange rather than a neutral ligand as in WP-1, arsenic is not loaded as the counter ion in the system, thus becoming a contaminant.

Chapter 5. Recovery of Gallium from Aqueous Systems

5.1 8-Hydroxyquinoline Chemistry Background and Research Goals

Recently, gallium has become a strategic metal in the computer industry because of the increased electron transfer rate of gallium arsenide compared to silicon in the semiconductor²². This metal has acquired significant commercial importance²³. The Bayer process, a sodium hydroxide leach of bauxite, is one of the major sources of gallium in the world²⁴. The process liquor usually contains 100 mg/L of gallium with 20,000 mg/L aluminum. Currently, the most efficient way of removing gallium from aluminum in Bayer solutions is by solvent extraction using Kelex 100²⁵. Solvent extraction using Kelex 100 was first reported by Leveque and Helegorsky²⁶. The active chemical in Kelex 100 is 8-hydroxyquinoline. Understanding the chemistry of 8-hydroxyquinoline and then, an overall goal of this thesis project was to incorporate onto a silica polymer matrix.

Incorporating 8-hydroxyquinoline onto a solid silica matrix has significant advantages relative to solvent extraction and styrene based ion exchange resins. Silica supports have no shrinking and swelling versus styrene based ion exchange resins suffer. Secondly, incorporation of 8-hydroxyquinoline onto a solid state ion exchange resin could increase capture kinetics of gallium from solution. Currently, in solvent extraction for gallium, reaction times take approximately 6 hours for successful gallium removal from aluminum in Bayer solutions. Furthermore, unwanted by-products which include contaminated organic solvent and “crud” formed at the aqueous organic interface, are produced as a result of solvent extraction technology. By successfully placing the molecule onto a silica based ion exchange support resin, these by-products will not be formed. The

research goal was to test the new silica supports for removal and recovery of gallium and other metals in both acidic and alkaline solutions.

Purity System Inc. (PSI) has two different silica based polymer gels that were utilized and tested for incorporation of 8-hydroxyquinoline onto the solid silica matrix.. The gels are WP-1, which consists of a polyethyleneimine functional group (Figure 5.1), and BP-1, which has a polyallylamine functional group (Figure 5.2).

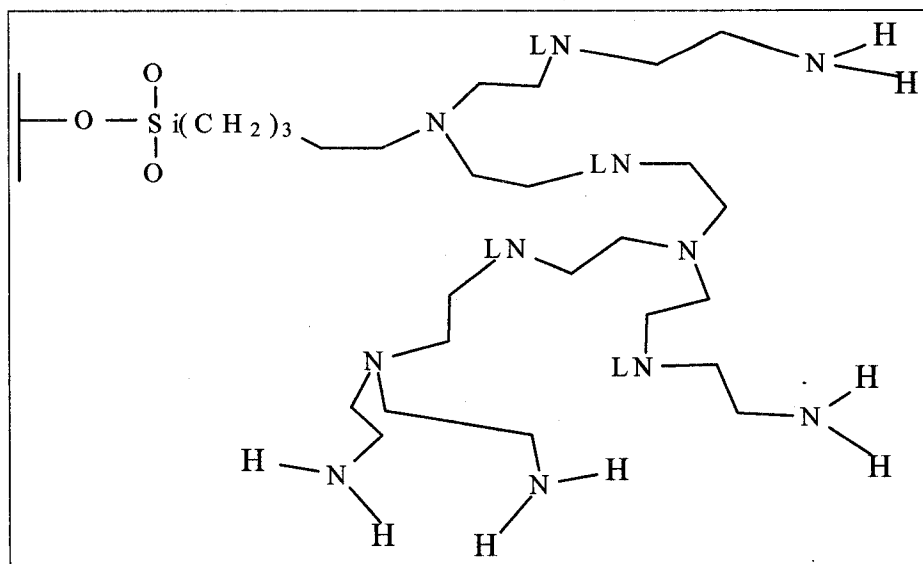


Figure 5.1. Structure of WP-1.

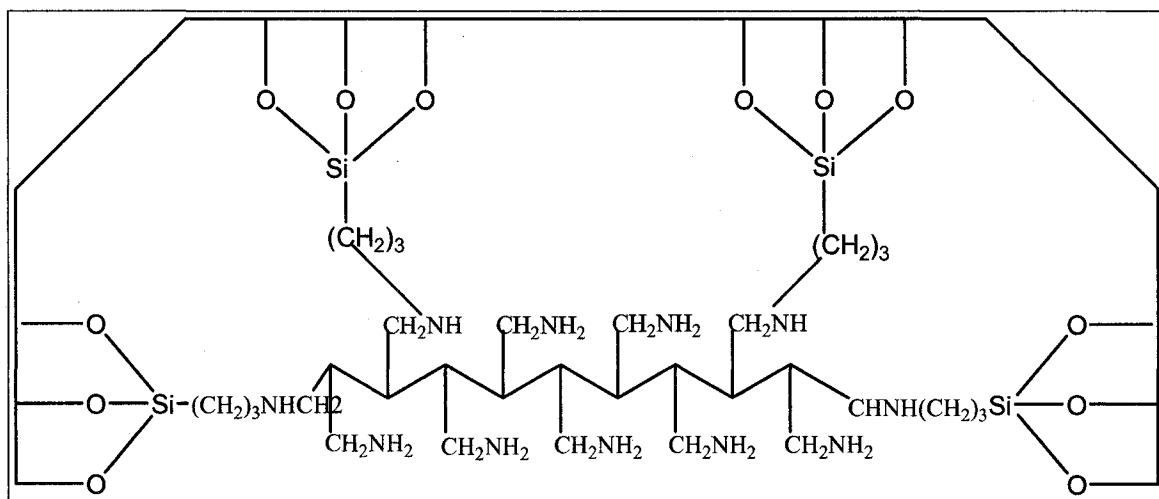


Figure 5.2. Structure of BP-1.

As seen from the structures, primary, secondary, and tertiary amines are used for binding and stripping of metals. These can also be used as reaction sites to extend the hydrophobic chain for incorporation of 8-hydroxyquinoline. The first experimental approach for making silica-based 8-hydroxyquinoline gel was formation of a Schiff base. The primary and secondary amines of the silica-based polymer gel reacts with aldehydes and ketones with the elimination of a water molecule to form an imine (Figure 5.3) Imines are nitrogen analogues of ketones or aldehydes with a carbon nitrogen double bond in place of the carbonyl group. A substituted imine is also called a Schiff base.

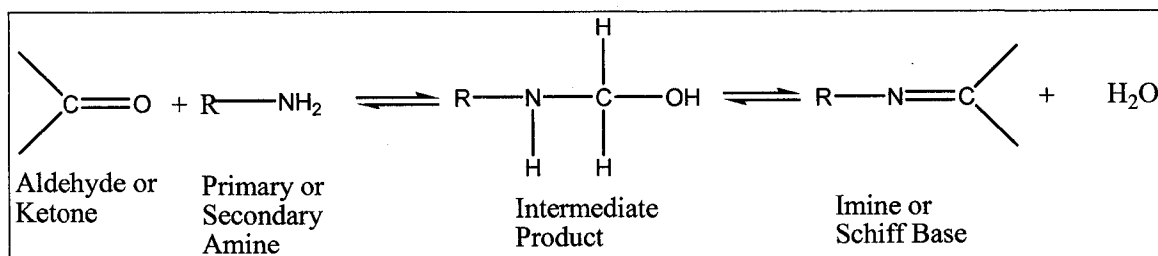


Figure 5.3. Schiff Base Formation and Reaction.

5.2 Fries Rearrangement Experimental Procedure.

In order to provide a ketone functionalized group, 8-hydroxy quinoline derivative was synthesized according to literature methods using the Fries Rearrangement²⁷. The reaction sequence for making 5-acetyl-8-hydroxyquinoline involves formation of a phenolic ester in the presence of a Lewis acid catalyst, anhydrous aluminum chloride, to form either ortho- or para phenolic ketones. Initially, the ester is by reacting sodium 8-hydroxyquinoline salt and acetyl chloride to form the 8-hydroxyquinoline acetate ester (Figure 5.4).

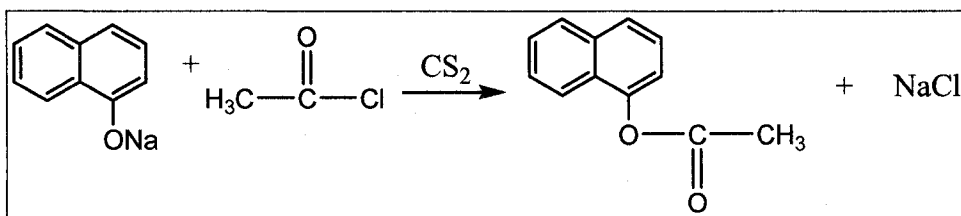


Figure 5.4. Formation of Ester.

For this approach, the Lewis acid, anhydrous aluminum chloride, attacks the ester bond to form an acylium ion. Since the hydroxide group on the 8-hydroxyquinoline molecule is an ortho- or para director, the acylium ion bonds to either position with a proton release to reform 8-hydroxyquinoline (Figure 5.5).

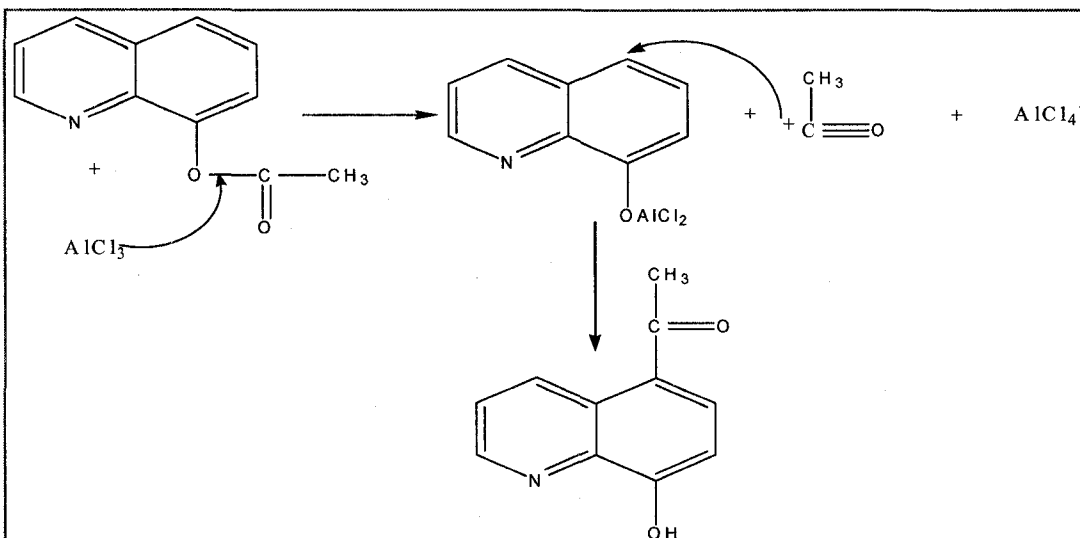


Figure 5.5. Fries Rearrangement Mechanism.

Several experiments were attempted using the Fries rearrangement to form the 5-acetyl 8-hydroxyquinoline. These attempts, however, were unsuccessful. The yields were less than 1% making this form of the Fries rearrangement was an unacceptable synthetic approach.

An alternative procedure to the Fries rearrangement was developed but not formally published by the late University of Montana Professor Emeritus, Forrest D. Thomas²⁸. According to his procedure, 5-acetyl 8-hydroxy quinoline can be synthesized in 70% yield. The main parameter differences between the Fries Rearrangement and the Thomas Fries Rearrangement are two-fold. The Thomas procedure used a more polar solvent of 1,2 dichloroethane compared to the prior work which used carbon disulfide. Secondly, the reaction was done at -35°C instead of 85°F. Because of the low reaction temperature conditions and the more polar solvent, a dissociation of the ionic intermediates was favored and side reactions were minimized.

5.3 Thomas Fries Rearrangement Results

Both the synthesis of the ligand and the subsequent reaction with the polyamine

appeared to be successful based on the infrared spectrum obtained (Figure 5.6).

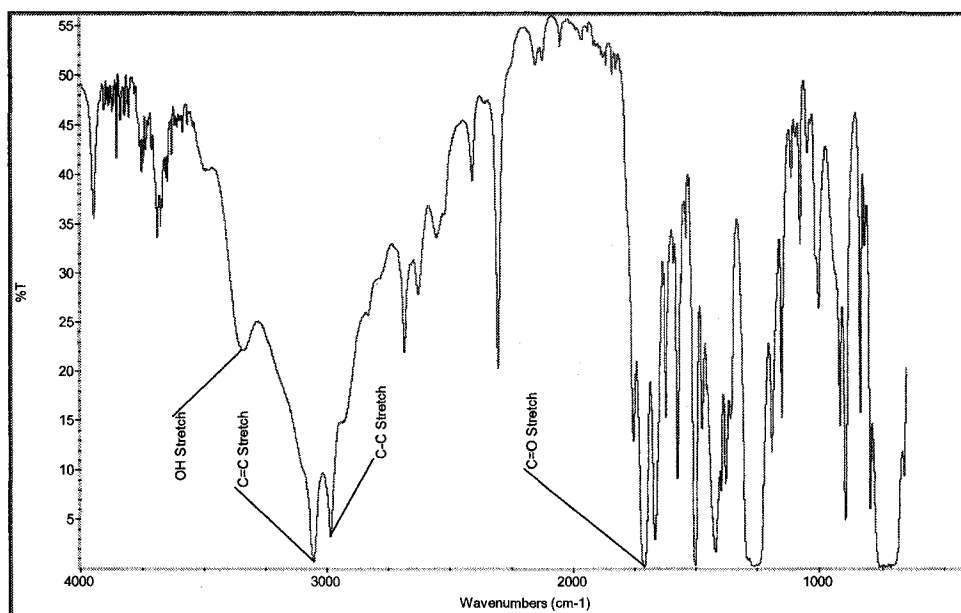


Figure 5.6. Infrared Spectrum of Thomas Fries Rearrangment Product of 5-Acetyl-8-hydroxyquinoline.

Using 1,2-dichloroethane, yields as high as 70% were achieved, however, because it employs a chlorinated hydrocarbon solvent, it would not be suitable in an industrial setting. Furthermore, the polyamine composite that resulted from the reaction of the 5-acetyl-8-hydroxyquinoline with the polyamine composite did not show very good kinetics.

5.4 Bonding of 8-Hydroxyquinoline to BP-1 and WP-1 Using the Mannich Reaction.

Given these rather disappointing results, we next turned to a very different approach to graft the 8-hydroxyquinoline ligand to the polyamine composite. Pyrell and Stork²⁹ used the Mannich reaction to bind an analog of 8-hydroxy quinoline onto silanized silica. We felt we could adapt it to our silica.

The Mannich reaction, in its simplest form, is the nucleophilic addition of an enol, represented by R_1 , to an iminium ion formed by the reaction of formaldehyde

with a primary or secondary amine. Figure 5.7 provides a generic example³⁰.

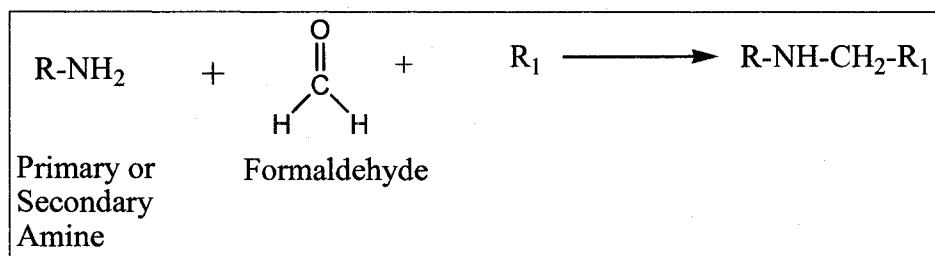


Figure 5.7. Mannich Reaction Example

Our specific application of the Mannich reaction employs WP-1 or BP-1 as the primary or secondary amine and 8-Hydroxyquinoline as R_1 . The mechanism for the Mannich reaction involves an acid-catalyzed equilibrium. The success of the Mannich reaction depends on being able to generate both nucleophilic and electrophilic carbon centers in the reaction mixture at the same time (Figure 5.7).

The mechanism of the Mannich reaction is somewhat complicated and is illustrated in Figure 5.8. Initially, since the reaction is acid catalyzed using acetic acid, both the amine, WP-1 or BP-1, and the formaldehyde are protonated to form an aminol molecule. The aminol is a good electrophile. Loss of water converts the aminol to an iminium ion that is an even better electrophile. Next, the 8-hydroxyquinoline is activated by a base. In this specific case, sodium hydroxide removes the proton from the alcohol group of 8-hydroxyquinoline. Because the hydroxyl group of the quinoline ring is an ortho- or para- director, nucleophilic attack of the iminium ion occurs from either position. Lastly, the final product is formed by ejection of proton from the nucleophile.

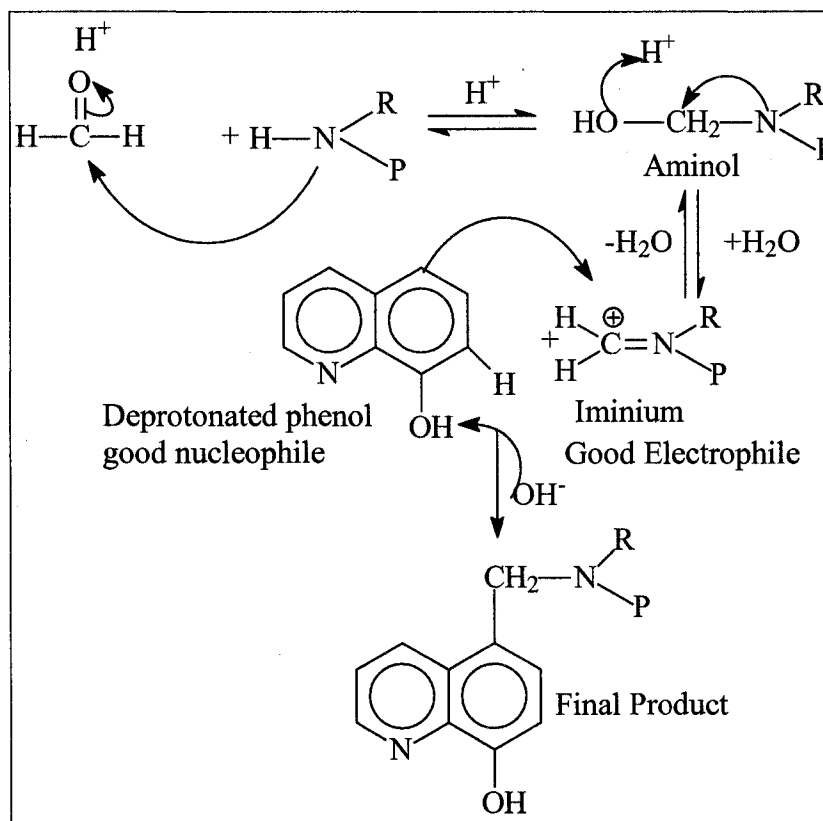


Figure 5.8. Mannich Reaction Mechanism.

5.5 Mannich Reaction Results

It should be noted that the initial WP-1 or BP-1 has a white color. After the Mannich reaction, however, the silica matrix shows a strong orange to pumpkin color. Since 8-hydroxyquinoline is commonly called “oxine”, the abbreviated name adopted for the BP-1-8-hydroxyquinoline combination was BPOX (Figure 5.9) and the WP-1 8-hydroxy quinoline was called WPOX (Figure 5.10).

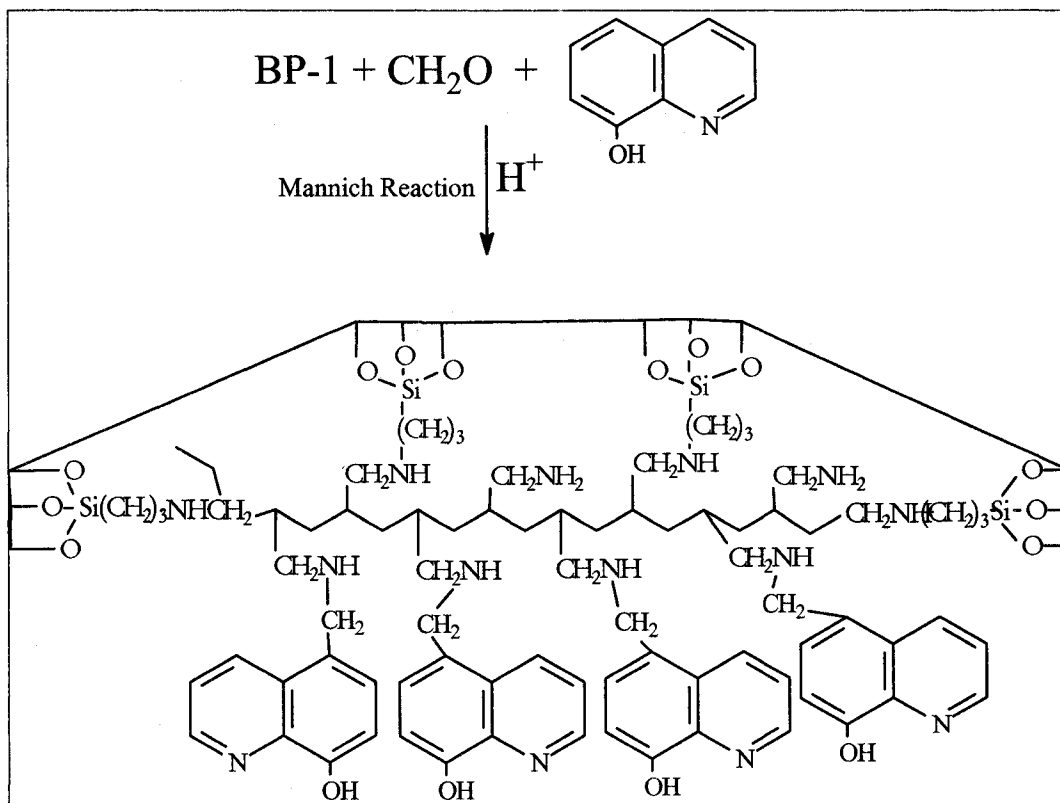


Figure 5.9. BPOX Structure

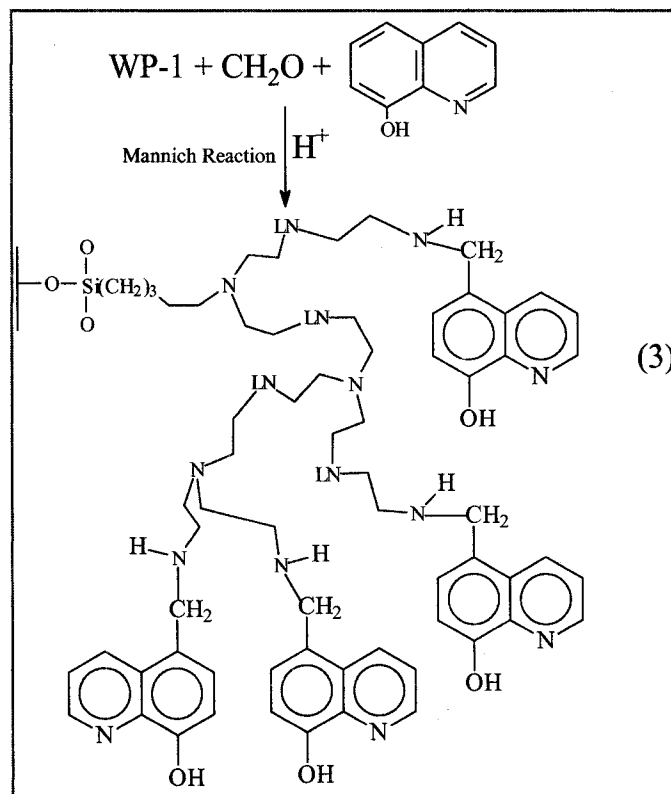


Figure 5.10. WPOX Structure

5.6 Infrared Spectra Analysis of Mannich Reaction Products.

After completion of the Mannich reaction experimental work, infrared spectrum were performed on both the starting, WP-1 and BP-1, and final, WPOX and BPOX, material.

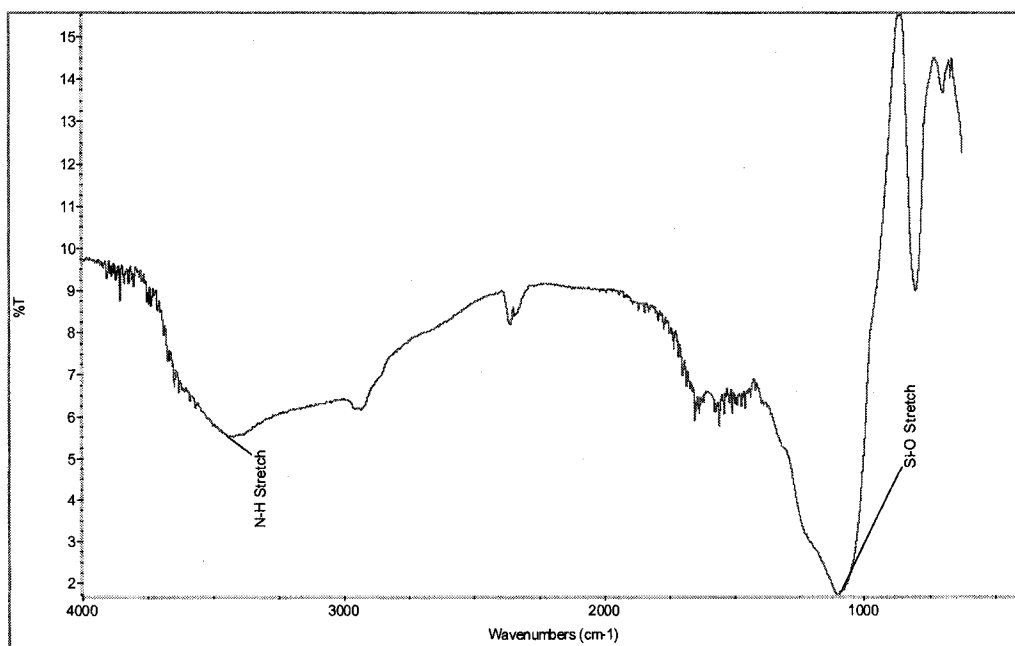


Figure 5.11. Infrared Spectra of BP-1

According to Figure 5.11, the infrared spectra of BP-1 showed nitrogen to carbon stretching at 3427 cm while alkane stretching occurred at 2925 cm. At 1100 cm, silicon to oxygen stretching was observed.

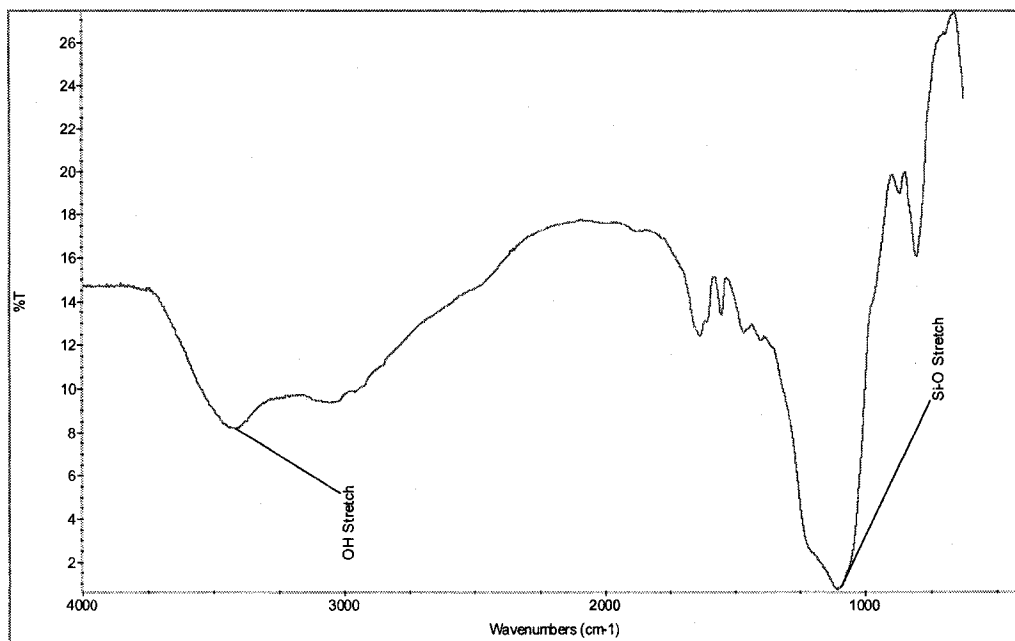


Figure 5.12 Infrared Spectrometer of BPOX.

The BPOX infrared spectra (Figure 5.12) shows a distinct increase in the intensity of the band in the 3400 cm^{-1} region relative to the hydrocarbon region which was attributed to the introduction of the 8-hydroxyquinoline.

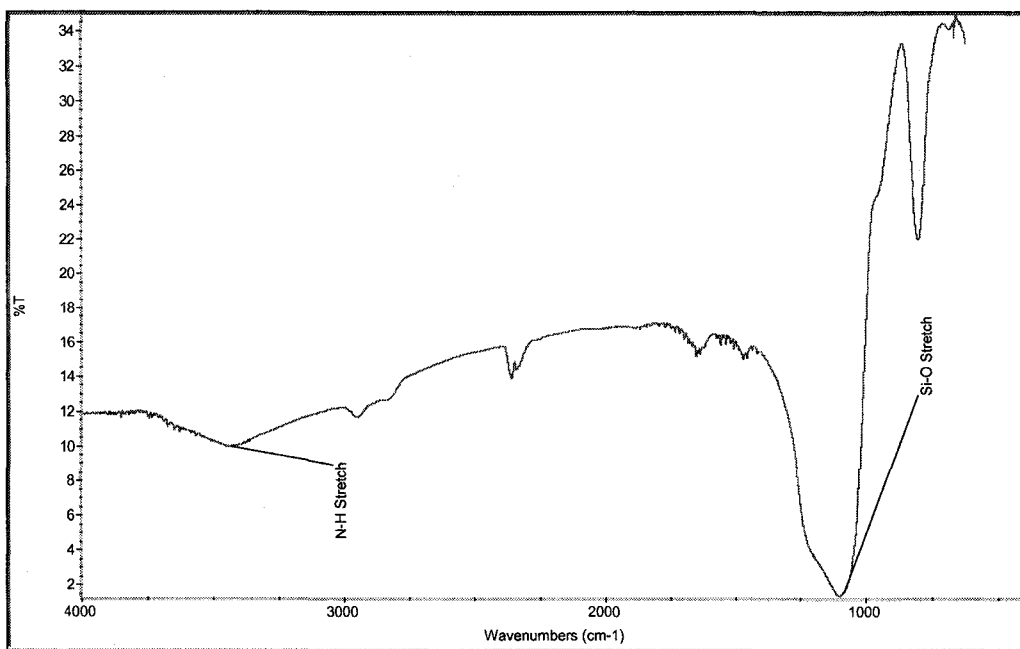


Figure 5.13. Infrared Spectrometer of WP-1

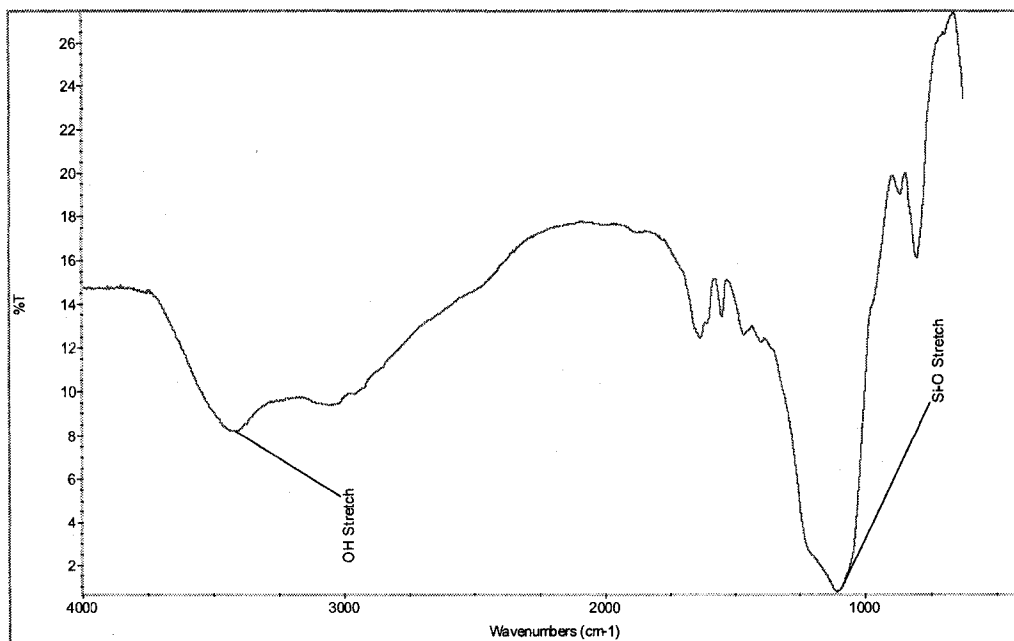


Figure 5.14 Infrared Spectrometer of WPOX.

The same trend was observed in the spectrum of WPOX (Figure 5.14) and here a new shoulder in the hydrocarbon region at 3062 cm^{-1} assignable to an aromatic stretching mode was also observed. Lastly, at 1103 cm^{-1} , the silica matrix was seen from Figure 5.14.

5.7 Elemental Analysis and Results

Samples were sent for elemental analysis. The samples included BP-1, WP-1, BPOX (Crossfield and Nanjing), and WPOX (Crossfield and Nanjing). Data was collected using the elemental analysis and calculations were performed to determine the amount of oxine loading onto each gel (Tables 5.1 to 5.4). For the calculation set, elemental percentage compositions for carbon, hydrogen, and nitrogen were initially converted to molar values for each data set.

Table 5.1. Elemental Analysis of BP-1 and WP-1.

Sample Name	% C	% H	% N
BP1	12.43	2.06	3.31
WP1	11.22	2.47	4.77

Table 5.2. Molar Elemental Analysis of BP-1 and WP-1.

Sample Name	Moles of C	Moles of H	Moles of N
BP1	0.01035	0.02044	0.00236
WP1	0.00934	0.02450	0.00340

Table 5.3. Elemental Analysis of BPOX and WPOX

Sample Name	%C	% H	% N
CR BPOX	24.95	3.60	4.51
NJ BPOX	20.62	3.17	4.85
CR WPOX	23.22	3.04	5.05
NJ WPOX	24.52	2.88	4.85

Table 5.4. Molar Elemental Analysis of BPOX and WPOX.

Sample Name	Moles of C	Moles of H	Moles of N
CR BPOX	0.02077	0.03571	0.00322
NJ BPOX	0.01717	0.03145	0.00346
CR WPOX	0.01933	0.03016	0.00360
NJ WPOX	0.02042	0.02857	0.00346

The amount of oxine loaded onto the gel was calculated by taking, for example BPOX, the total amount of carbon and nitrogen loaded onto the gel and subtracting the amount of starting material (BP-1). The oxine loading gels were then calculated the same way as the previous data set. The elemental percentage was converted to molar amount (Tables 5.5 and 5.6).

Table 5.5. Oxine Loading Calculation.

Sample Name	%C	% H	% N
CR BPOX	12.52	1.54	1.20
NJ BPOX	8.19	1.11	1.54
CR WPOX	12.00	0.57	0.28
NJ WPOX	13.30	0.41	0.08

Table 5.6. Oxine Loading Moiar Calculation.

Sample Name	Moles of C	Moles of H	Moles of N
CR BPOX	0.01042	0.01528	0.00086
NJ BPOX	0.00682	0.01101	0.00110
CR WPOX	0.00999	0.00565	0.00020
NJ WPOX	0.01107	0.00407	0.00006

The overall goal was to calculate the amount of oxine loaded onto each silica gel. This calculation was done by using the nitrogen in each gel. By knowing the amount of nitrogen added to silica composite, a ratio was determined for final loading of the oxine molecule. For this calculation, the ratio $N(\text{BPOX})/N(\text{BP1})$ determined the overall loading for oxine onto the silica composite (Table 5.7).

Table 5.7. Nitrogen-Oxine Ratio.

Sample Name	Moles of N (Total)	Moles of N (Oxine)	Ratio
CR BPOX	0.00322	0.00086	3.74
NJ BPOX	0.00346	0.00110	3.15
CR WPOX	0.00360	0.00020	18
NJ WPOX	0.00346	0.00006	57

According to the data and calculations for Crossfield BPOX, one oxine molecule was placed onto the polyamine for every four nitrogen groups (Figure 5.15). Eight out of every twenty nitrogens were bound to the silica surface (based on calculations from elemental analysis of CP Gel and BP-1) and, assuming these were not available for

binding to the oxine then five of the remaining twelve were functionalized with oxine.

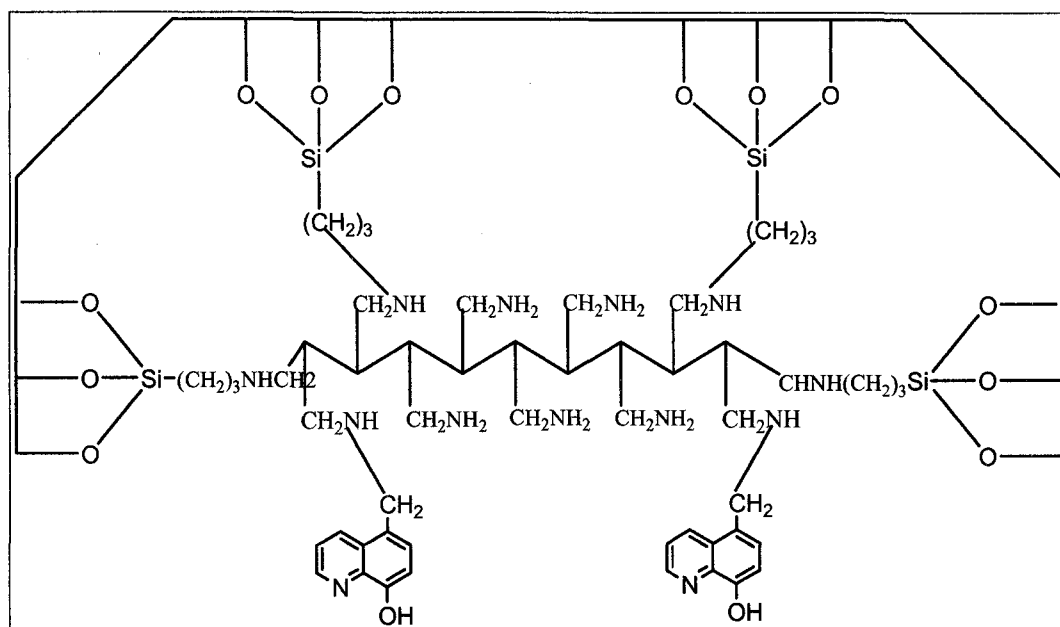


Figure 5.15. BPOX Structure Determination after Elemental Analysis.

This is a lower percentage, 42% than for Cu-WRAM, where 75% of the available nitrogen groups are functionalized. This is undoubtedly due to the larger size of the 8-hydroxyquinoline group relative to the picolyl group in Cu-WRAM (see Figure 4.1). For Nanjing BPOX, an oxine group was placed onto the molecule every third available nitrogen group. For the WPOX series, according to the data, only a small amount of oxine was placed onto the silica composite. For Crossfield WPOX, one out of every 18 nitrogens was bound to oxine while one out of every 57 was loaded using Nanjing silica gel.

5.8 Results

Infrared spectra (Figures 5.12 and 5.14) and elemental analyses (Tables 5.3) were in good agreement with the structures proposed above and, in this case, the resulting composites. Experimental testing to bind 8-hydroxyquinoline onto the silica gel matrix was difficult at times.

Using the Fries rearrangement procedure, very little, less than 1%, of the needed 5-acetyl-8-hydroxyquiniline product was created. Because of the low yield, the Fries rearrangement procedure was abandoned.

Using the Thomas Fries rearrangement, over 70 percent of the desired product was made, however, attempts to bind the 5-acetyl-8-hydroxyquiniline onto WP-1 and BP-1 produced poor kinetic capture, so this method was also abandoned. . It was indeed surprising that going from a double bond between carbon and nitrogen to a single bond completely changed the behavior of the material with regard to metal capture kinetics even when using the same silica gel and the same polyamine. This was undoubtedly due to the rigid nature of the double bond that prevents the ligand from adopting a minimum energy conformation with regard to its nearest neighbor ligands and thus decreases access of the metal ions to the active binding sites of the ligand.

Finally, the Mannich reaction was a very facile way to link ligands to the polyamine via a carbon-nitrogen single bond and the success encountered here can be and will be extended to the design and synthesis of other metal selective silica polyamine composites.

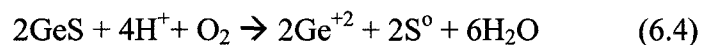
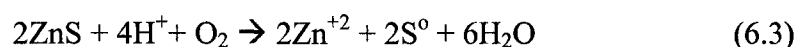
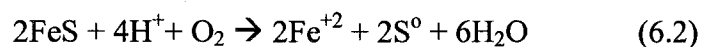
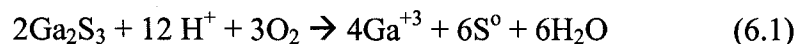
The testing of these new resins revealed Crossfield silica gel to be a better silica matrix for the large 8-hydroxyquinoline structure. The reasoning is that Crossfield silica gel has a larger pore size (225 angstroms) than the Nanjing silica gel (100 Angstroms). The molecule cannot either get into the Nanjing pores or the pore size completely blocks tefficient binding of 8-hydroxyquinoline. Previous studies performed in our group using large molecules have revealed the same trends. The advantage of the Nanjing silica was that it can be obtained more cheaply and in larger particle sizes. Larger particle sizes are

more advantages from the standpoint of giving less back pressure in a column configuration. The results obtained with the 300 angstrom silica gel prove the above hypothesis. This Crossfield gel was also cheap but the larger pores result in lower surface areas for a given particle size.

Chapter 6. Experimental Testing of WPOX and BPOX for Gallium Recoveries

6.1 Background and Introduction

Purity Systems Inc. received a solution from Pasminco Inc., an Australian mining company which has a mine located in Gordonsville, Tennessee and processes zinc containing ores³¹. A solid processing waste product was found to contain large amounts of iron, zinc, gallium, and germanium. Since both gallium and germanium are quite valuable, PSI was contacted for removal and concentration of both metals using the silica gel polyamine technology. The first step was to dissolve the metals into solution using the nitrogen catalyzed pressure leach¹⁸ developed Dr. Corby Anderson to dissolve the metals into solution. The total reaction for the dissolution of metals into solution can be summarized by the following reactions:



After leaching the metals into solution, PSI technology was used to recover and concentrate both gallium and germanium.

The testing of both new gels, WPOX and BPOX, was carried out in a 25 mL syringe column. The actual zinc ores were supplied by Pasminco Inc.. They contained both germanium and gallium as well as zinc, aluminum and iron (Table 6.1). The pH of the solution was adjusted to 2.1 as this proved to be the optimal pH for gallium recovery (Figure 6.1). Monitoring of pH is very important for gallium recoveries. If the pH of the testing solution goes above 2.1, both gallium and iron, as ferric, will begin to precipitate

and will clog the frits contained within the column during testing.

Table 6.1 Metal Profile of Pasmenco Challenge Solution.

Element	Concentration (mg/L)
Aluminum	1,944
Gallium	2,191
Germanium	200
Iron (as ferrous)	36,980
Zinc	5,381

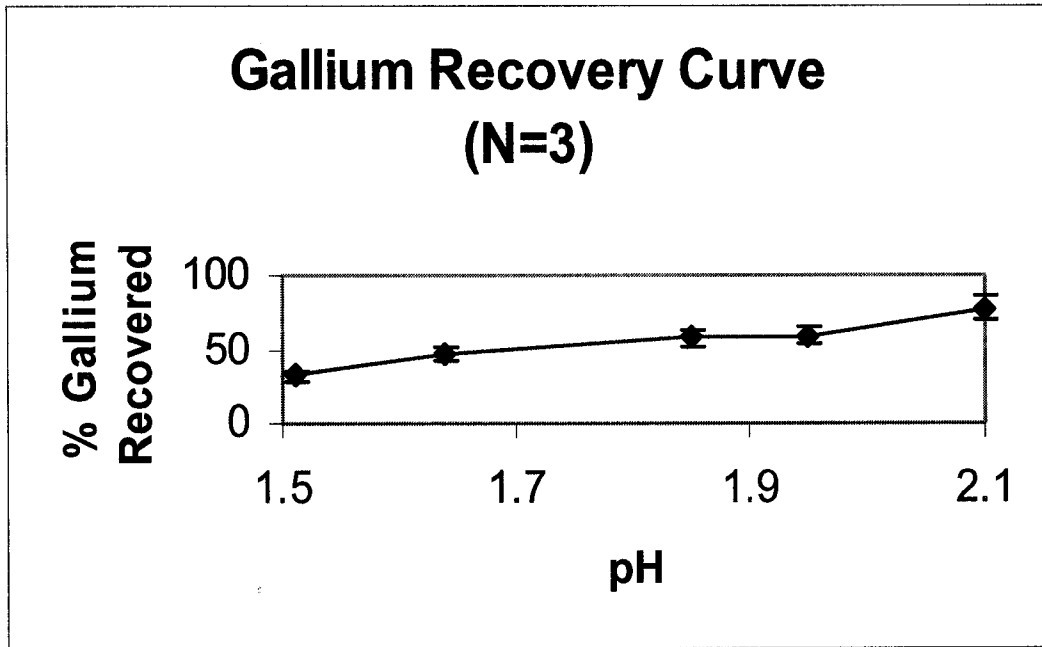


Figure 6.1 pH profile for gallium recovery using WPOX.

6.2 Gallium Recovery with WPOX

WPOX made on Crossfield silica gel gave excellent results for removal of gallium from solution. According to Figure 6.2, gallium breakthrough does not occur until seven bed-volumes. It should be noted that the initial solution of gallium contains 2.1 g/L and only 25 mL columns are used for the testing. Gallium breakthrough results can be seen below (Figure 6.2). The gallium capacity of WPOX was calculated at 25.95 milligrams gallium per gram of gel. WPOX was also very selective with regard to the separation of gallium from other metals in the system including aluminum, iron and zinc. The silica gel composite passed the other metals while mainly retaining gallium (Figure 6.3). The strip metal ratios of the column produced excellent results especially considering the huge excesses of iron and zinc present in the solution (Table 6.2).

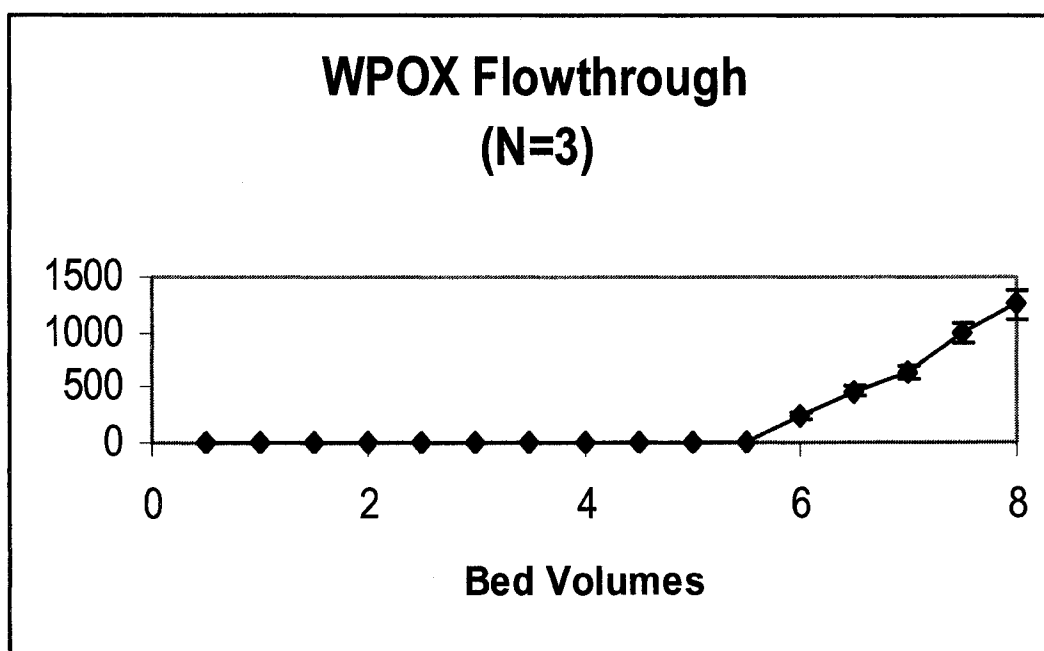


Figure 6.2 Gallium breakthrough curve for WPOX with the acidic ore leach solution.

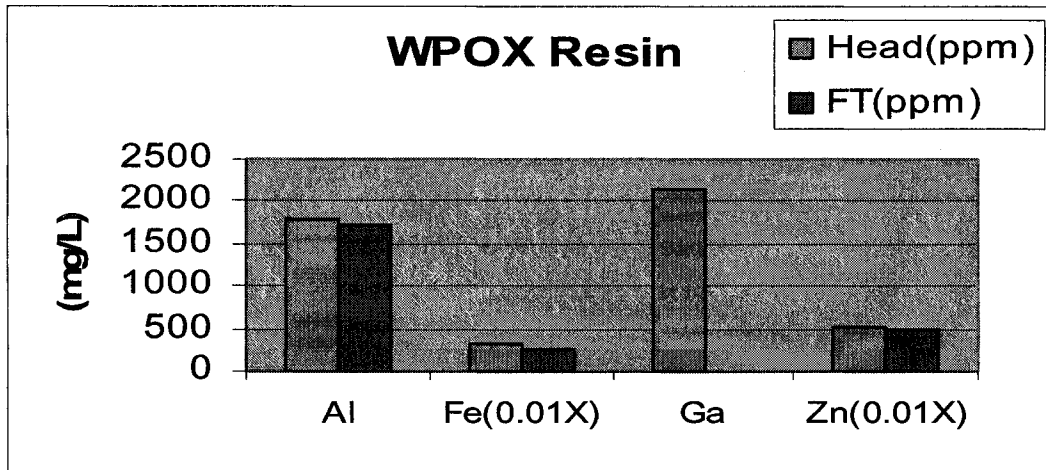


Figure 6.3 Comparison of feed and flowthrough concentrations for acidic ore leach containing gallium.

Table 6.2 WPOX Metal Strip Ratio

Gallium to Metal Ratio	Ratio
Aluminum	40.62
Iron	3.44
Zinc	92.32

6.3 Gallium recovery with BPOX

Like WPOX, the Crossfield based BPOX has shown excellent removal of gallium from the acidic ore leach solution. Gallium breakthrough is similar to that for WPOX and does not occur until seven bed volumes (Figure 6.4). The gallium capacity of BPOX was calculated at 25.00 milligrams gallium per gram of resin. BPOX, like WPOX, was also very selective for gallium removal from the other metals in the system such as aluminum, iron, and zinc. The silica gel composite passed the other metals while mostly retaining gallium (Figure 6.5). The metal strip ratios for BPOX are given in Table 6.3. Interestingly, although the measured gallium capacities are very similar for both BPOX and WPOX, the metal selectivities are somewhat different. BPOX shows better selectivity for gallium over aluminum while WPOX shows much better selectivity for

gallium over zinc. Selectivity for gallium over ferrous is about the same for both resins (Table 6.3).

Table 6.3 BPOX Metal Strip Ratio.

Gallium to Metal Ratio	Ratio
Aluminum	92.41
Iron	4.87
Zinc	6.81

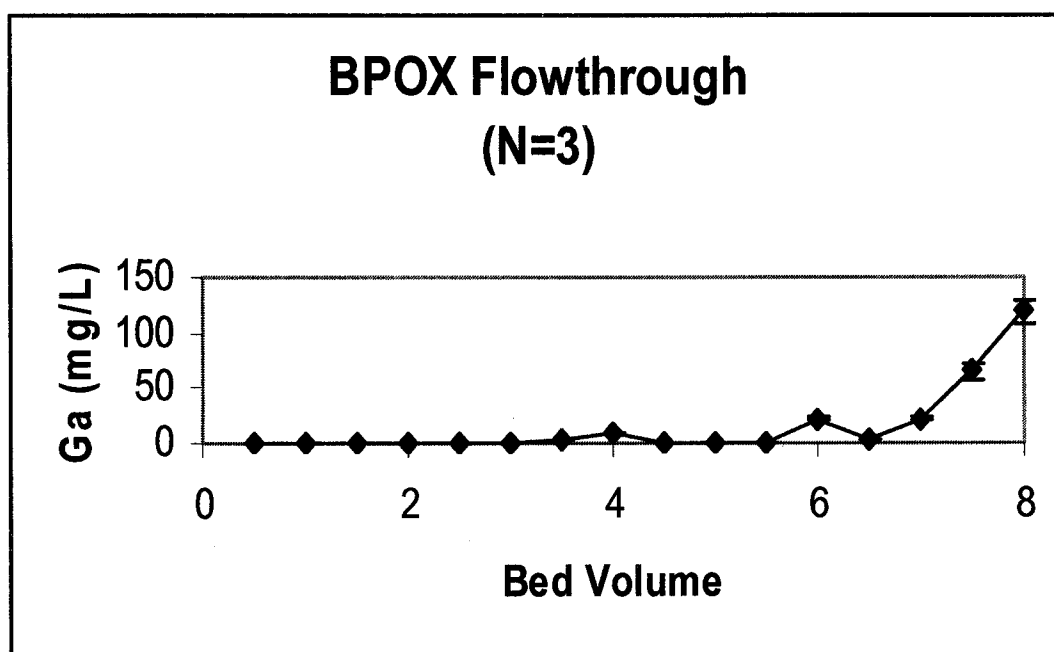


Figure 6.4 Gallium breakthrough curve for BPOX with acidic leach solution.

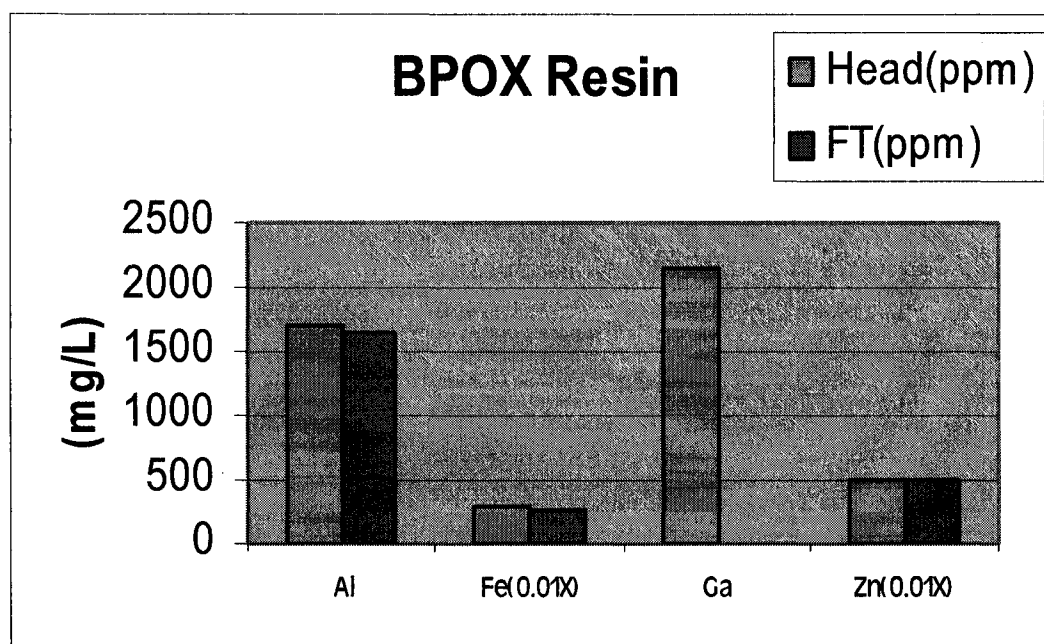


Figure 6.5 Comparison of Feed and Flowthrough Concentrations Containing Gallium.

6.4 Gallium Recovery from Alkaline Bayer Solutions

In addition to acidic solution studies, alkaline solutions were also tested using the silica composites. In the gallium industry, Bayer leachates are used to recover gallium from bauxite (aluminum oxide) ores using solvent extraction with Kelex-100²³. The Bayer process consists of leaching ore bodies with a strong alkaline base (sodium hydroxide). The resulting solutions contain large amounts of aluminum along with small amounts of gallium. The overall goal using the PSI technology was to selectively separate and concentrate the gallium in the Bayer solutions. Initial challenge concentrations of the Bayer solutions are given in Table 6.4. The challenge solutions were made up to reflect the actual concentrations of Bayer solutions in aluminum recovery plants. Since Bayer solutions contain large amounts of sodium hydroxide, the Bayer solution pH was extremely high, greater than 14. Initial challenge solution

samples were taken and measured on ICP.

Table 6.4 Initial Bayer Challenge Solution.

Metal	Concentration (mg/L)
Aluminum	9,381
Gallium	198.8

Purity Systems Inc. tested a synthetic Bayer solution on the BPOX, WPOX, and tethered BPOX. As with previous work, the flow rate was 0.2 bed-volumes per minute. Samples were taken every bed volume and measured by ICP. After loading, the columns were stripped with 4N sulfuric acid to remove the captured gallium from the column. Tables 6.5 to 6.7 show flow through data for all the PSI composite studies.

Table 6.5 BPOX Flow through Data for Bayer Solutions.

Bed Volume	Gallium (mg/L)	Aluminum (mg/L)
1	24.58	500.9
2	171.7	5,421
3	156.6	6,432
4	187.5	5,103

Table 6.6 WPOX Flow through Data for Bayer Solutions.

Bed Volume	Gallium (mg/L)	Aluminum (mg/L)
1	45.34	2,210
2	141.9	6,086
3	175.6	6,953
4	192.4	5,477

Table 6.7 Tethered BPOX Flow through Data for Bayer Solutions.

Bed Volume	Gallium (mg/L)	Aluminum (mg/L)
1	112.5	4,125
2	195.8	5,623
3	198.2	6,087
4	203.6	6,782

At first glance, the flow through data indicated poor results for gallium removal from Bayer leach solutions. Previous solvent extraction studies point out kinetics may have a major role in removal of gallium from solution. In the solvent extraction

process the solution is agitated for over six hours before the gallium was stripped from the organic phase. In order to improve the initial poor results, it was decided to slow down flow rate and recycle the test solution through the column. The hypothesis here was that the selectivity for gallium was overwhelmed by the large aluminum to gallium ratio and that eventually, given enough contact time gallium would displace aluminum from the column. The strip (Tables 6.8 to 6.10) confirmed the small amount of gallium bound to the silica composites. However, aluminum has bound to the sites and it might be possible to displace the aluminum by increasing contact time with the resin. The poor gallium loading compared to the acidic solutions may be due to a combination of poor mass transfer kinetics due to the high viscosity of the solution and the different speciation of gallium at pH=15 versus pH=2. On the positive side it should be noted that the silica gel composites survived exposure to strong base even though silica itself readily dissolves in alkaline solution.

Table 6.8 BPOX Strip Data for Bayer Solutions.

Bed Volume	Gallium (mg/L)	Aluminum (mg/L)
1	3.87	1,083
2	28.98	1,489
3	7.52	219.3

Table 6.9 WPOX Strip Data for Bayer Solutions.

Bed Volume	Gallium (mg/L)	Aluminum (mg/L)
1	4.97	545.8
2	12.75	2,389
3	8.59	2,042

Table 6.10 Tethered BPOX Strip Data for Bayer Solutions.

Bed Volume	Gallium (mg/L)	Aluminum (mg/L)
1	9.68	1,455
2	5.89	968

Because of the poor kinetics test for removal of gallium from Bayer solutions, a second set of experimental research was conducted. During the first testing of Bayer solution, the amount of time the solution spent reacting with the column was 5 minutes per bed volume. As previously discussed, industry allows the Bayer solution to react with solvent extraction for a minimum of six hours for effective removal of gallium from the Bayer solution. During the experimental phase, 100 mLs of Bayer solution was pumped through the column containing the BPOX silica resin. The flow through solution was then recirculated into the feed solution tank. Flow rate for the system was 0.2 bed volumes per minute. The feed solution was then sampled every hour up to six hours and analyzed on the ICP for gallium and aluminum.

According to Table 6.11, better results were obtained using BPOX silica resin for removal of gallium from Bayer solutions. The table shows that kinetics are involved in effective removal of gallium from solution. As contact time with the gel increases, the amount of gallium in solution decreases. Only 50% of the gallium was effectively removed from solution after six hours (Table 6.11).

Table 6.11 BPOX Bayer Solution Testing.

Hours	Aluminum (mg/L)	Gallium (mg/L)
2	12,552	334.5
4	10,200	278.8
6	8,756	223.6

6.5 BPOX/WPOX Experimental Testing Conclusions.

In acidic solutions contain gallium, ferrous iron, aluminum, and zinc, the silica based oxine bound ligands, such as WPOX and BPOX, had shown excellent kinetics and selectivity for both removal and stripping of gallium from solution. During experimental testing, the pH of the solution was important. For optimal testing, a pH of 2.1 was determined to remove over 75% of gallium from solution. By lowering the pH of the test solution, gallium recovery results were significantly lowered to 33%. Loading capacities for BPOX and WPOX were calculated and very similar. Gallium capacity for BPOX was measured at 25.00 mg gallium per gram of gel while WPOX capacity was 25.95 mg gallium per gram of gel. During alkaline testing, BPOX was successful in removing 50% of gallium from Bayer solution, however, the poor results may be a direct result of poor mass transfer do to the viscosity of the Bayer solutions.

Generally, the oxine based ligand will bind and successfully remove trivalent cations, such as aluminum, ferric, or gallium, from solution while binding little of divalent cations, such as zinc, nickel, and ferrous.

The success for gallium removal versus other metals from solution using oxine based ligands can be argued by the ability of gallium as a “soft” or more polarizable element. Because of this, gallium is selectively removed from the Pasminco solution over aluminum, and other divalent cations such as ferrous iron and zinc.

From a literature review, gallium was generally removed from solution using the Bayer process, a sodium hydroxide leach³². The Pasminco solution, using the nitrogen species catalyzed leach, offers a very unique situation for successful removal of gallium from solution from a process ore. Using Kelex-100, experimental data favors gallium recoveries from strong alkaline solutions. According to literature, the ligand will co-load ferric iron in acidic solutions along with gallium from solution. By leaching the ore along with ferric reduction to ferrous iron with elemental zinc, a very distinctive solution was made for gallium recovery. The BPOX/WPOX silica gel provided an easy remediation for gallium separation from ferrous iron compared to solvent extraction or precipitation techniques. The silica gel was able to separate and concentrate gallium from solution based on experimental work.

6.6 Two Step Separation of Germanium and Gallium

The solutions received from Pasminco Inc in Gordonsville, TN contained high concentrations of iron, zinc, and gallium as well as smaller amounts of germanium and aluminum (Table 6.12). The goal for remediation of the solution was to selectively remove and concentrate gallium and germanium from iron, zinc and aluminum. A pilot study was done with 100 lbs of WP-2 at the Pasminco plant in May of 2002 effectively recovered the gallium in sufficient purity for direct formation of gallium metal by electrolysis³¹. It was also desirable to recover the germanium

The WP-2 resin contains an aminoacetic acid functional group. At pH 2.1 WP-2 rejects iron, as ferrous, zinc, and aluminum. Initial experiments for the gallium-germanium separation used stacked columns of WP-2 and BPOX. After adjustment to

pH 2.1 with sodium hydroxide, the solution was passed through the columns at a flow rate of 0.2 bed volumes per minute. Samples were collected every bed volume for analysis by ICP (Table 6.12). After the columns were loaded with the test solution, two bed volumes of distilled water were run through the column to remove any residual test solution in the column. The columns were stripped (Table 6.13) using 4N sulfuric acid.

Table 6.12. Flow Through Results for the WP-2-BPOX Two Column System.

	Al (mg/L)	Fe(mg/L)	Ga(mg/L)	Ge(mg/L)
Bed Volume 1	4.29	9.47	0.00	0.00
Bed Volume 2	422.2	6,846	0.98	0.00
Bed Volume 3	1,297	21,010	16.56	0.00
Bed Volume 4	1,593	26,870	41.03	33.82
Bed Volume 5	1,550	25,990	50.37	79.66
Bed Volume 6	1,671	28,440	75.81	151.8

Table 6.13. Strip Results for the WP-2-BPOX Two Column System.

Strip	Al (mg/L)	Fe(mg/L)	Ga(mg/L)	Ge(mg/L)
BPOX BV 1	234.1	4,536	227.3	71.73
BPOX BV 2	14.81	289.2	171.4	126.3
WP2 BV1	161.6	26,070	375.1	432.1
WP2 BV2	128.0	21,050	5,080	483.7
WP2 BV3	512.6	8,767	3,714	537.9
WP2 BV4	193.4	3,257	1,966	441.1

Previous studies with the Pasmenco solution showed the WP-2 resin to be very selective for removal of gallium from iron, aluminum, and zinc. It should be noted that the resin rejects ferrous iron but not ferric. The Pasmenco testing solution was over six months old and oxidation of ferrous to ferric had occurred in the solution as evidenced by the large amount of iron in the strips relative to that observed in the previous work (Figures 6.6 and 6.7). The main point is that germanium and gallium co-loaded on both resins.

We repeated the above experiments after reduction of the ferric ion to ferrous and adjusted the pH to 2.1 after passing the solution through WP-2. The results are much

improved and indicated that a two step process could be used to separate germanium and gallium. Figures 6.6 and 6.7 and Tables 6.14 and 6.15 showed the flow through data after passing the solution through WP-2 and then BPOX. Co-loading of both gallium and germanium on WP-2 was still observed but the BPOX shows a much higher affinity for germanium. The strip data revealed an effective capacity of 20.4 mg/g and 6.6 mg/g for gallium and germanium respectively on WP-2 and 25.5mg/g and 19.5 mg/g respectively on BPOX. Based on the large difference in effective capacity between WP-2 and BPOX for germanium, it was possible to remove almost all the germanium by passing the solution through BPOX first and then through WP-2 to remove all the gallium.

Table 6.14. ICP data for Pasmenco Flow Through Using BPOX.

BPOX Bed Volume	Ge(mg/L)	Ga(mg/L)	Al(mg/L)	Fe(mg/L)
1	0.00	87.52	986.3	12,532
2	25.23	35.63	1,222	28,562
3	20.23	420.3	1,198	26,352
4	45.23	435.2	1,250	27,564
5	56.63	444.3	1,333	27,860
6	120.32	478.6	1,350	28,521
7	222.31	480.6	1,352	28,321

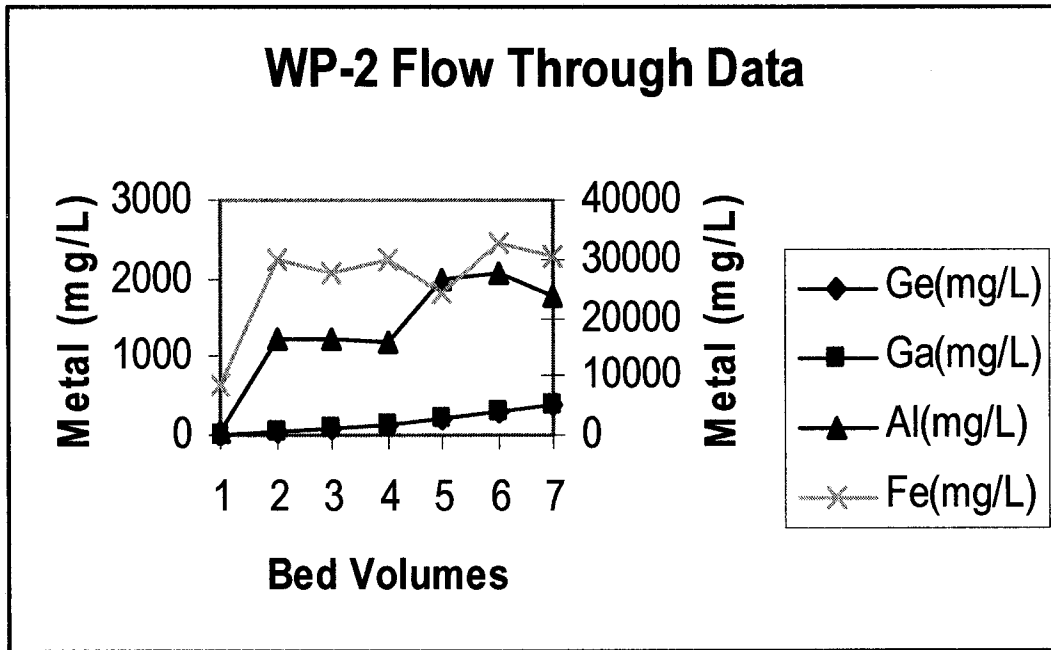


Figure 6.6. Breakthrough curves for the acidic ore leach after adjustment to pH = 2.1 and passing through the WP-2 column (N=1).

Table 6.15. ICP data for Pasmenco Flow Through Using WP-2.

WP-2 Bed Volume	Ge(mg/L)	Ga(mg/L)	Al(mg/L)	Fe(mg/L)
1	0.00	0.00	25.32	8,563
2	55.62	60.23	1,223	29,650
3	76.63	78.32	1,219	27,563
4	125.6	120.5	1,198	29,989
5	218.3	220.5	2,003	24,326
6	292.3	302.6	2,056	32,563
7	375.8	380.3	1,756	30,236

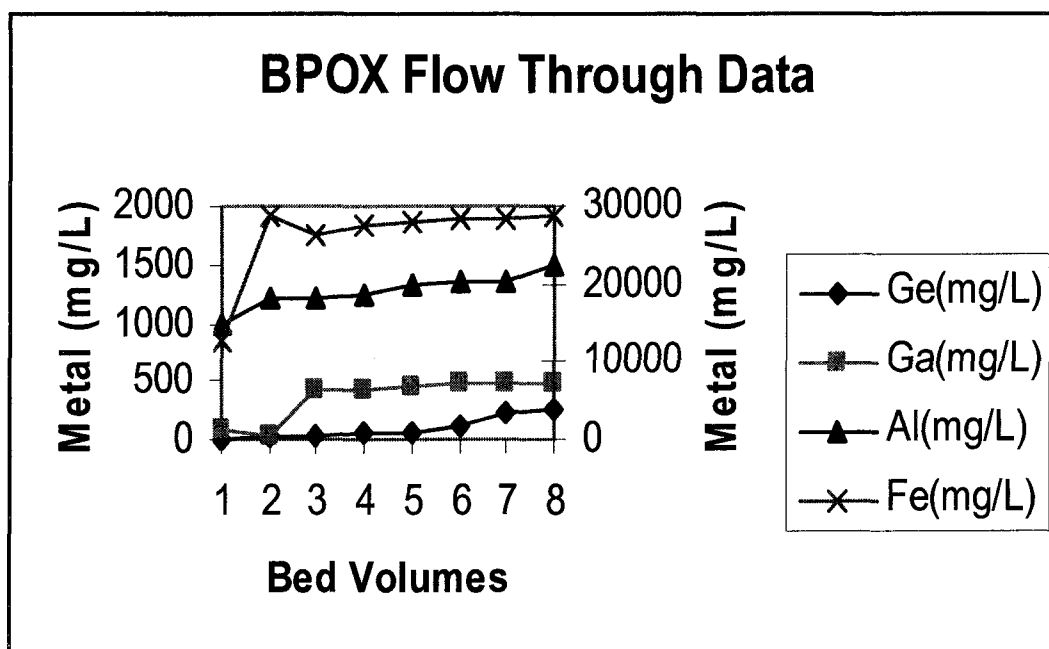


Figure 6.7. Breakthrough curve for acidic ore leach after readjusting pH to 2.1 on BPOX (N=1).

6.7 Two Step Separation Conclusions

Both WP-2 and BPOX had a high affinity for gallium and germanium while passing ferrous iron and aluminum. Further work for complete loading and separation of gallium and germanium from acidic solution needs to be investigated. Previous WP-2 (Figure 6.6) experimental work revealed co-loading of both metals while BPOX had shown separation of gallium from germanium from solution (Figure 6.7).

Initially, further experimental work could use WP-2 to co-load both metals from solution until both gallium and germanium are completely removed from solution. After metal loading, the column could be stripped using 4N sulfuric acid and pH adjusted to 2.1 using sodium hydroxide. Next, a large column of BPOX would be used to selectively load gallium from germanium in solution. The flow through could then either be pH adjusted with sodium hydroxide to precipitate the germanium, or another additional column of WP-2 could be used to concentrate the germanium from solution.

Chapter 7. Tethered BPOX

7.1 Mounting the 8-Hydroxy Quinoline Ligand via a Tether and its Impact on Kinetics

With the success of attaching 8-hydroxyquinoline to the various polyamine composites, it was decided to try to improve the capture kinetics of the resin by attaching a short tether to the polyamine prior to using the Mannich reaction to attach the ligand. It was well known from prior research in the area of polymer anchored catalysts that extending the catalyst in the solution form the polymer matrix improves the captivity of the anchored catalyst. By adding a two carbon tether to BPOX, faster kinetics for removal of gallium would occur.

The reaction of 2-bromo ethylamine with BP-1 yielded a modified polyamine which was then reacted with 8-hydroxyquinoline to yield the tethered BPOX. Elemental analyses (Table 7.1) and the weight gains were all consistent with the successful addition of the tether and the grafting of the 8-hydroxyquinoline to the silica polyamine composite.

Table 7.1. Elemental Results of Tethered Product, BPOX and WPOX.

Silica Gel	% Carbon	% Hydrogen	% Nitrogen
BPOX	18.73	4.13	3.42
WPOX	25.95	3.23	4.02
Tethered BPOX	25.28	3.77	4.22

Incorporation of the tether did have a favorable impact on gallium capture. By addition of a two carbon tether, faster kinetics for removal of gallium occurred (Figure 7.2). Most importantly, the gallium adsorption kinetics for the tethered system is faster than for the original BPOX. The tethered system had a higher equilibrium adsorption capacity suggesting that the tether made more sites available to ligand modification as

well as improving the adsorption kinetics.

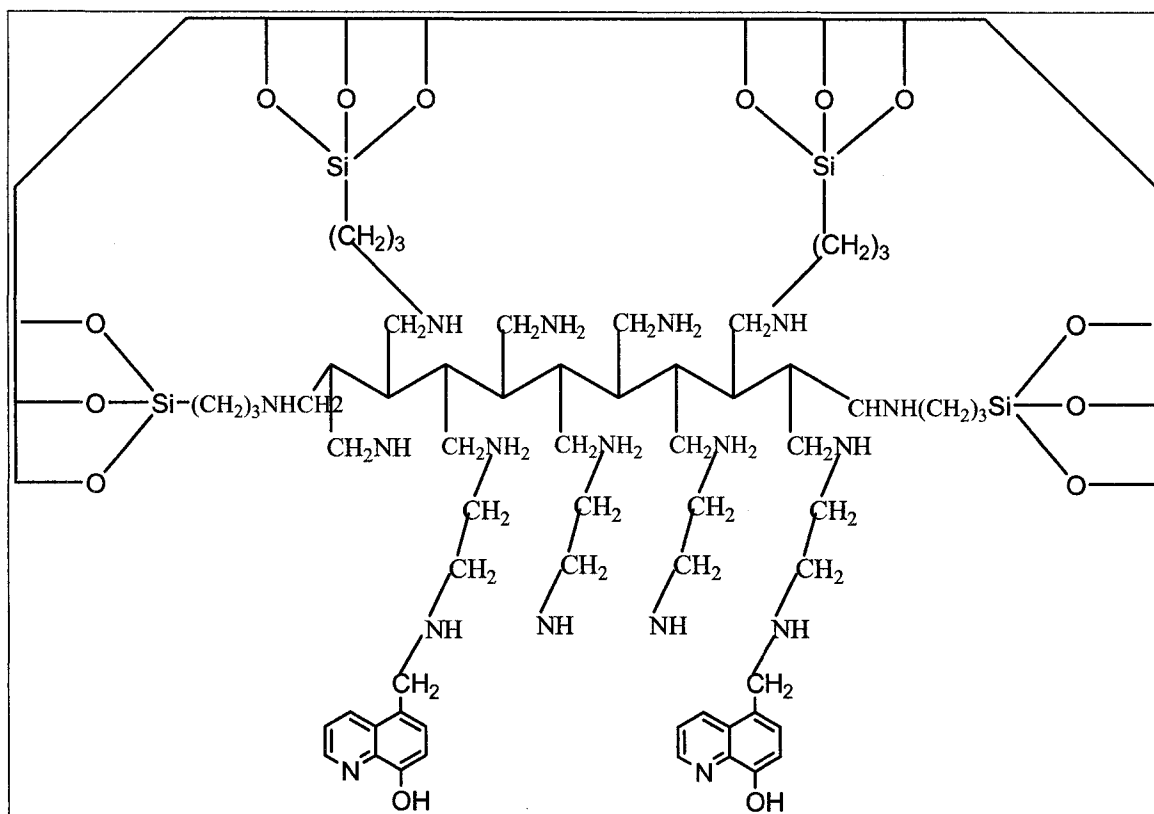


Figure 7.1. Tethered BPOX Structure.

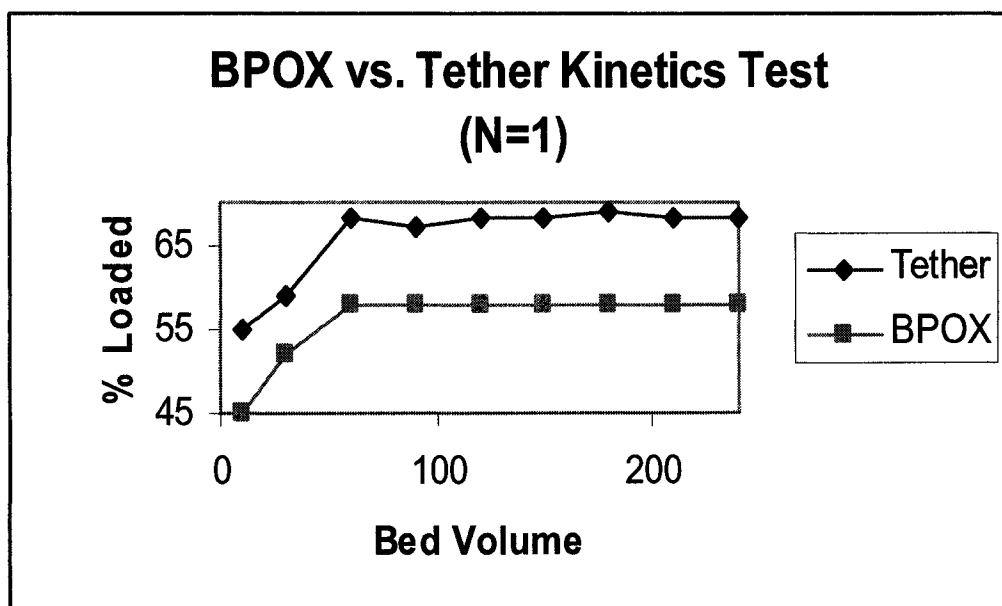


Figure 7.2. Kinetics Test of BPOX vs. Tethered BPOX.

7.2 Tethering Conclusions

By creating a tethered version of BPOX using 2-bromo-ethylamine followed by the Mannich reaction with 8-hydroxyquinoline, faster kinetics for removal of gallium from acidic solutions were observed. Experimental testing of Pasminco solution (Figure 7.2) with the tethered BPOX silica gel had shown a 14% increase in metal uptake for the tethered BPOX resin compared to molar BPOX resin. Since this was only a modest improvement, further testing should be investigated by adding longer tethers of alkyl chains to the resins. However, using longer chains may not be feasible due to the lack of commercially available 1°, 1° amino halides. Secondly, the risk of using longer hydrophobic chains could fold on themselves. Experimental tests to make the 3, 4, 5, and 6, carbon tethers followed by the Mannich reaction should be done for further research.

Chapter 8 Nickel-Ferric Separations using BPOX

8.1 Experimental Testing of BPOX for Nickel-Ferric

After testing BPOX for successful gallium removal from solutions, further experimental studies showed the resin could be used to remove ferric iron in acidic conditions containing divalent transition metal ions. In order to meet the requirements for such separations, the oxine based resin should have a high affinity for ferric iron while having a low affinity for nickel in acidic conditions during the experimental phase. Secondly, after successful loading of the ferric ion in solution, the stripping kinetics must be completed within two column bed volumes.

Tests were conducted using a 30 mL syringe column filled with 14.22 grams of Crossfield BPOX. A solution containing 1,472 mg/L of ferric iron made from ferric ammonium sulfate dodecahydrate ($(\text{FeNH}_4(\text{SO}_4)_2 \cdot 12\text{H}_2\text{O})$) and 486.4 mg/L nickel made from nickel sulfate hexahydrate ($(\text{NiSO}_4) \cdot 6\text{H}_2\text{O}$). The pH of the solution was adjusted to 1.5 with sulfuric acid. The testing procedure used a flow rate of 5 mLs per minute. Samples were taken every three bed volumes and analyzed for nickel and iron on ICP. After running 15 bed volumes of solution, a column volume of pH 1.5 distilled water was passed through the column to remove any residual solution from the resin. Next, 10 mLs of 4N sulfuric acid was placed into the column followed by distilled water. For each strip solution, one column volume or 30 mLs was collected and analyzed for nickel and iron in solution. Nickel and iron separation results are shown in Table 8.1 and Figure 8.1.

Table 8.1 Nickel-Iron Separation Results.

Bed Volume	Fe (mg/L)	Ni (mg/L)
Challenge	1,472	486.4
3	8.92	538.6
6	8.43	491.3
9	6.95	492.9
12	9.54	496.3
15	5.46	488.4

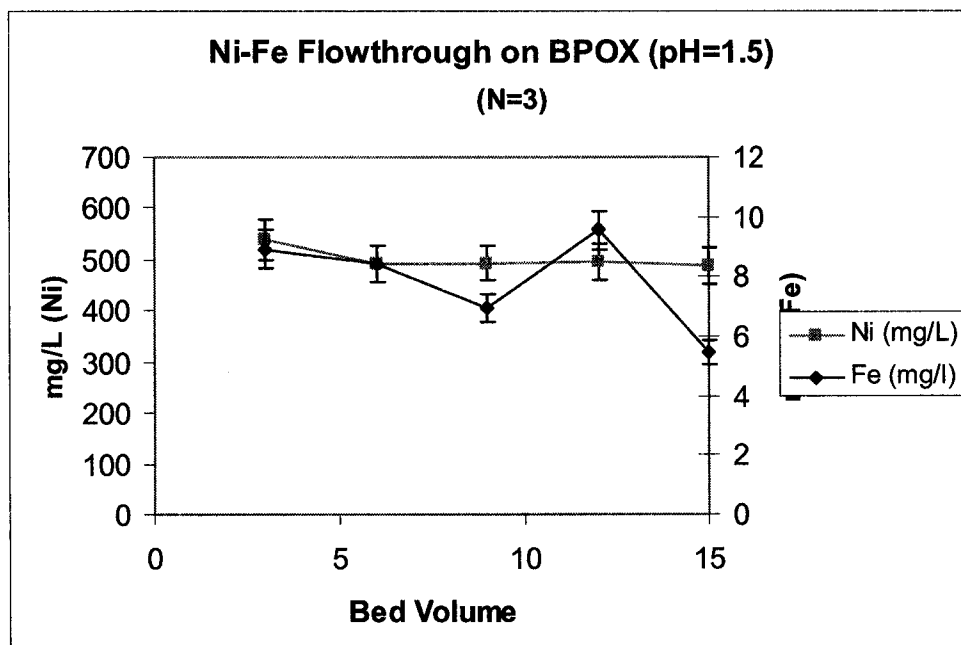


Figure 8.1 Nickel-Iron Flowthrough Results.

Results for BPOX indicated excellent removal capabilities for ferric iron in the presence of nickel in acidic conditions. The oxine resin was able to successfully reduce ferric iron from solution to less than 10 mg/L from 1,500 mg/L. The experimental work showed nickel completely passed through the column and the oxine resin had little or no affinity for nickel at pH 1.5. Observation of Table 8.2 showed BPOX had a capacity of 30.88 mg ferric iron per gram of BPOX gel during experimental work.

Table 8.2. Ferric Capacity Calculations.

Bed Volume	Ferric Loading (mg/L)	Ferric Loading (mg)
3	1463.08	87.7848
6	1463.57	87.8142
9	1465.05	87.903
12	1462.46	87.7476
15	1466.54	87.9924
	Total	439.242

The second criteria for successful removal of ferric in acidic conditions involved stripping kinetics. As previously stated, the requirement was to effectively remove and strip the ferric iron from the column within two column bed volumes. Observation of Table 8.3 and Figure 8.2 are shown with excellent removal kinetics for stripping ferric iron from BPOX Crossfield resin.

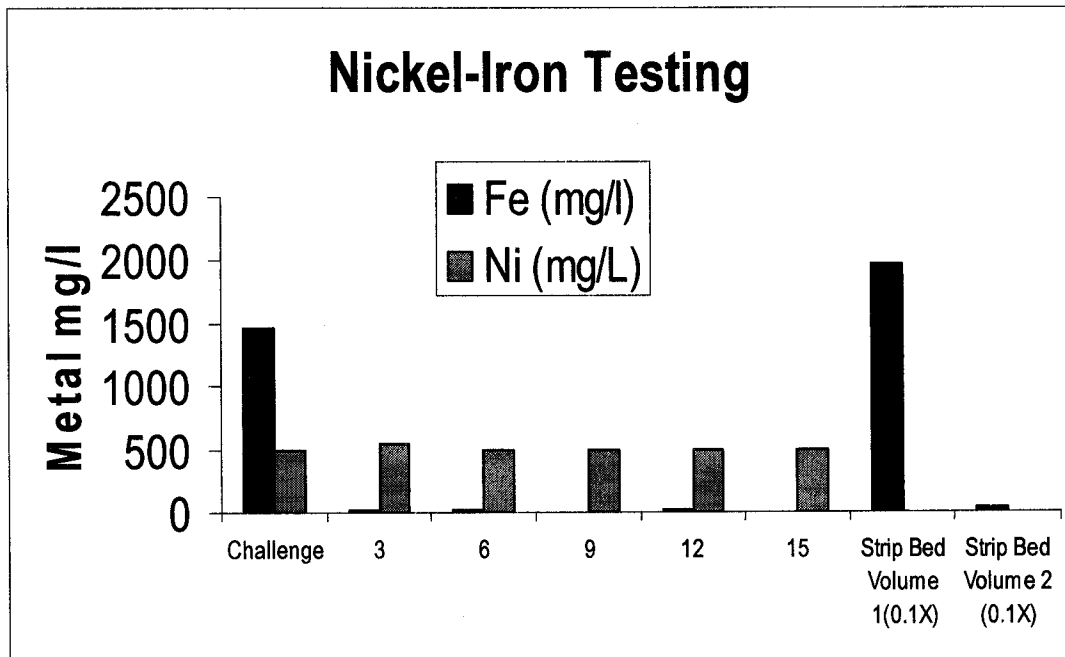


Figure 8.2 Nickel-Iron Flow Through and Strip Results.

Table 8.3 Nickel Iron Strip Results.

	Ferric Strip (mg/L)	Ferric Strip (mg)
Strip 1 (20 mL)	19,680	393.6
Strip 2 (20 mL)	374.8	7.496
	Total	401.096
	Percent Recovery	91.31549

8.2 BPOX pH testing

Additional experimental work was done with nickel and ferric iron in acidic solutions with respect to pH adjustment. The ferric and nickel ion loading was measured at pH of 1.0 and 2.0. The same flow rate, as in previous experimental procedures, was used, however, instead of sampling occurring at every third bed volume, samples were taken every bed volume. Results from pH 1.0 and 2.0 experimental work are shown in Tables 8.4 and 8.3.

Table 8.4. Nickel-Iron Flowthrough at pH 1.0.

	Nickel (mg/L)	Iron (mg/L)
Head	543	1,500
	Ni Flowthrough (mg/L)	Fe Flowthrough (mg/L)
1	0.00	0.00
2	540.3	1.81
3	536.2	3.01
4	507.6	3.36
5	529.8	6.62
6	525.7	16.51
7	513.9	1,352
8	506.4	1,200
9	516.2	1,320
10	521.1	1,380

Table 8.4 showed ferric breakthrough after five bed volumes. Compared the experimental testing at pH 1.5, BPOX has lower affinity for removal of ferric ion from solution. Table 8.5 indicated ferric capacity calculations of 13.89 mg ferric and nickel

capacity 2.73 mg nickel per gram of BPOX gel.

Table 8.5 Nickel-Ferric Loading calculations at pH 1.0.

Nickel Loading (mg/L)	Ferric Loading (mg/L)	Nickel Loading (mg)	Ferric Loading (mg)
543	1498.19	2.715	7.49095
3	1496.99	0.015	7.48495
0	1496.64	0	7.4832
0	1493.38	0	7.4669
0	1483.49	0	7.41745
0	148	0	0.74
0	148	0	0.74
0	300	0	1.5
0	180	0	0.9
0	120	0	0.6
	Total	2.73	41.82345

The pH of the system was adjusted to 2.0 with one molar sodium hydroxide solution and experimental work was repeated. Samples were taken every bed volume and flow rate was consistent with previous experimental work at 0.2 bed volumes per minute. Flow through results can be seen in Table 8.6.

Table 8.6 Nickel-Iron Flowthrough at pH 2.0.

	Ni (mg/L)	Fe (mg/L)
Head	500.3	1,500
Bed Volume	Ni (mg/L)	Fe (mg/L)
1	33.25	2.87
2	50.35	6.25
3	556.3	11.72
4	611.5	16.49
5	922.7	14.27
6	702.8	21.23
7	556.4	15.91
8	549.2	15.55
9	563.0	22.22
10	542.6	44.45

Table 8.7 Nickel-Ferric Loading calculations at pH 2.0.

Ni (mg/L)	Fe (mg/L)	Ni (mg)	Fe (mg)
467	1497.13	2.335	7.48565
450	1493.75	2.25	7.46875
0	1488.3	0	7.4415
0	1483.51	0	7.41755
0	1485.73	0	7.42865
0	1478.8	0	7.394
0	1484.09	0	7.42045
0	1484.45	0	7.42225
0	1477.78	0	7.3889
0	1455.6	0	7.278
	Total	4.585	74.1457

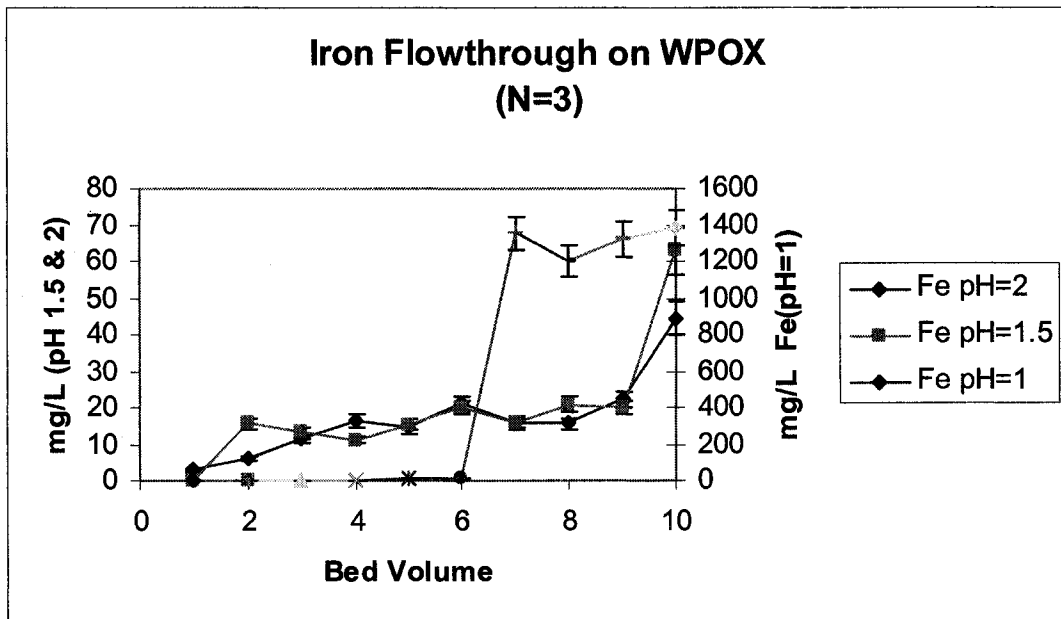


Figure 8.3. Ferric Flowthrough Testing on WPOX

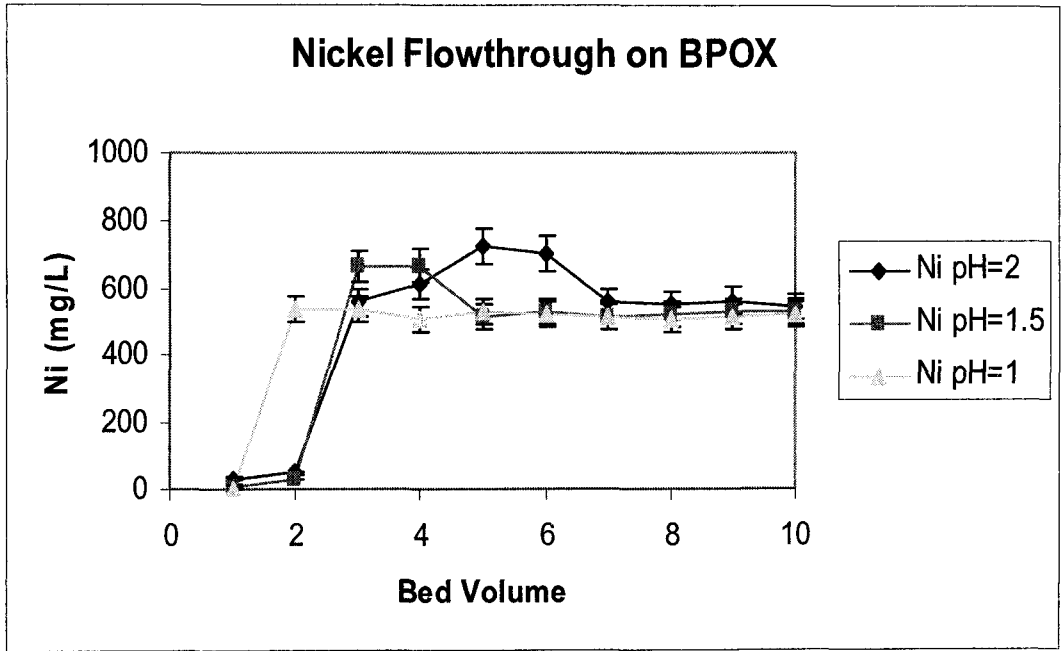


Figure 8.4. Nickel Flowthrough Testing on BPOX.

Table 8.8. Nickel-Ferric Loading Calculations.

pH Testing Value	Ni (mg/g)	Fe (mg/g)
1.0	0.906977	13.89483
1.5	1.591362	24.59326
2.0	1.523256	24.63312

8.3 Nickel-Ferric Conclusions

According to Table 8.8 and Figures 8.3 and 8.4, Crossfield based BPOX shows excellent removal of ferric iron from solution in the presence of nickel. The oxine ligand binds and removes ferric ion from solution with little affinity for nickel. For the oxine based ligand, binding affinity of the gel was preferentially effective in removal of trivalent cations, such as ferric or gallium, from solution. The ligand had little or no affinity for divalent cations such as nickel or ferrous. As the pH of the solution was lowered to 1.0, the ferric iron capacity drops to 50% of higher pH levels of 1.5 and 2.0. As the pH of the solution was raised to 2.0, the capture kinetics of iron are the same as pH 1.5. At pH 2, ferric removal was the highest experimental level which can be achieved. If the solution was raised above pH 2, precipitation of ferric hydroxide will occur from solution.

During experimental testing and loading the oxine based silica gel, over 99% of the ferric was successfully removed from solution at pH 1.5, while 100% of the nickel was passed through the column. Stripping kinetics of ferric from the loaded columns was easily achieved with 91% recovery within the required two column volumes.

An additional literature search was completed for comparison of current iron removal technology using solvent extraction techniques. From literature³³, Kelex-100, which uses an 8-hydroxyquinoline derivative as its ligand, can successfully remove ferric iron from solution. During extraction of iron, several experimental differences occurred from current experimental test work. Initially, pH of known process solvent extraction solutions were measured at 0.5 while BPOX experimental work was completed from pH 1 to 2. Removal of ferric iron was adequate, however, according to BPOX ferric iron

removal, kinetics of iron removal are much slower using solvent extraction compared to silica based ion exchange technology. During solvent extraction, residence times for successful removal of ferric iron were up to 60 minutes while BPOX residence times were 5 minutes to pass solution through columns.

Secondly, from the literature research, metal test solutions were much higher than BPOX experimental test solutions. According to the literature, solvent extraction concentrations were measured between 5 and 20 g/L of ferric iron. After testing, ferric iron was not completely removed and final iron concentrations were lowered to 0.8 g/L. Because of this fact, BPOX has improved kinetics for selective removal of ferric iron from solutions containing low concentrations of ferric iron. From a required discharge standard for iron, BPOX has both excellent affinity and capacity to selectively remove ferric iron from acidic solutions.

Lastly, using Kelex-100, substantial stripping problems occurred with the loaded ferric iron solvent. By using strong sulfuric acid, as in BPOX, ferric would not be selectively strip from the solvent. The ferric iron must be reduced to ferrous before stripping occurs in Kelex-100. By using this technique, both additional cost and steps would occur for successful removal of ferric iron. With a one step stripping process, BPOX has a great advantage over Kelex-100 solvent extraction technology for removal of iron from solution.

Chapter 9. Arsenic and Selenium Removal Using Zirconium(IV) Loaded Silica Polyamine Composites

9.1 Introduction

Arsenic and selenium are extremely toxic elements to human health and the environment³⁴. The development of effective remediation methods for these elements would be beneficial both scientifically and economically. Arsenic can increase lung, kidney, and skin cancer³⁵. Selenium has been found to be harmful to organisms including humans despite being recognized as an essential micronutrient³⁶. Due to these facts, both arsenic and selenium discharge levels continue to become stricter. Water supplies from mining and industrial sources are polluted with high concentrations of these elements. Therefore, the removal of arsenic and selenium from industrial and mining solutions has become increasingly more important. Both arsenic and selenium are predominately present as oxo-anions. The conjugate acids for arsenic(III) is H_3AsO_3 while arsenic(V) is H_3AsO_4 . The conjugate acids for selenium(IV) is H_2SeO_3 while selenium(VI) is H_2SeO_4 . Currently, both co-precipitation and coagulation processes are used for removal of arsenic and selenium³⁷. These processes require large amounts of chemicals and produce a wet bulky sludge. Solvent extraction has been tested; however, its application is limited to pre-concentrated solutions. Recently, experimental tests have shown that aluminum oxide, zirconium(IV) loaded activated charcoal, hydrous zirconium oxide, and lanthanum oxide have a favorable affinity for removal of oxo-anions which are capable of forming weak conjugate acids such as arsenic and selenium. After doing a literature research study on arsenic and selenium removal from aqueous solution, a paper was found for effective removal of arsenic and selenium from test solutions using an EDTA

functionalized polystyrene resin loaded with zirconium(IV)³⁸.

9.2 Zirconium Background

The initial work of Suzuki *et. al.* immobilized zirconium on a specially prepared polystyrene resin containing the ethylenediamine tetraacetic acid (EDTA) ligand using $ZrOCl_2 \cdot 8H_2O$. Using WP-2 instead of using polystyrene based ion exchange resins, several advantages occurred. Since the experimental procedure for placing the zirconium cation uses one molar hydrochloric acid, the silica based WP-2 resin is very robust and stable in strong acidic conditions. Under these strong oxidizing acid conditions for styrene based ion change resins, studies have shown degradation of the styrene based gel. There was a significant advantage for silica based over styrene based ion exchange resins. From Suzuki work, zirconium loading was measured at 0.8mmol/g. Previous WP-2 loading for similar type transition metals was much greater and measured at 40 mg/metal per gram gel. By loading more metal onto the WP-2, the process would greatly enhance removal of oxo-anions from solution by providing more metal sites along with faster kinetics for oxo-anion removal. This provided the impetus for us to try to immobilize the same metal using our previously reported WP-2, a silica polyamine resin functionalized with amino acetic acid groups (Figure 9.1).

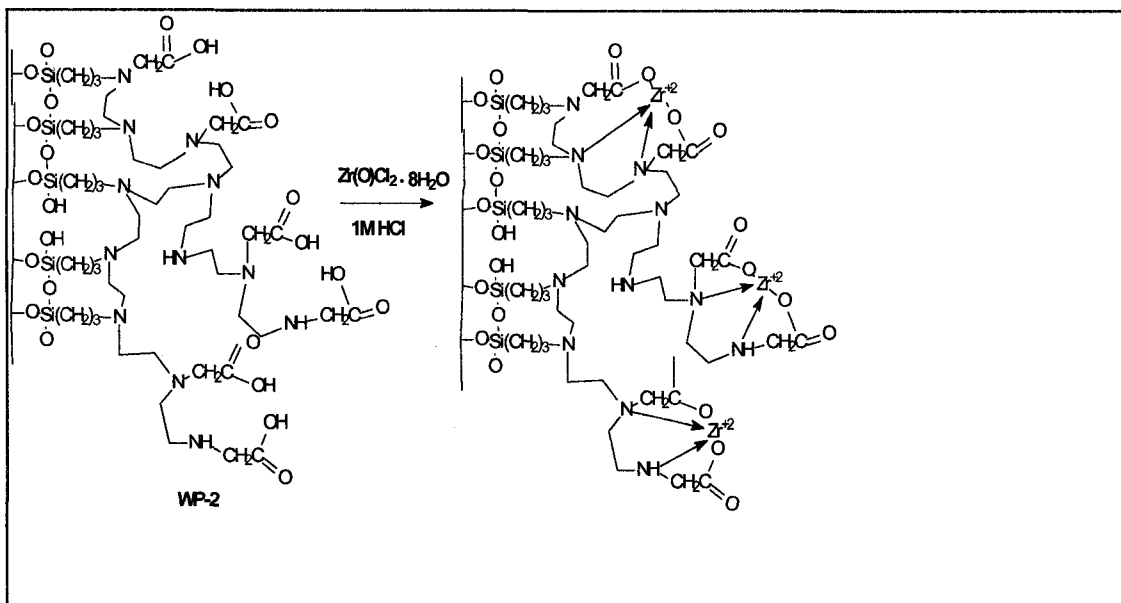


Figure 9.1 Schematic representation of the immobilization of zirconium on WP-2. (WPAN).

During the experimental procedures, aliquot samples were taken before and after the reaction and tested for zirconium loading onto WP-2 using ICP. The experimental procedure was done three times and the results were placed into Table 9.1. According to the data, zirconium loading was measured at 41.09 mg zirconium per gram of gel.

Table 9.1 Zirconium Capacity Loading onto WP-2 Silica Gel.

Experimen Test	Initial Zr Concentration mg/L	Ending Zr Concentration mg/L	Zr Loaded mg/L	Mg Zr Loaded	WP-2 Capacity
1	81,330	71,110	10,220	2,044	40.88
2	75,920	70,700	5,220	1,044	41.76
3	76,230	71,150	5,080	1,016	40.64
				Average	41.09

Zirconium loading onto the resin averaged about 40mg/g resin (0.46 mmol/g). Based on elemental analysis of the starting resin and the zirconium loading, it was estimated that approximately two amino acetic acid residues are bound to each

zirconium. The zirconium loading was lower than reported by Suzuki *et. al* (0.8 mmol/g) and the properties of the materials were different in interesting ways. The resin was referred to as WPAN from now on.

A potential research problem using WPAN silica gel was stripping kinetics. Since the resin showed excellent potential for remove of arsenic from solution, the resin must be able to effective strip the oxo-anion and be able to regenerate the resin effectively. By loading and stripping the oxo-anions repeatedly, the silica resins would be more viable commercially for removal of arsenic from solution. From the research paper³⁶, previous stripping techniques for removal of oxo-anions used one molar sodium hydroxide solution. From previous experimental work, using the strong alkaline base with silica based resin had devastating effects on the silica backbone of the gel itself. Silica gel was easily dissolved in strong bases and cannot be used for stripping of the oxo-anions such as arsenic and selenium. Several different experimental stripping procedures were tested and evaluated using WPAN resin on both arsenite and arsenate anions. Procedures included using synthetic mock solutions as well as real mining test solution acquire from a smelter located in East Helena, Montana.

9.3 WPAN Experimental Strip Study

After several experimental attempts for removal and stripping of selenium and arsenic using BPAN silica technology, the results had shown poor stripping kinetics. Further experimental research was attempted and included using hydrochloric acid, sulfuric acid, and sodium phosphate brine strips. The research goal was to find a stripping method capable of removing both arsenic and selenium species from zirconium loaded WPAN resin. Experimental stripping results are seen in Tables 9.2 to 9.3.

Table 9.2. Hydrochloric Acid Stripping Results.

	mg/L selenium	
Head	244.5	
Bed Volume	mg/L selenium	Mg selenium loaded
4	8.827	28.28
8	5.347	28.70
12	5.258	28.71
Stripping Bed Volume	Total	85.69
1	96.66	1.93
2	80.56	1.61
3	67.88	1.36
4	35.71	0.71
5	25.85	0.52
	mg recovered	6.13
	Percent Recovery	7.16

According to Table 9.2, hydrochloric acid had shown little effect on stripping of selenium loaded WPAN. The percent recovery using this method yielded only 7.16% of recovered selenium from solution.

Table 9.3. Sulfuric Acid Stripping Results.

	mg/L Se	
Head	123.2	
Bed Volume	mg/L Se	mg selenium loaded
4	0.00	14.78
8	0.00	14.78
12	0.00	14.78
16	0.00	14.78
Stripping Bed Volume	Total	59.14
1	10.23	0.20
2	175.9	3.52
3	432.6	8.65
4	663.9	13.28
	584.1	11.68
	mg recovered	37.33
	Percent Recovery	63.13

Using sulfuric acid, as the stripping reagent, better results were produced with

hydrochloric acid, however, according to experimental data, only 63% of the selenium was recovered from WPAN. The goal was to completely remove selenium from WPAN for potential regeneration and reuse the experimental WPAN column for further testing.

Table 9.4. Sodium Phosphate Strip.

20 mL Sample	Se mg/L	mg stripped
1	157.6	3.152
2	674.2	13.484
3	418.4	8.368
4	158.7	3.174
5	75.68	1.5136
6	49.75	0.995
7	35.08	0.7016
8	29.67	0.5934
9	24.64	0.4928
10	22.33	0.4466
	Total mg	32.921
	% Recovery	75.921314

Table 9.5. Sulfuric Acid Strip.

20 mL Sample	Se mg/L	mg stripped
1	24.98	0.4996
2	159.9	3.198
3	73.59	1.4718
4	19.39	0.3878
5	8.29	0.1658
6	30.11	0.6022
	Total mg	6.3252
	% Recovery	14.586966

For selenite stripping, phosphate (Tables 9.4 and 9.5) showed excellent capabilities of removal of selenite from WPAN. By using the sodium phosphate strip, over 75% of selenium was effectively removed from solution. Removing of phosphate from WPAN, an additional 15% of selenite was removed from solution. Overall 100% of selenite was completely removed from solution, and 90% was recovered from the loaded column.

9.4 Selenate Flow Through Experimental Testing

The initial head solution contained 134.6 mg/L selenium and 80 mg/L sulfate. Table 9.6 indicated excellent removal capabilities of selenate from solution using WPAN. After 10 bed volumes, flow through data was still below ICP detection limits. The additional experimental work was performed to duplicated to verify completed stripping using pH=4 100g/L phosphate solution followed by sulfuric acid. Samples were collected from loaded selenate column and analyzed using ICP. Results are shown in Table 9.7.

Table 9.6. Duplicate Experimental Work for Selenate Strip Data.

	Head mg/L	134.6
Head Se(mg/L)	ICP	
Bed Volume	Se mg/L	Se mg loaded
1	0.00	4.818
5	0.00	19.272
10	0.00	24.09
	Total	48.18

Table 9.7. Selenate Flow Through Data.

20 mL Sample	Se mg/L	Se mg stripped
1	1,139	22.78
2	680.6	13.612
3	379.5	7.59
4	57.49	1.1498
5	22.56	0.4512
6	20.17	0.4034
7	17.15	0.343
8	16.09	0.3218
9	13.86	0.2772
10	12.82	0.256
	Total	47.1844
	% Recovery	97.933582

Table 9.7 showed excellent recovery of selenate from selenium loaded WPAN.

According to the experimental data, 100% of the loaded selenium was removed from the column using the 100 g/L pH 4 phosphate solution followed by sulfuric acid.

9.5 Batch Testing for Selenate

An experimental study to calculate selenium capacity on WPAN was performed using batch tests. Both selenium species were observed for batch capacity using WPAN. Batch capacity results can be observed in Table 9.8.

Table 9.8. Selenate Capacity Calculations.

Batch Number	Se mg/L	Selenate Load	Selenate Capacity
Head	5,635	mg/L	mg/G gel
1	4,125	1,510	30.2
2	4,274	1,361	27.22
3	4,280	1,355	27.1
	Average	1,408	28.17

Batch capacities for removal of selenate species from solution were very good. For selenate, the capacity was calculated at 28.17 mg selenate per gram of WPAN.

9.6 Flow Testing for Selenate Species.

Additional experimental work was performed to calculate the flow capacity for selenate species on WPAN. The work consisted of using synthetic solutions which contained a high concentration of selenate. While making the synthetic solutions, additional sulfate was added to the system by pH adjustment to 4 using two molar sulfuric acid. Both sulfate and selenate breakthrough curves can be observed in Figure 9.2 and Figure 9.3 and results for selenium and sulfate loading were calculated and can be observed in Tables 9.9 and 9.10.

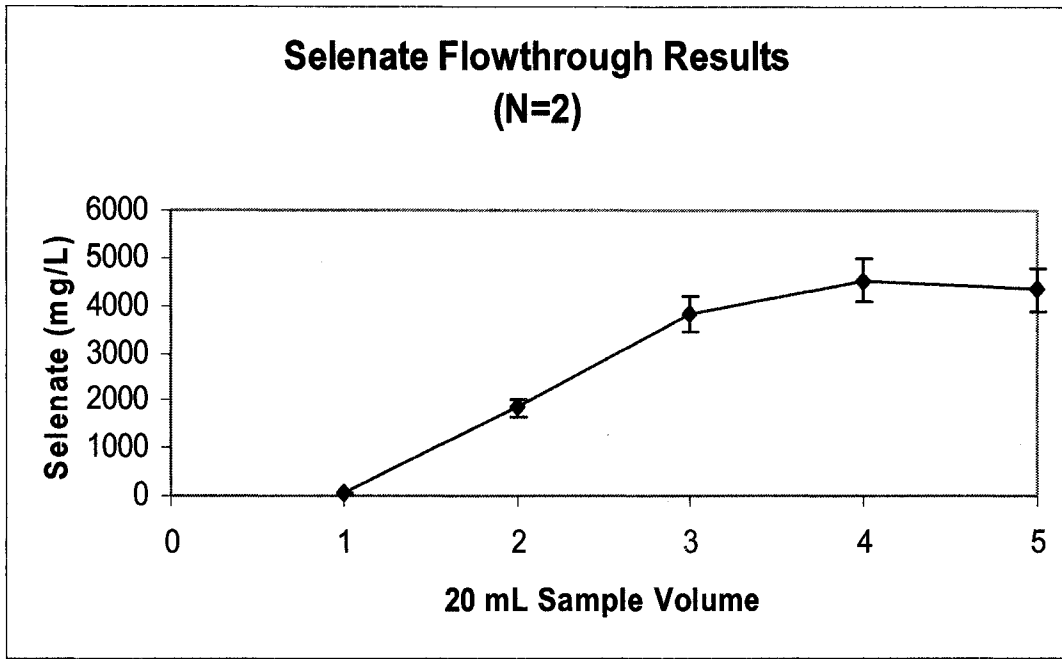


Figure 9.2. Selenate Breakthrough Curve.

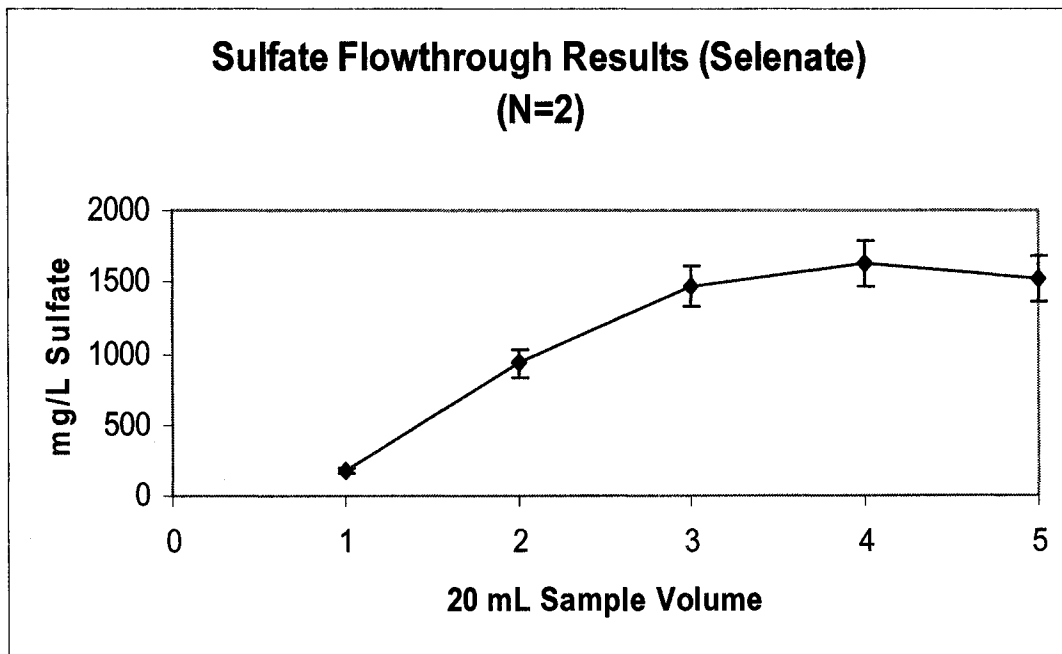


Figure 9.3. Sulfate Breakthrough Curve with Selenate.

Table 9.9. WPAN Loading Calculations of Selenate.

	Selenate Head (mg/L)	5,649
20 mL Sample Volume	Selenate Load mg/L	Selenate Load mg
1	5,607	112.15
2	3,816	76.32
3	1,825	36.50
4	1,113	22.26
5	1,316	26.32
	Total	273.55
	Selenate Capacity	27.35

Table 9.10. WPAN Loading Calculations of Sulfate in Presence of Selenate.

	Sulfate Head (mg/L)	1,469
20 mL Sample Volume	Sulfate Load (mg/L)	Sulfate Load mg
1	175.6	25.87
2	931.5	10.75
3	1,468	0.02
4	1,624	0.00
5	1,524	0.00
	Total	36.64
	Sulfate Capacity	3.66

Both Figures 9.2 and 9.3 and Table 9.9 and 9.10 showed excellent results and capacities for selenate in solution. Even though some sulfate was co-loaded, WPAN removed selenate from solution in the presence of sulfate. Flow capacities were calculated at 27.55 mg selenium per gram of WPAN gel. Compared to the value of the batch testing of 28.17 mg selenium per gram of gel, the results are within experimental error and showed fast kinetics for selenate removal from solution. Sulfate calculation showed a capacity of 3.66 grams of sulfate per gram of gel.

9.7 Flow Testing for Selenite Species.

Further experimental work was performed to calculate the flow capacity for selenite species on WPAN. The work consisted of using synthetic solutions which contained a high concentration of selenite. While making the synthetic solutions, additional sulfate was added to the system by pH adjustment to 4 with 2 molar sulfuric acid. Both sulfate and selenite breakthrough curves are observed in Figures 9.4 and 9.5 and results for selenium and sulfate loading were calculated and can be observed in Tables 9.11 and 9.12.

The initial head solution contained 5,635 mg/L selenium and 1,428 mg/L sulfate. Table 9.11 have shown excellent capabilities for removal of selenite from solution using WPAN. Both sulfate and selenite breakthrough curves are seen in Figures 9.4 and 9.5 and results for selenium and sulfate loading were calculated and observed in Tables 9.11 and 9.12.

Table 9.11. WPAN Loading Calculations of Selenite.

	Selenite Head (mg/L)	5,635
20 mL Sample Volume	Selenite Load mg/L	Selenite Load mg
1	5,429	108.59
2	4,327	86.54
3	3,273	65.46
4	2,278	45.56
5	1,604	32.08
	Total	338.23
	Selenite Capacity	33.82

Table 9.12. WPAN Loading Calculations of Sulfate in Presence of Selenite.

	Sulfate Head (mg/L)	1,428
20 mL Sample Volume	Sulfate Load (mg/L)	Sulfate Load mg
1	1,252	25.04
2	496.5	9.93
3	0.00	0
4	0.00	0
5	0.00	0
	Total	34.97
	Sulfate Capacity	3.50

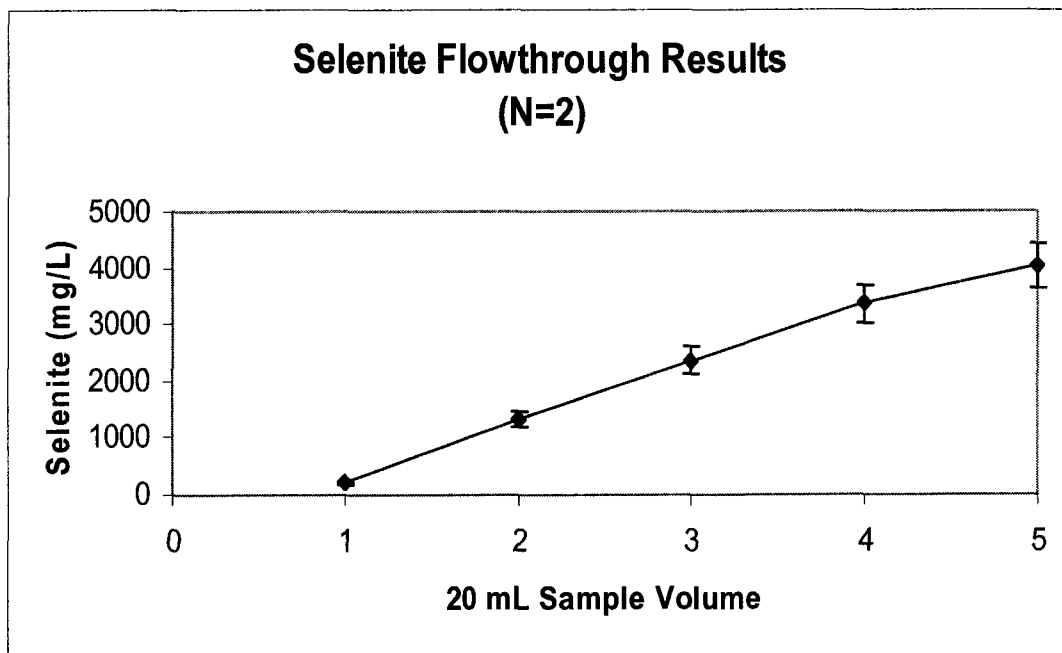


Figure 9.4. Selenite Breakthrough Curve.

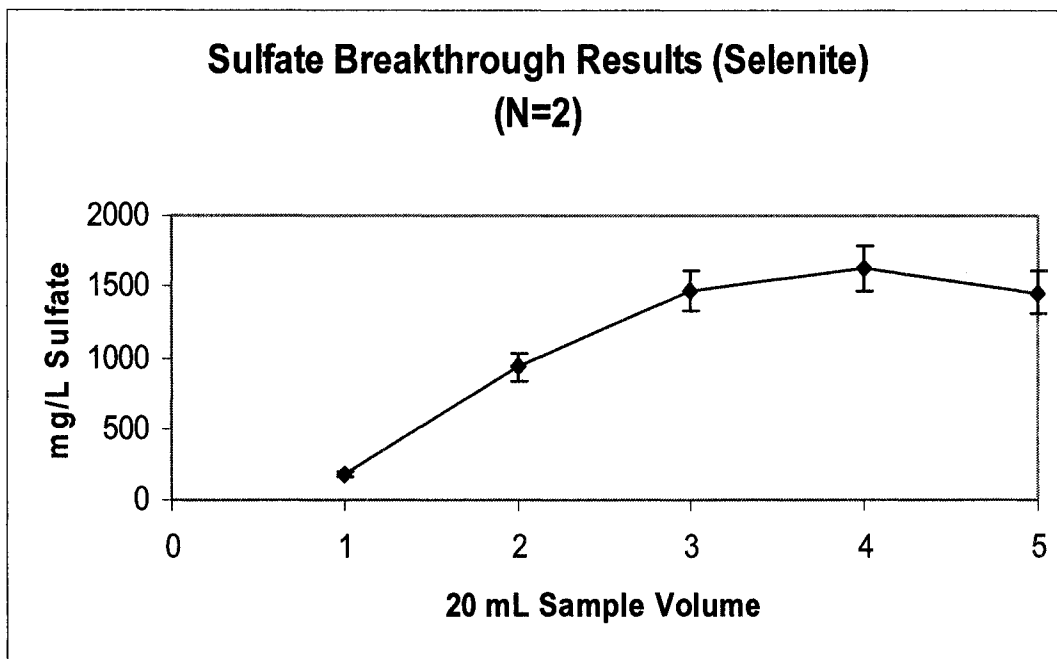


Figure 9.5. Sulfate Breakthrough Curve with Selenite.

For selenite species in the presence of sulfate, WPAN has excellent potential to successfully remove the selenite species from solution. The flow capacities were calculated for selenite at 33.82 mg selenite per gram of WPAN gel while sulfate capacities were calculated at 3.50 mg sulfate per gel gram. Compared to the batch capacities studies of selenite of 39.4 mg per gel gram, selenite kinetics are comparable to batch studies. Because the both batch and flow capacities were similar, kinetics were very fast for removal of selenite from solution in the presence of sulfate.

9.8 Selenium Process Test Solution Experimental Work

Further experimental work was tested on a mine waste solution from Kennecott Inc. located in Magma, Utah. The solution was contaminated with selenium and sulfate. The initial test solution was measured for selenium and sulfate on ICP. Selenium concentrations were 0.939 mg/L while measured sulfate was 80.23 mg/L. Since the

solution speciation of selenium has little effect on WPAN removal capabilities, speciation was not done. Results can be observed in Figures 9.6 and 9.7 and Tables 9.13 and 9.14.

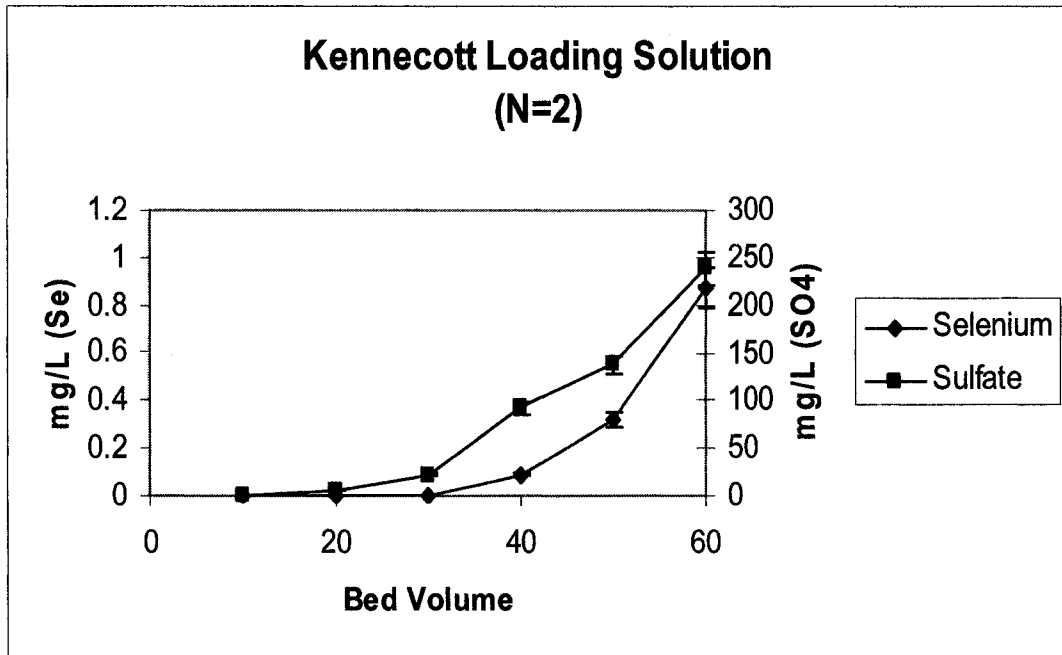


Figure 9.6. Kennecott Flowthrough Curve.

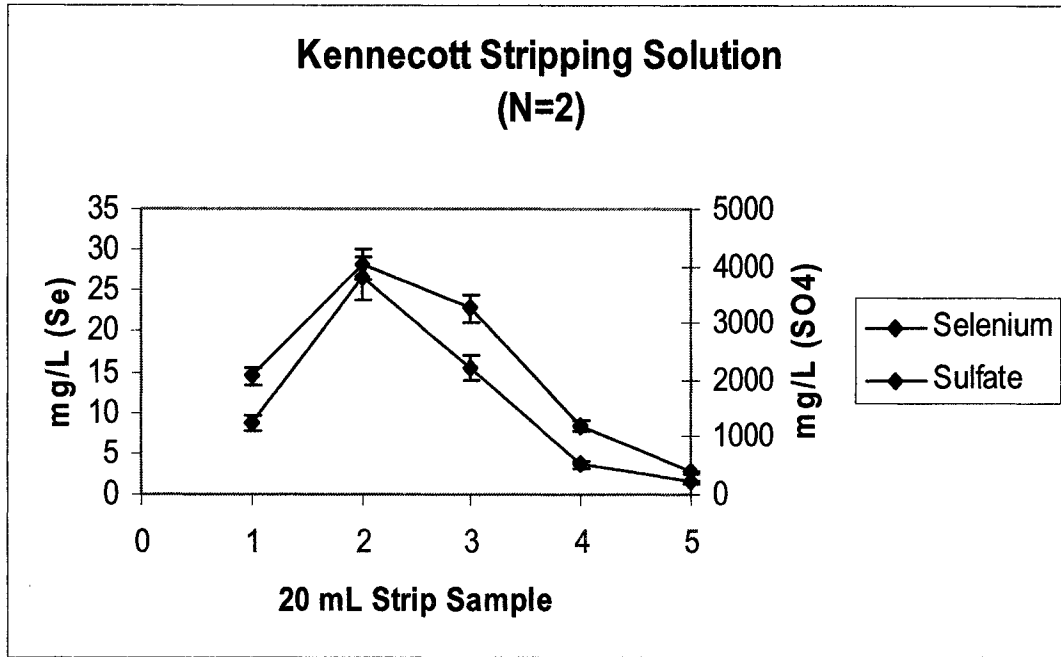


Figure 9.7. Kennecott Stripping Curve.

Table 9.13. Kennecott Flowthrough Data.

Bed Volume	Selenium (mg/L)	Sulfate (mg/L)
10	0.00	0.5499
20	0.00	5.23
30	0.00	21.91
40	0.089	91.77
50	0.3209	137.7
60	0.8701	237.8

Table 9.14. Kennecott Stripping Data.

20 mL sample	Selenium (mg/L)	Sulfate (mg/L)
1	8.59	2,069
2	26.54	4,029
3	15.54	3,257
4	3.577	1,180
5	1.533	379

Using a real process solution, such as Kennecott solution, excellent results occurred. During the first 40 column volumes, solution breakthroughs, less than 10 ug/L, were observed. After 40 column volumes, selenium began to breakthrough. It

was noted that co-loading of sulfate also occurred, however, by using a slower flow rate, selenium may remove sulfate from WPAN. For selenium, mass balances were excellent. According to Table 9.15, over 85% of selenium was recovered in the pH phosphate strip.

Table 9.15. Selenium Mass Balance.

Head	Se (mg/L)	0.939	
Bed Volume	Se Load (mg)	20 mL sample	Se Strip (mg)
10	0.2817	1	0.1718
20	0.2817	2	0.5308
30	0.2817	3	0.3108
40	0.255	4	0.07154
50	0.18543	5	0.03066
60	0.02067		
Total	1.3062	Total	1.1156
		Percent Recovery	85.4080539

9.9 Batch Testing for Arsenite and Arsenate Species

Batch testing procedures were also done on arsenic species which include arsenite and arsenate. Both arsenate and arsenite species were observed for batch capacity using WPAN. Batch capacity results can be observed in Tables 9.16 and 9.17.

Table 9.16. Arsenate Batch Capacity.

Batch Number	Arsenate mg/L	Arsenate Load	Arsenate Capacity
Head	5,196	mg/L	mg/G gel
1	3,852	1,344	26.88
2	3,765	1,431	28.62
3	3,826	1,370	27.4
	Average	1,381	27.63

Table 9.17. Arsenite Batch Capacity.

Batch Number	Arsenite mg/L	Arsenite Load	Arsenite Capacity
Head	4,645	mg/L	mg/G gel
1	4,274	371	7.42
2	4,282	363	7.26
3	4,340	305	6.1
	Average	346.33	6.93

Excellent results for removal of oxidized arsenic species from solution were

produced. WPAN batch capacities were calculated at 27.63 mg arsenate per gram of WPAN gel. The resin showed excellent potential for removing arsenate species. Observation of Table 9.17, arsenite batch capacity, indicated that arsenite removal from solution was fair compared to arsenate results. Batch capacities were much lower at 6.93 mg arsenite per gram of gel. Because of the different protonated species of the arsenate and arsenite (Figure 9.8 and 9.9), different capture kinetics for each species can be observed.

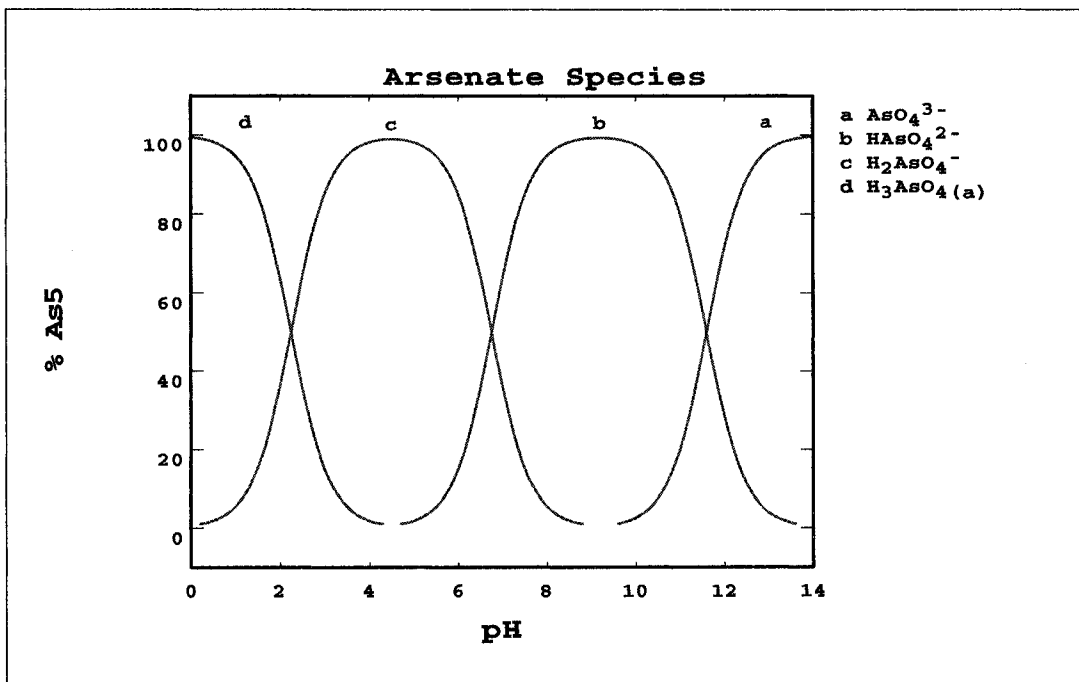


Figure 9.8. Arsenate Species in Aqueous Systems.

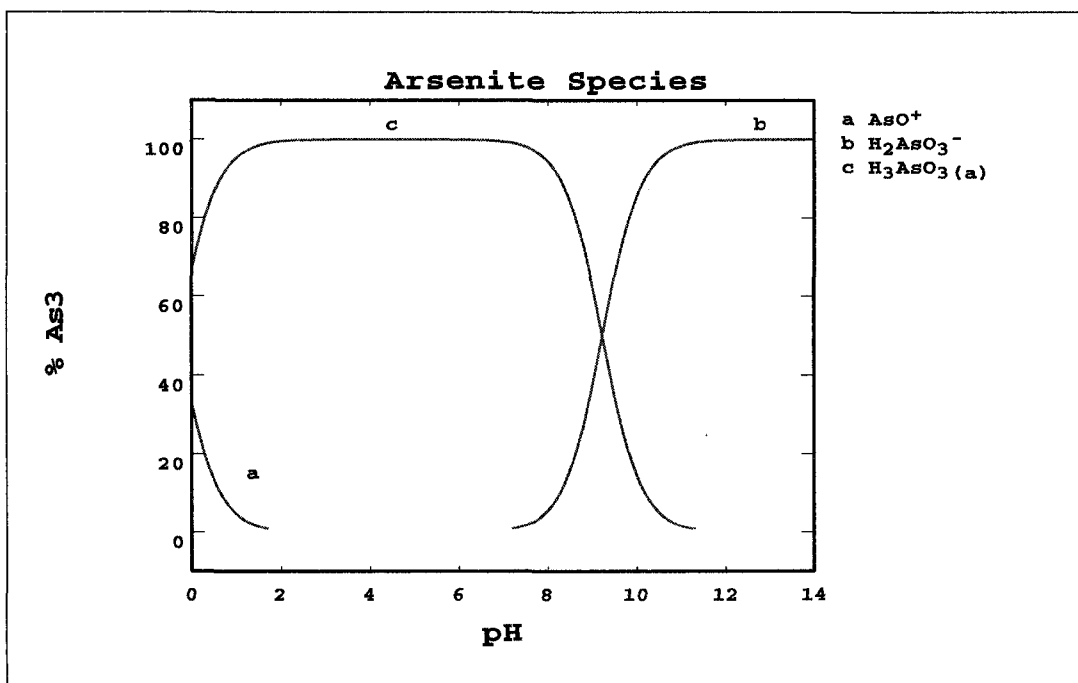


Figure 9.9. Arsenite Species in Aqueous Systems.

According to the Figures, WPAN produced adequate removal of arsenate at pH 4 while arsenite removal had shown lower capture kinetics. By using STABCAL solubility modeling diagrams, it was shown that the species for arsenate at pH 4 was HAsO_4^{-2} and had a strong affinity to adsorb onto the zirconium loaded WPAN. Because the zirconium contained a highly positively charged ion, the negatively charged arsenate ion can easily bind to the resin. However, because of the chemistry of arsenite at pH 4, the molecule was neutral. The species at this pH was H_3AsO_3 , therefore, did not have the negatively charged molecule needed to bind to the positively charged zirconium ion.

9.10 Flow Testing for Arsenite and Arsenate Species

Initial testing of arsenic solutions consisted of dissolving arsenic salts into solution and adjusting to pH 4 with sulfuric acid. Results for arsenate and arsenite

removal can be observed in Tables 9.18 and 9.19.

Table 9.18. Arsenite Flowthrough Results.

Arsenite Loading	Arsenite Head	168.5
Head As(mg/L)	ICP Value	
BV FT	mg/L	mg loaded
1	13.07	4.6629
5	161.9	0.792
10	167.8	0.084
	Total	5.5389

Observation of Table 9.18 showed similar results in removal of arsenite from solution in flow through testing. As shown in batch studies, at pH 4 arsenite was not removed from solution using WPAN.

Table 9.19. Arsenate Flowthrough Results.

Arsenate Loading	Arsenate Head(mg/L)	168.5
Head As(mg/L)	ICP Value	
BV FT	mg/L	mg loaded
1	0.00	5.055
5	0.00	20.22
10	0.00	25.275
	Total	50.55

Table 9.20. Phosphate Strip Results.

20 mL PO4 Strips	As (mg/L)	As mg stripped
1	0.00	0.00
2	404.7	8.09
3	940.8	18.82
4	461.4	9.23
5	147.2	2.94
6	64.2	1.28
7	37.99	0.76
8	29.17	0.58
9	23.43	0.47
10	19.05	0.38
	Total	42.56
	% Recovery	84.19

Table 9.21. Sulfate Strip Results.

20 mL SO4 Strips	As(mg/L)	As mg stripped
1	17.06	0.3412
2	47.63	0.9526
3	327.7	6.554
4	101.8	2.036
5	21.13	0.4226
6	8.07	0.1614
	Total	10.4678
	% Recovery	20.70781

Results from Tables 9.20 and 9.21 indicated excellent removal and stripping of arsenate from solution using WPAN. Since results were similar to batch testing, capture kinetics were very fast for removal of arsenate from solution. Since breakthrough never occurred, it was impossible to calculate flow through capacity of arsenate. During stripping of arsenic from WPAN, 84.19% of arsenic was successfully removed from the column, further stripping was done using sulfuric acid. Mass balances show complete recovery of arsenic using WPAN. Since 20% of arsenic was left on the gel after phosphate stripping, poor rinsing could have occurred of remaining phosphate and arsenic on the column. Since breakthrough never occurred, it was impossible to calculate loading capacity. Further experimental work with higher arsenic solutions for complete saturation of arsenic onto the gel was done to calculate flow capacity.

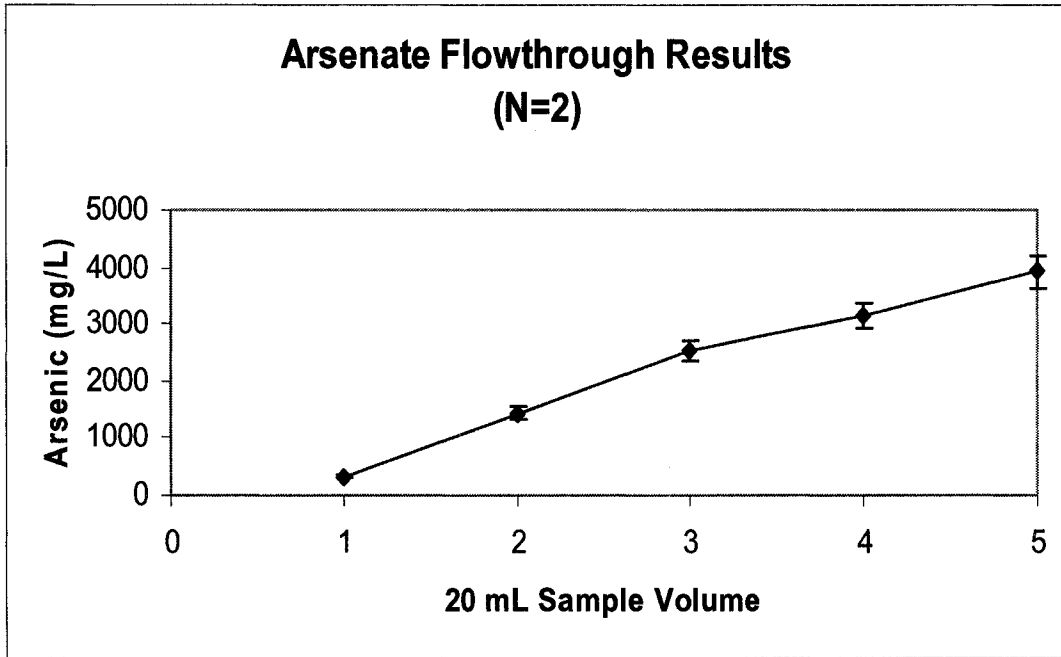


Figure 9.10. Arsenate Flow Through Results.

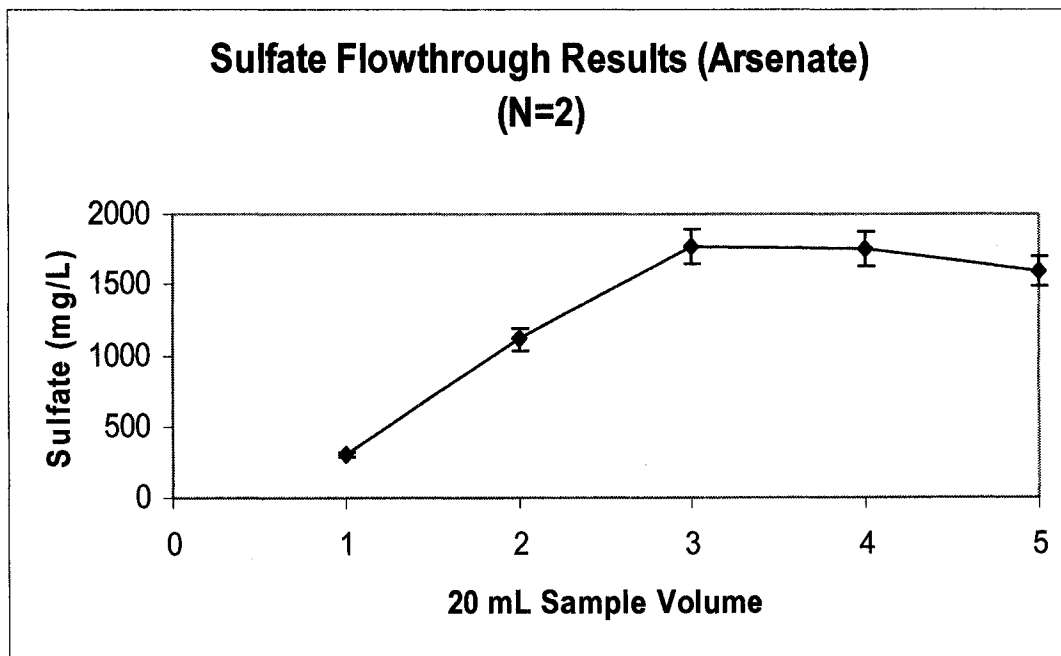


Figure 9.11. Sulfate Flow Through Results in Arsenate Solution.

Table 9.22. Arsenate Capacity Calculations.

	Arsenate Head (mg/L)	5,196
20 mL Sample Volume	Arsenate Load (mg/L)	Arsenate Load mg
1	4,875	97.50
2	3,762	75.24
3	2,662	53.24
4	2,041	40.82
5	1,280	25.6
	Total	292.40
	Arsenate Capacity	29.24

Table 9.23. WPAN Loading Calculations of Sulfate in Presence of Arsenate.

	Sulfate Head (mg/L)	1,224
20 mL Sample Volume	Sulfate Load (mg/L)	Sulfate Load mg
1	921.2	18.42
2	116.3	2.32
3	0.00	0
4	0.00	0
5	0.00	0
	Total	20.74
	Sulfate Capacity	2.07

Experimental data (Tables 9.22 and 9.23) indicated WPAN had a high capacity for removal of arsenate species from solution even in the presence of a small amount of sulfate. Since the capacity was measured at 29.24 mg of arsenate per gram of WPAN gel, the kinetics for arsenate removal are very fast and comparable to batch capacity of 27.63 mg of arsenic per gram of WPAN gel. Sulfate loading of WPAN was measured at 2.07 mg sulfate per gel gram. This data was similar to selenium species testing of sulfate which was measured at 3.5 mg sulfate per gel gram. Overall, arsenate has a strong binding affinity at pH 4 for zirconium loaded silica gels.

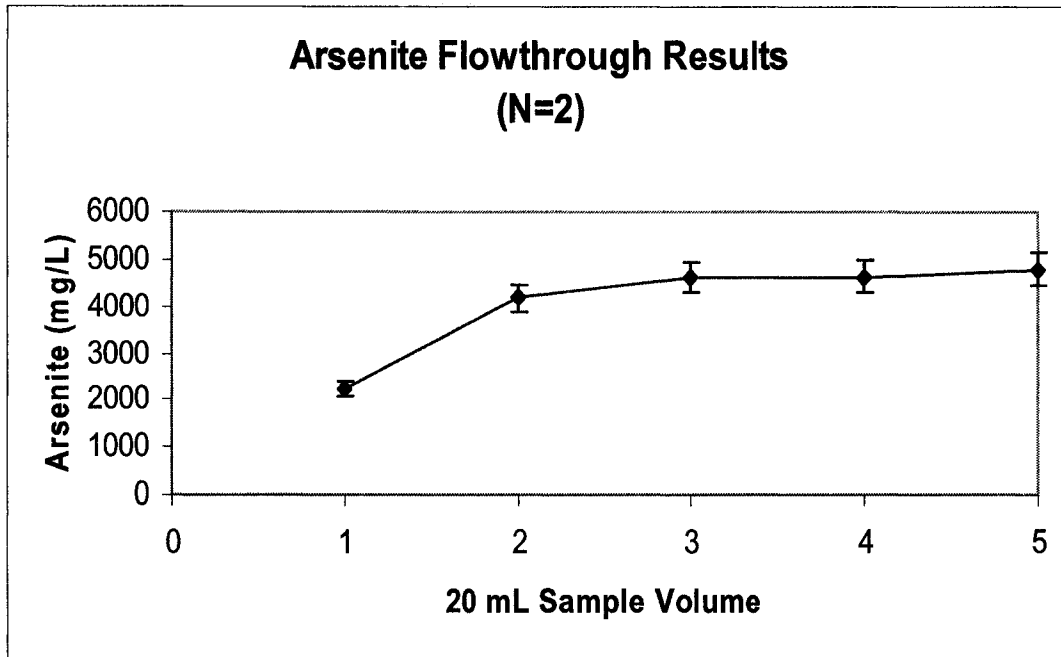


Figure 9.12. Sulfate Flow Through Results in Arsenite Solution.

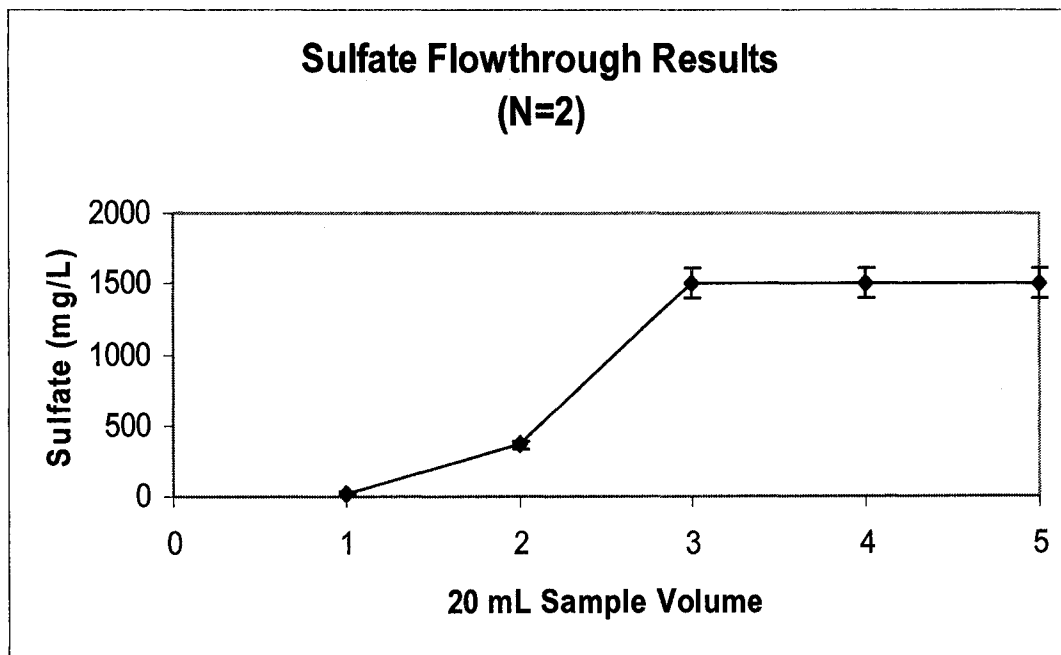


Figure 9.13. Sulfate Flowthrough Results in Presence of Arsenite.

Table 9.24. Arsenite Capacity Calculations.

	Arsenite Head (mg/L)	4,645
20 mL Sample Volume	Arsenite Load mg/L	Arsenite Load mg
1	2,400	48
2	473	9.46
3	45.23	0.9
4	0.00	0
5	0.00	0
	Total	58.36
	Arsenite Capacity	5.84

Table 9.25. WPAN Loading Calculations of Sulfate in Presence of Arsenite.

	Sulfate Head (mg/L)	1,481
20 mL Sample Volume	Sulfate Load (mg/L)	Sulfate Load mg
1	1,455	29.10
2	1,115	22.31
3	0.00	0
4	0.00	0
5	0.00	0
	Total	51.41
	Sulfate Capacity	5.14

As seen with previous batch testing data (Table 9.24 and 9.25), WPAN has little affinity for arsenite from solution at pH 4. Because of the neutral charged ion (H_3AsO_3), the positively charge zirconium had little effect on removal of arsenite from solution. The WPAN arsenite capacity was calculated at 5.84 mg arsenite per gram of gel. Previous batch results show a capacity of 6.93 mg arsenite per gram of WPAN gel. This data confirms that the neutrally charged reduced species of arsenite has little binding capacity at flow through kinetics as well as the slower batch kinetic experiments.

9.11 Arsenic Mining Process Solution Flow Through Testing

An arsenic bearing mining process should was obtained from East Helena, Montana. The solution contained 7.2 mg/L of arsenic. Flow through results can be seen in Figure 9.14 and 9.15 and Table 9.26 and 9.27.

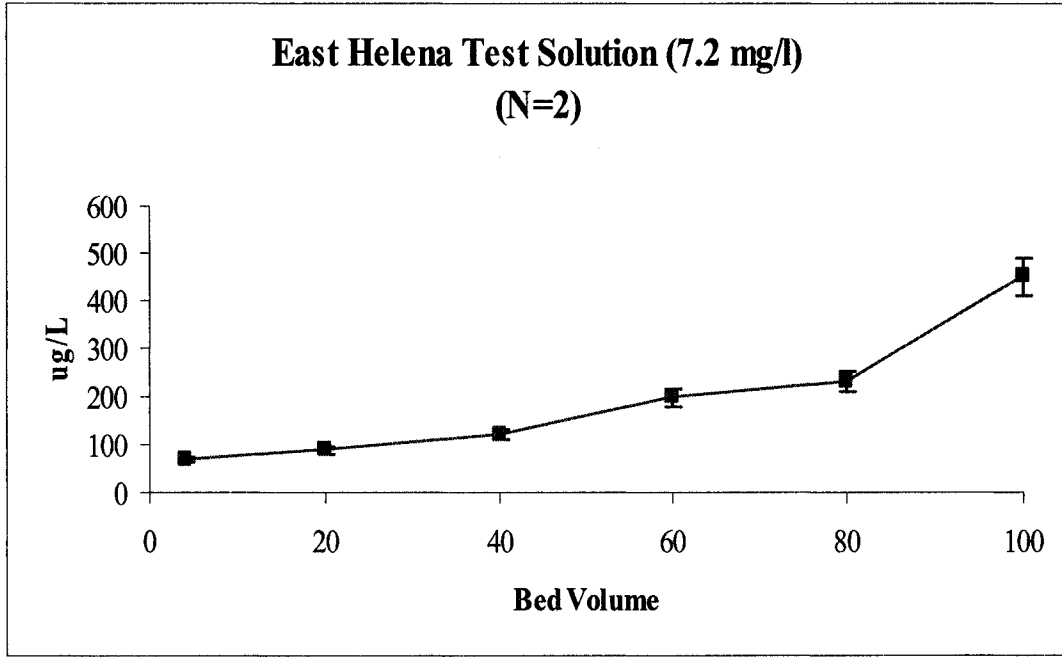


Figure 9.14. Flowthrough Results of East Helena Solution

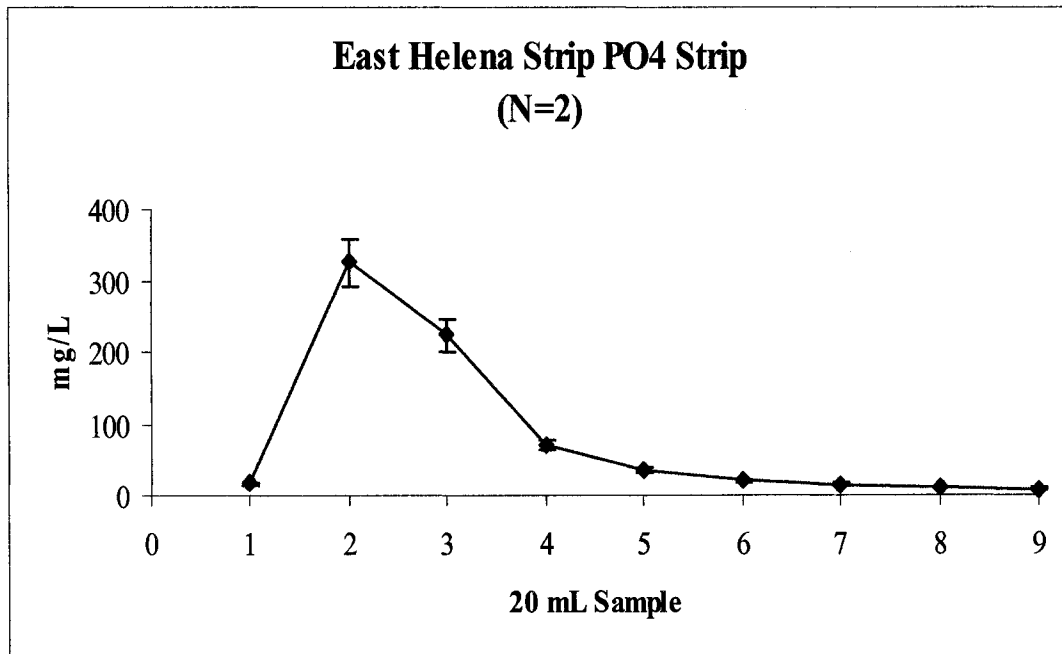


Figure 9.15. Strip Results of East Helena Solution.

Table 9.26. Flowthrough Results of East Helena Solution.

Bed Volume	As (ug/L)	As Loading
4	67.6	0.855888
20	89.3	3.413136
40	118.7	4.24878
60	197.4	4.20156
80	230.1	4.18194
100	450.1	4.04994
	Total	20.951244

Table 9.27. Strip Results of East Helena Solution.

Strip	As (mg/L)	As Loading
1	17.06	0.5118
2	325.2	9.756
3	223.6	6.708
4	68.81	2.0643
5	33.56	1.0068
6	20.33	0.6099
7	14.55	0.4365
8	10.93	0.3279
9	8.38	0.2514
	Total	21.6726
	Percent Recovery	103.443

WPAN results of the East Helena mining solution had shown significant breakthrough of arsenic compared to previous results. Further indications of the poor results come from pH adjustment. The initial process solution pH was 9 and was never adjusted to the proper pH level of 4. At this pH the species of arsenic in solution was HAsO_4^{2-} instead of the species at pH 4 of H_2AsO_4^- . This speciation could have a dramatic effect on arsenic removal from solution using WPAN. Secondly, because the initial addition of potassium permanganate was not mixed properly in the solution, not all of the arsenic may have been oxidized to arsenate. Previous experimental results show that arsenite in solution is not easily removed using zirconium loaded silica polymers.

9.12 East Helena Solution Second Experimental Research

Because of the poor results for arsenic removal, a second set of experiments were performed for removal of arsenic from solution in the East Helena Process Solution (Figure 9.16 and Table 9.28)

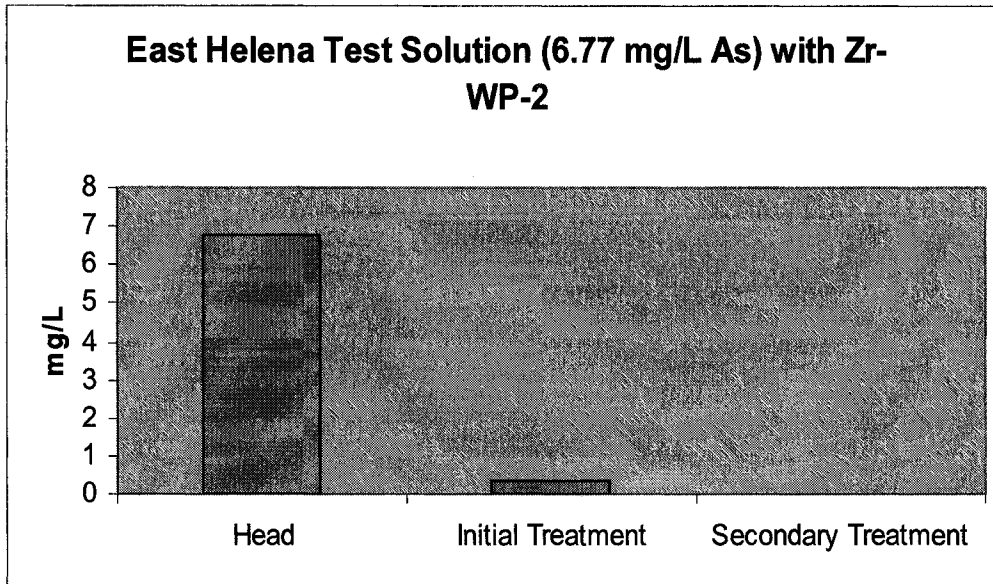


Figure 9.16. East Helena Experimental Work.

Table 9.28. Experimental Results of Second East Helena Testing Solution.

	As(mg/L)	Percent Retained	Percent Removed
Head	6.771	100	0
FT 1	0.3278	4.841235	95.15877
FT2	0.01245	0.183872	99.81613

Further experimental work indicated excellent removal of arsenic using the East Helena process test solution. After the first pass using WPAN, over 95% of the arsenic was effectively removed from solution. The second pass removed over 99.8% of arsenic from the test solution. It was important to note that pH and speciation of arsenic are very important parameters for effect removal of arsenic from solution.

9.13 WPAN Testing on Arsenic and Sulfate Solution.

Purity System Inc. received a sample from the Zortman-Landusky mine located near Yellowstone National Park³⁹. Initial concentrations of the solution were measured and contained 283 ug/L arsenic and 150.2 mg/L sulfate. Sulfate concentration was important due to its negative anion charge and may compete for the zirconium(IV) sites on the gel. The goal was to selectively remove arsenic to less than ICP detectable levels, less than 5 ug/L, using WPAN silica gel. Flow rates for the testing procedure were 0.2 bed volumes per minute. Samples were taken every bed volume and analyzed for arsenic and sulfate.

9.14 WPAN Results on Arsenic and Sulfate Solution

According to Figure 9.17, arsenic removal with sulfate competition using WPAN produced excellent results. Even after 50 bed volumes of test solution, arsenic concentrations were below ICP detection limits. According to the data, zirconium(IV) had a high affinity for effective removal of arsenic in competition with sulfate in solution.

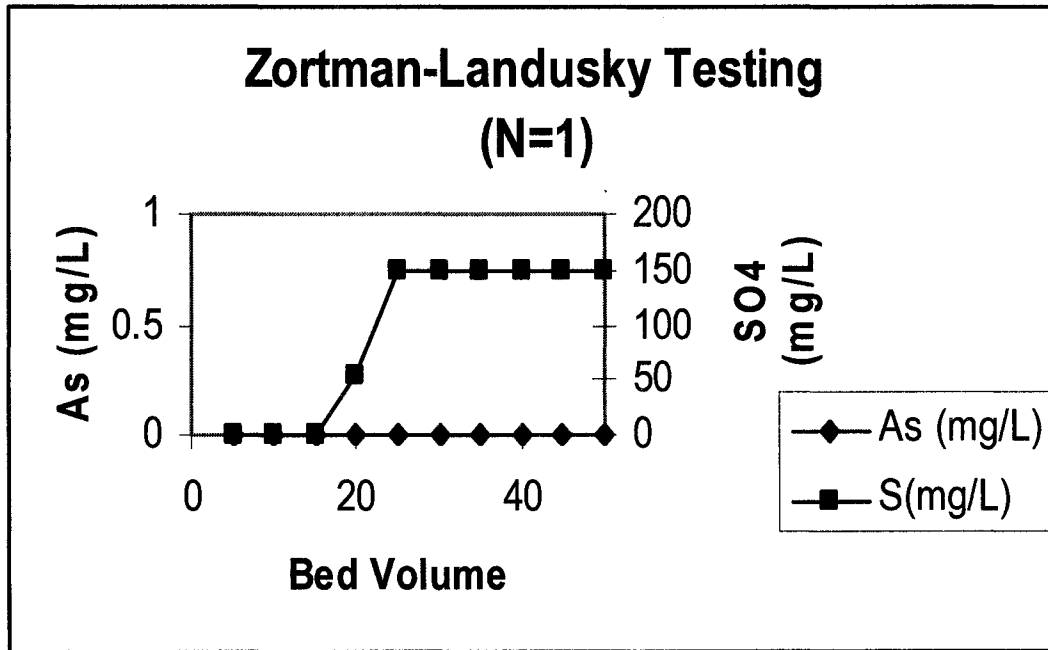


Figure 9.17. WPAN Results on Arsenic and Sulfate Solution.

9.14 Montana Tech Design Team Solution

In 2004, an environmental design competition was held in Las Cruces, New Mexico. One of the tasks of the Western Environmental design competition was to remove arsenic from an acidic solution. The initial concentration of arsenic in solution was measured at 10.2 milligrams per liter. The solution pH was 2.0. The solution was tested using WPAN by a group of students from Montana Tech, located in Butte, Montana. A 30 mL syringe column was used for the testing procedure. The solution pH was adjusted to 4 with potassium hydroxide and the solution was run through the column at a flow rate of 3 mLs per minute. Samples were taken at intervals of 166.67 mLs and analyzed on the ICP for arsenic. Results can be observed in Table 9.29 and Figure 9.18.

Table 9.29. Arsenic Results from Montana Tech Design Team.

mL Flowthrough	ug/L As
166.67	14
333.33	12
500.00	13
666.67	13
833.33	12
1000.00	11
1166.67	12
1333.33	10
1500.00	10
1666.67	10
1833.33	9
2000.00	9
2166.67	11
2333.33	11
2500.00	13
2666.67	10
2833.33	13
3000.00	11

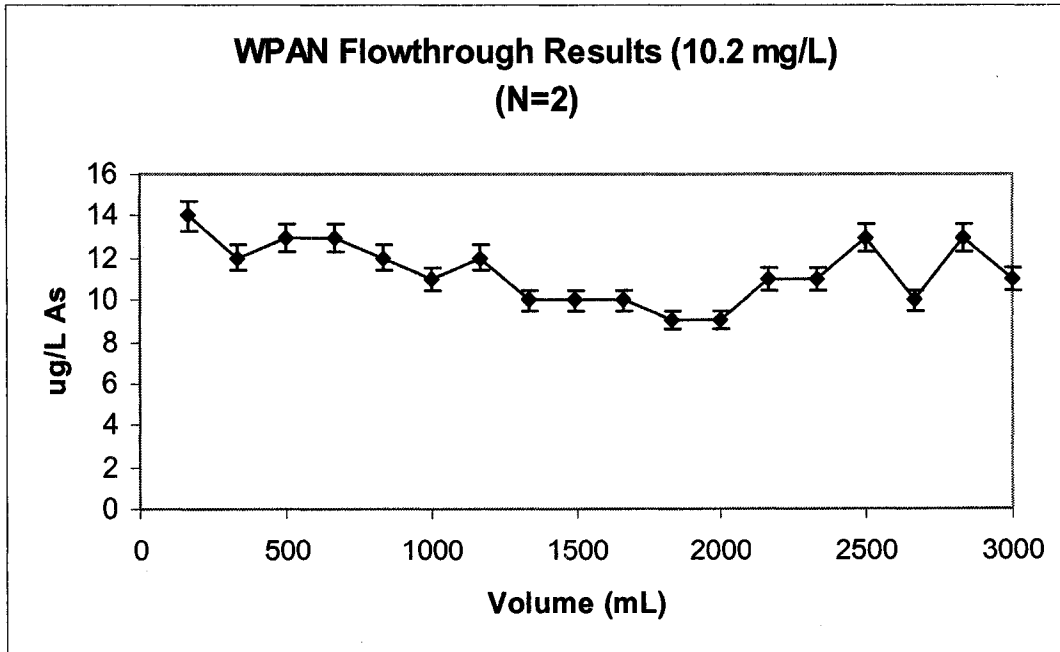
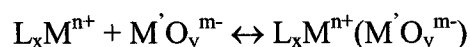


Figure 9.18. Experimental Results of Arsenic Solution from Design Team.

Experimental results indicated excellent removal of arsenic from solution using WPAN. Even at a higher concentration of arsenic (10.2 mg/L), WPAN was effective in removing the arsenic from solution to low levels of 15 ug/L or less during the entire testing phase.

9.16 Zirconium Loaded Silica Conclusions

Compared to literature results, Suzuki material captured arsenite but WPAN/BPAN did not capture the anion. On the other hand, WPAN/BPAN captured selenate as well as selenite while the Suzuki resin only captured selenite. Both capture arsenate anions at pH 8. These results were difficult to rationalize but a working hypothesis was that WPAN/BPAN had an overall higher average charge on the zirconium making it capable of capturing SeO_4^{2-} which was a weaker Lewis base than SeO_3^{2-} and existed as HSeO_3^{1-} at the reported pH of 4. The Suzuki resin captured arsenite was more difficult to understand in that it existed as a neutral compound up to pH=10. It may be that the zirconium ion center was essentially neutral or only +1 and therefore captured only neutral or +1 ions as reported (As(V) exists $\text{H}_2\text{AsO}_4^{1-}$ at pH 4). At pH 8, the performance of both systems fell off presumably because of increasing ionization and competition with hydroxide. It would appear from this initial data that whether a given oxyanion was captured or not was a combination of the net charge on the immobilized metal anion complex and the matching of the covalent binding characteristics of the pair. If the complex had a net negative charge binding will be weak while neutral or net positive complexes can be stable if there was sufficient donor acceptor bonding to outweigh hydration energy.



The current technology for stabilization of selenium from solution uses the ferrihydride process⁴⁰. This process utilizes iron sulfate or chloride salts which are initially dissolved in solution with selenite ions. The acidic solution pH is then raised to 8 with a strong base. Since the ferrihydride, freshly precipitated ferric hydroxide, has a strong positive charge, the selenite anion is removed from solution. Finally, a solid-liquid separation is done for total removal of selenite from solution.

Compared to current technology, WPAN was significantly better for removal of selenium from solution. Using ferrihydride technology, the process can only selectively remove the reduced form, selenite, from solution. In industry, a reduction step for selenium is performed. From the current study, WPAN is selective for both species of selenium. Secondly, using the ferrihydride process, large amounts of ferric iron sludge are produced for successful removal of selenium from solution. WPAN, however, was able to concentrate and remove selenium from solution. By concentrating the selenium anions, smaller amounts of by-product sludge are produced.

For arsenic remediation, the ferrihydride process⁴¹ is still considered the Best Demonstrated Available Technology (BDAT). As with the selenium removal process, iron salts are dissolved into the arsenic containing solution. The pH is then adjusted between 4 and 6 to successfully remove arsenate from solution. A solid-liquid separation is then performed to remove arsenic from solution.

For removal of arsenic from solution, the ferrihydride process was comparable. Both technologies are only capable of successfully removing the oxidized form of arsenic from solution. For both processes to be successful in industry, an initial oxidation step must be performed to remove arsenic from solution. Furthermore, WPAN technology have an

advantage over the ferrihydride process. As with selenium removal, the process produces a tremendous amount of sludge by-product compared to WPAN technology. The zirconium silica based ion exchange resins have the ability to concentrate arsenic from solution, therefore, lowering the amount of sludge created by the ferrihydride process.

References

1. A. Gupta, E.F. Johnson, and R.H. Schlossel, *Industrial and Engineering Chemistry Research*. **26**, 588 (1987).
2. R.W. Bartlett, "Solution Mining," Gordon and Breach, Amsterdam, 1992
3. G. Amos, W. Hopkins, S. Izatt, R. L. Breuning, J. B. Dale in "Environmental Improvements in Mineral Processing and Extractive Metallurgy," (M.A. Sanchez, F. Vergara, S. H. Castro, Eds.), University of Concepcion, Chile, 1997.
4. J.W. Patterson, and R. Passino, "Metals Speciation Separation and Recovery," Lewis Chelsea, Michigan, 1986.
5. K. Periasamy, and C. Namasivayam, *Waste Management* **15**, 63 (1995).
- 6a. J. Chang, R. Law, and C. Chang, *Water Res.* **31**, 1651 (1997).
b. L. Zhang, L. Zhao, Y. Yu, and C. Chen, *Water Res.* **32**, 1437 (1998).
7. R.C. Gatrone, M.L. Dietz, and E.P. Horwitz, *Solvent Extraction and Ion Exchange*. **11**, 411 (1993).
- 8a. S. Alexandratos, *Sep. and Purification Methods* **21**, 1 (1992).
b. S. Alexandratos, and D. Quillen, *Reactive Polymers* **13**, 255 (1990).
c. R. Fish, et.al., *Reactive Polymers* **6**, 255 (1987).
- 9a. R. Grinstead, *J. Metals* **31**, 13 (1979).
b. G.D. Del Cul et. al., *Separation Science and Technology*. **32**, 431 (1997).
10. A.M. Mathur, and A.B. Scranton, *Sep. Sci. and Tech.* **32**, 285 (1997).
11. E. Rosenberg, and D. Pang, U.S. Patent No. 5,695,882, 1997. Assignee: The University of Montana.
- 12.a) S. T. Beatty, R. J. Fischer, D. Pang, and E. Rosenberg; *Sep Sci and Tech.* **34**, 2723 (1999).
b) S. T. Beatty, R. J. Fischer, D. Pang, and E. Rosenberg, *Sep Sci and Tech.* **34**, 3125 (1999).
c) S. T. Beatty, R. J. Fischer, D. L. Hagars, E. Rosenberg, *Industrial and Engineering Chemistry Research* **38**, 4402 (1999).
13. E. Rosenberg, "Symposium Proceedings of the International Conference on Materials and Advanced Technologies," eds. T. White, D Sun, Mat. Res. Soc., Singapore, 2001, Volume I, p. 173.

14. U.S. Filter Hexavalent Chromium Contamination Treatment for Public Drinking Water Supply Case Study, May 2003.
15. F. Habashi, "All That Glitters. Readings in Historical Metallurgy," *Bull. Hist. Chem.* **4**, 33 (1990).
16. G.C. Westby, "Nitric Acid and Copper Ores", *Metallurgical and Chemical Engineering*, **18**, (6), 290-296, 1918.
17. J.D Prater, P.B. Queneau, and T.J. Hudson, "Nitric Acid Route to Processing Copper Concentrates", *Trans. Min. Eng. AIME* **254** (2) 117-222, 1973.
18. C.G. Anderson, K.J. Harrison, and L.E. Kryz, "The Application of Sodium Nitrite Oxidation and Fine Grinding in Refractory Precious Metals Concentrates Pressure Leaching", *Transactions of the Society for Mining, Metallurgy, and Exploration*, Volume 299, 1996.
19. E. Peters, *Hydrometallurgical Process Innovation*, *Hydrometallurgy*, **29**, 1992.
20. C.G. Anderson et. al., "Treatment of Metal Bearing Mineral Material", U.S. Patent No. 5,096,0486, March 17, 1992.
21. R.J. Fischer, *Development of a copper selective silica-polyamine composite*, University of Montana Dissertation, 1992.
22. S. Mahajam, *Role of Materials Science in Development of InP/InGaAsP Light Emitting Diodes for Light Wave Communication*, *Trans. IIM* **41** (1988) 205-217.
23. G.M. Phatak, K. Gangadharan, *Extraction of Gallium from Bayer Liquors: A Report on the Indegenous Research and Development. Proc. of the Xth ISAS National Symposium on Strategic and Hi-Tech Metals Extraction and Process Characterization*, Udaipur Chapter, India, 1994, pp. 4-6.
24. I. Mikaylove, P.A. Distin, *Gallium Solvent Extraction in Hydrometallurgy: An Overview*, *Hydrometallurgy* **28** (1992) 13-27.
25. D. Bauer, Y. Pescher-Cluzeau, *Liquid-liquid Extraction of Aluminum and Gallium with 5-substituted 8-hydroxyquinolines*, *Hydrometallurgy* **18** (1987) 465-483.
26. A. Leveque, J. Helegorsky, *The Recovery of Gallium from Bayer Process Aluminate Solutions by Alkylated Hydroxyquinolines*, *Hydrometallurgy* **16** (1986) 315-324.
27. M.J.S. Dewar, L.S. Hart, *Aromatic Rearrangement in the Benzene Series*, *Tetrahedron*, Vol. 26, pp. 1001-1008.

28. F.D. Thomas, New Synthetic Formation of 5-acetyl-8-hydroxyquinoline, Unpublished Dissertation.
29. U. Pyell, G. Stork: Preparation and properties of an 8-hydroxyquinoline silica gel, synthesized via Mannich reaction, *Fresenius J. Anal. Chem.* **342** (1992) 281-286.
30. C. Mannich, W. Krosche, *Arch. Pharm.* **250**, 647 (1912).
31. C.G. Anderson, Personal Communication.
32. T. Sato, and H. Oishi, Solvent Extraction of Gallium(III) from Sodium Hydroxide Solution by Alkylated Hydroxyquinoline, *Hydrometallurgy*, **16** (1986) 315-324.
33. G.P. Demopoulos, Iron(III) Removal from Base Metal Electrolyte Solutions by Solvent Extraction, *Hydrometallurgy*, **12** (1984) 299-315.
34. L. Fishbien, *Fundamental Applied Toxicology*, 1983, 3, 411.
35. C.J. Chen, *Br. J. Cancer*, 1992, 66, 888.
36. E. Marshall, *Science* 1985, 229, 144 Selenium in Biology and Human Health, ed., Burk, R.F. Springer-Verlag, New York, 1994.
37. M.L. Pierce, C.B. Moore, *Water Res* 1982, 16, 1247; S.K. Gupta, K.Y. Chen, J. *Water Pollut. Control Fed.*, 1978, 50, 493; Chang, R.C., Liang, S., Wang, H., Bueler, M.D., *Journal American Water Works Association*, 1995, 64, 105.
38. T.M Suzuki, T. Pacheeco, L. Tanco, M. Kanosato, T. Yokoyama, Adsorption and removal of oxo-anions of arsenic and selenium on zirconium(IV) loaded polymer resin functionalized with diethylenetriamine-N,N,N,N-polyacetic acid.
39. J. Kueth, Montana Department of Quality.
40. L.G. Twidwell, The Removal of Toxic Species from Waste Solutions by the Formation of Stable and Filterable Precipitates, Quarterly Report, USBM Mineral Industry Waste Treatment and Recovery Generic Center, Univ. of Nevada Reno, NV.
40. R.G. Robins, C.Y. Huang, T. Nishimura, and G.H Khoe, The Adsorption of Arsenate Ion by Ferric Hydroxide, *Arsenic Metallurgy Fundamentals and Applications*, Eds. TMS-AIME Symposium Proceedings, Phoenix, AZ, The Metallurgical Society, Warrendale, PA, pp. 99-112.